D'Hondt, S.L., Jørgensen, B.B., Miller, D.J., et al., 2003
Proceedings of the Ocean Drilling Program, Initial Reports Volume 201

1. Leg 201 Summary[1]

Shipboard Scientific Party[2]

ABSTRACT

Ocean Drilling Program Leg 201 was the first ocean drilling expedition dedicated to the study of life deep beneath the seafloor. Its seven sites were selected to represent the general range of subsurface environments that exist in marine sediments throughout most of the world's oceans. In water depths as great as 5300 m and as shallow as 150 m, the expedition drilled as deep as 420 m into oceanic sediments and the underlying rocky crust. The sediments ranged in temperature from 1° to 25°C and in age from 0 to almost 40 Ma.

To document metabolic interactions in deeply buried marine sediments and the differences between those interactions in ocean-margin sediments and in open-ocean sediments, shipboard scientists measured an unprecedented array of metabolic reactants and products in the interstitial waters of Leg 201 sediments. To document subsurface communities, shipboard scientists initiated an unprecedented number and range of microbial experiments. To document the nature of subsurface environments, shipboard scientists documented an exhaustive range of core and downhole geophysical and sedimentological properties.

Active prokaryotic respiration occurs throughout the sediment column at every site. Subseafloor respiration is supported at all sites by the diffusion of sulfate from the overlying ocean, as well as by the dissolution of iron- and manganese-bearing minerals. At the open Pacific sites, respiration deep beneath the seafloor is also supported by the transport of sulfate, nitrate, and dissolved oxygen from water circulating through the underlying basaltic crust. At both the open Pacific sites and the Peru margin sites, methanogenesis consistently co-occurs with electron-accepting processes that are often assumed to outcompete it, including sulfate reduction, iron reduction, and manganese reduction. In all of the sedimentary environments sampled during Leg 201, sedimentary

[1]Examples of how to reference the whole or part of this volume.
[2]Shipboard Scientific Party addresses.

Ms 201IR-101

properties and, by inference, past oceanographic conditions affect current rates of prokaryotic activities.

Prokaryotic abundances are much higher in sediments buried on the continental shelf of Peru than in sediments of the open Pacific Ocean. The open Pacific sites contained some of the lowest average prokaryote concentrations ever observed in deep-sea sediments. In contrast, some of the sediments recovered on the Peru shelf contained the highest concentrations of prokaryotes ever observed beneath the seafloor. At the Peru shelf sites, the concentration of sedimentary prokaryotes was highest in a narrowly focused zone of anaerobic methanotrophy tens of meters beneath the seafloor.

The recovered sediments and fluids will be studied further to document the composition of subseafloor prokaryotic communities, the principal controls on rates of subsurface activity, the influence of past oceanographic conditions on current activity in deeply buried sediments, and the effects of subseafloor biogeochemical processes on Earth's surface world.

INTRODUCTION

The Ocean Drilling Program (ODP) is uniquely positioned to sample one of the least known and potentially strangest ecosystems on Earth—the microbial biosphere of deep marine sediments and the oceanic crust. The growing international interest in the study of this subsurface biosphere is driven by a variety of factors, including the role of subsurface microbial activity in Earth's biogeochemical cycles, the possibility of life on other planets, and sheer fascination with the nature of life at the apparent margin of existence.

Nearly 20 years ago, Deep Sea Drilling Project (DSDP) experiments with methane concentration and radiotracer uptake first demonstrated active microbial processes in cores recovered from deeply buried marine sediments (Oremland et al., 1982a; Whelan et al., 1986; Tarafa et al., 1987). Over the last 15 years, studies of ODP cores have extended our understanding of those processes (e.g., Cragg et al., 1992; Getliff et al., 1992) and consistently identified abundant prokaryotes in deeply buried oceanic sediments (e.g., Cragg et al., 1990, 1992; Thierstein and Störrlein, 1991; Parkes et al., 1994, 2000). Prokaryotes have been recovered from burial depths as great as 800 meters below the seafloor (mbsf) (Shipboard Scientific Party, 1999). Recent contamination tracer experiments suggest that the prokaryotes reported from ODP cores are indigenous to the drilled sediments (Smith et al., 2000b).

The number and biomass of prokaryotes in the subsurface biosphere of oceanic sediments have been estimated by extrapolation from direct counts of sedimentary prokaryotes at a small number of ODP sites. Based on that extrapolation, the marine subsurface biosphere has been estimated to compose as much as one-tenth (Parkes et al., 2000) or even one-third (Whitman et al., 1998) of the world's living biomass. In situ metabolic activity by at least a portion of this biosphere is spectacularly demonstrated by hydrates of methane produced by prokaryotes in deep-sea sediments. On a global scale, these hydrates contain 7,500 to 15,000 gigatons of carbon—four to eight times as much carbon as in living surface biosphere and soils combined (Kvenvolden, 1993). Interstitial water chemical studies (Borowski et al., 1996) and recent microbiological discoveries (Hinrichs et al., 1999; Boetius et al., 2000) suggest that, on an ongoing basis, the methane produced in deep-sea sediments

is primarily destroyed by the sulfate-reducing activity of prokaryotes in overlying sediments.

Despite these recent advances, very little is known about the nature and activity of life in deep marine sediments. In particular, we know almost nothing about (1) the continuity of subsurface life from one oceanographic region to another, (2) metabolic interactions in deeply buried marine sediments, or (3) the conditions under which subsurface prokaryotes are active or inactive and living or dead.

Background

There is abundant evidence of both microbial populations and microbial activity in subsurface marine sediments throughout the world ocean. Prokaryotic cells have been found in surprisingly high numbers in buried sediments at every site that has been assayed for their presence (Parkes et al., 2000). The abundance of those cells varies in a systematic and fairly predictable manner. For example, deeply buried shelf sediments from the Peru margin (high surface-ocean productivity and shallow water depth) contain 10^8–10^9 cells/cm^3, and sediments from the eastern equatorial Pacific (low surface-ocean productivity and abyssal water depth) contain only 10^6 cells/cm^3 (Parkes et al., 2000).

Interstitial water chemical data from hundreds of DSDP and ODP sites document the presence of subsurface metabolic activity in sediments throughout most of the deep ocean (D'Hondt et al., 2002). Bacterial sulfate reduction, methane production, and methanotrophy are common processes in deeply buried marine sediments. Other metabolic processes are known to occur in subsurface marine sediments but have been studied very little (such as manganese and iron reduction).

Despite the ubiquity of prokaryotic cells in deeply buried marine sediments and the clear interstitial water evidence of in situ microbial metabolism, the identity and structure of these communities and the metabolic adaptations of the prokaryotes that constitute them remain largely unknown. Most probable number (MPN) experiments have demonstrated that viable cells are present in deeply buried marine sediments (Parkes et al., 2000). However, these viable cells represent only the barest fraction (0.00001% to 0.6%) of the total cells enumerated in the sediments sampled (Parkes et al., 2000). The extent to which this discrepancy between enumerated and viable cells reflects a culturing bias, known also from surface sediments, or the extent to which it reflects a real difference between a small active population and a very large inactive (dormant or dead) population remains to be determined.

The importance of this issue for our understanding of subsurface population structure and metabolic adaptation is underscored by estimates of the mean sulfate reduction per enumerated subsurface cell (D'Hondt et al., 2002). If all of these enumerated cells are alive, their rates of sulfate reduction are zero to two orders of magnitude lower in the ocean-margin anaerobic methanotrophy zone and four or more orders of magnitude lower in open-ocean sediments than per-cell rates inferred in surface marine sediments (Jørgensen, 1978; Knoblauch et al., 1999; Ravenschlag et al., 2000; D'Hondt et al., 2002). In contrast, if subsurface cells actually utilize sulfate at the lowest rates inferred for cells in surface marine sediments, as few as 1 in 100 may be actively respiring in the sulfate-reducing methanotrophy zone of the most microbially active sites and fewer than 1 in 10,000 is actively respiring at the most microbially active open-ocean sites. In short, most of the subsurface prokaryotes enumerated by direct microscopy in marine sediments

must be either adapted for extraordinarily low levels of metabolic activity or dormant—or even dead. This conclusion is supported by available estimates of mean generation times of up to 1 m.y. for deep subsurface prokaryotes (Parkes et al., 2000).

Metabolic Diversity

The metabolic diversity and rates of microbial processes in deep subsurface sediments can be inferred from a broad range of geochemical information, including modeling of interstitial water profiles of ions, gases, and low molecular weight organic molecules, mass balance calculations of changes in solid-phase constituents, and stable isotope fractionation. Basically, the same types and sequences of microbial processes may occur deep beneath the seafloor as are known from the much more active surface sediments of ocean margins. The mechanisms and regulation of the exceedingly slow hydrolytic degradation of macromolecular organic compounds are, however, only poorly understood. So, too, are the fermentative pathways that produce substrates for the terminal mineralization processes such as sulfate reduction or methanogenesis.

The buildup of bicarbonate and ammonium are indicators of the diagenesis of organic material in all marine sediments. Sulfate reduction appears to dominate biogeochemical processes down to the depth of sulfate depletion, many tens or hundreds of meters below the seafloor, where it is followed by methanogenesis. Although methane formation is very slow, the continuous production of a diffusible gas over millions of years results in vast methane accumulations, either dissolved in the interstitial water or in the condensed form of gas hydrates. In both cases, an upward flux of methane reaches the sulfate zone and supports an interface of enhanced microbial activity based on methane oxidation. In shallow marine sediments, this anaerobic process appears to be catalyzed by a syntrophic community consisting of archaea, which convert methane back to an intermediate such as hydrogen or acetate, and sulfate-reducing bacteria, which oxidize the intermediate (e.g., Hoehler et al., 1994; Valentine and Reeburgh, 2000; Boetius et al., 2000; Orphan et al., 2001). Based on interstitial water modeling of sulfate and methane profiles, the same process appears to drive a significant part of sulfate reduction in the seabed (e.g., Borowski et al., 1999; D'Hondt et al., 2002). This interface is of particular importance, since it constitutes a barrier against the escape of methane up into the ocean water and eventually into the atmosphere.

In deep-sea sediments, such as the Peru Basin sites drilled during Leg 201, manganese oxide may provide an important oxidant of organic material and its reduction can be traced tens of meters below the seafloor (Yeats, Hart, et al., 1976). The reduction of iron oxides is also expected to play a greater quantitative role in deep-sea sediments than in ocean-margin sediments. Iron(III) bound in mineral phases may provide a slow but continuous source of oxidation potential.

Hydrogen is an important intermediate in the microbial degradation pathways of shallowly buried ocean-margin sediments, where its interstitial water concentration appears to be strictly regulated by the uptake potential of the prokaryotic community and the energy yield of their hydrogen metabolism. Thus, the hydrogen partial pressure in the sulfate reduction zone is maintained below the threshold level required by archaea to drive methanogenesis (Hoehler et al., 1998). The key role of hydrogen, known from the metabolic competition among microbial

populations in surface sediments, may also be critical for the deep subsurface biosphere. The potential sources for microbial energy metabolism need to be surveyed with an open mind toward new and unexpected types of redox processes and mineral surface reactions.

Microbial Diversity

The phylogenetic and physiological diversity of deep sediment communities remains virtually unknown. Only two isolates of sulfate-reducing bacteria from subsurface sediments (80 and 500 mbsf) have been characterized (Bale et al., 1997). These isolates (from a single site in the Japan Sea) are of a new barophilic species, *Desulfovibrio profundus*. Its unusually wide growth temperature range (15°–65°C) has no counterpart in any other known sulfate-reducing bacterium. It is metabolically flexible; it possesses the capability to reduce oxidized sulfur species, nitrate, and iron(III). Whether deeply buried sulfate-reducing communities throughout the world ocean are dominated by close relatives of *D. profundus* or are composed of a host of other organisms remains to be tested.

The record of methanogenic isolates from the subsurface is surprisingly spare. MPN enumerations of methanogens in deep marine sediments have yielded cultured methanogens in much smaller numbers than sulfate-reducing bacteria (in the Peru margin; Cragg et al., 1990) or not at all (in the Japan Sea; Cragg et al., 1992). These surveys have not, to our knowledge, led to the description of new methanogen species from the marine subsurface. Hence, the phylogenetic composition of marine subsurface methanogenic communities remains essentially unknown.

Organisms responsible for methanotrophy in nearshore surface sediments have been biomarker fingerprinted and phylogenetically identified but not yet cultured (Hinrichs et al., 1999; Boetius et al., 2000; Lanoil et al., 2001; Teske et al., 2002). Whether or not similar microbial communities (composed of sulfate-reducing bacteria and previously unknown members of the archaea Methanosarcinales) are responsible for methanotrophy in the more deeply buried biosphere throughout the world ocean (in both ocean-margin and open-ocean environments) remains to be seen.

Novel forms of prokaryotic metabolism with subsurface potential are constantly being discovered. For example, systematic studies of sulfate- and sulfur-reducing bacteria and archaea have shown that many representatives of these organisms, among them an astonishing set of phylogenetically very deep lineages (Vargas et al., 1998), share an unexpected capacity for iron(III) reduction (Lonergan et al., 1996). A *Thermus* sp. isolated from a deep South African gold mine used dissolved oxygen, nitrate, iron(III), S^0, manganese(IV), cobalt(III), chromium(VI), and uranium(VI) as electron acceptors (Kieft et al., 1999). Respiration of metal oxides could allow bacteria and archaea a respiratory mode of life even after other electron acceptors, including oxidized sulfur species, become depleted with increasing distance from the oxidized biosphere. The metabolic flexibility of *D. profundus* and the South African *Thermus* sp. allows multiple scenarios of subsurface phylogenetic diversity. One possible scenario is that a certain prokaryotic community becomes buried below the sediment surface and basically persists in its phylogenetic diversity and physiological potential over millions of years. This community may be responsible for nitrate reduction, manganese reduction, iron reduction, and sulfate reduction throughout the vertical expanse

of a single sediment column—and even dominate the subsurface respiratory realm throughout the sediments of the world ocean (at least within a broad temperature range, such as 0°–30°C or 30°–60°C). A second (and perhaps more likely) scenario is that the phylogenetic composition of subsurface communities may be shaped by variables other than the type of electron acceptors available. For example, it may be controlled by electron donor availability, micronutrient availability, or the ability of well-tuned species or communities to out-compete each other under slightly different local environmental conditions, such as different concentrations of metabolic products and reactants. Also, physical factors such as available pore space, ability to migrate in the sediment, interactions with mineral surfaces, or distance to solid substrates may be important.

Global Biogeochemical Effects

The subsurface biosphere of marine sediments may affect the surface Earth in a variety of ways. It is now widely recognized that release of methane from marine sediments may affect atmospheric carbon stocks and climate (Dickens et al., 1995; Dickens, 2000; Kennett et al., 2000; Hesselbo et al., 2000; Hinrichs, 2001). It is less widely recognized that sulfate reduction by the buried biosphere may also change Earth's surface chemistry and climate. Such reduction is a major sink of sulfate from the world ocean (Holland, 1984). Because sulfate is the second most abundant anion in seawater (Pilson, 1998) and sulfate reduction followed by sulfide precipitation results in the production of two equivalents of alkalinity per mole, subsurface sulfate reduction may affect total oceanic alkalinity and, consequently, the partitioning of carbon dioxide between atmosphere and ocean over geologic time (D'Hondt et al., 2002). The ultimate effect of this process on the surface Earth will depend on the extent to which reduced sulfur is fixed in the sediment rather than diffusing back into the overlying ocean to be oxidized.

Why the Equatorial Pacific and Peru Margin?

In short, we know almost nothing about the population structure, metabolic strategies, community composition, and global biogeochemical influence of the marine deep biosphere. We also know almost nothing about how the chemical and physical characteristics of subseafloor sediments control the prokaryotic communities and activities that occur within those sediments. Consequently, we also know little about how modern prokaryotic communities are constrained by past oceanographic history. If we are to develop a coherent understanding of the prokaryotic communities that are deeply buried in marine sediments, a focused and interdisciplinary program of deep biosphere study is required. Leg 201 presents a crucial early step in the development of such a program.

Sampling of the Leg 201 sedimentary environments allows us to document the activity, composition, and biogeochemical effects of the subsurface biosphere in environments representative of essentially the entire range of subsurface conditions that can be found in relatively cool (2°–25°C) marine sediments. These include equatorial Pacific sediments typical of the open ocean, Peru margin sediments typical of a nearshore upwelling regime, and Peru Basin sediments. Much of the geochemical and sedimentological character of these sediments has been documented during previous ODP and DSDP legs (DSDP Leg 34, Peru margin

ODP Leg 112, and equatorial Pacific ODP Leg 138) (Yeats, Hart, et al., 1976; Mayer, Pisias, Janecek, et al., 1992; Suess, von Huene, et al., 1990; Pisias, Mayer, Janecek, Palmer-Julson, and van Andel, 1995). In short, several widely different marine sedimentary regimes were explored during this single drilling leg. Few regions in the world contain within a relatively short distance so many marine sedimentary regimes that have been so well characterized.

The environments that were examined include (1) carbonate and siliceous oozes of the equatorial Pacific, (2) clays and nannofossil-rich oozes of the Peru Basin, (3) organic-rich silty sediments of the shallow Peru shelf, and (4) a hydrate-bearing deepwater sequence off the continental shelf of Peru (see Fig. **F1**).

The first two environments are characteristic of open-ocean sedimentary regimes. Leg 138 studies identified the presence of subsurface prokaryotes throughout the sediment column in this equatorial Pacific region (Cragg and Kemp, 1995). Shipboard chemical analyses from Legs 138 and 34 (Pisias et al., 1995; Yeats, Hart, et al., 1976) suggest that the deeply buried prokaryotic communities of these two regions rely primarily on sulfate and manganese reduction, respectively. Despite these studies, the subsurface extent of electron acceptors with similar or intermediate standard free-energy yields (nitrate, oxygen, and iron oxides) in these regions was unknown prior to Leg 201.

The second two environments are characteristic of ocean-margin regimes. Studies of Leg 112 samples identified abundant subsurface prokaryotes in Peru shelf sediments (Cragg et al., 1990). At all sites but one, these shallow-water sediments and the deepwater hydrate-bearing sediments are rich in dissolved sulfate at shallow burial depths (down to a few meters below seafloor) and rich in methane at greater burial depths (starting a few meters below seafloor or tens of meters below seafloor) (Suess, von Huene, et al., 1990). The remaining site is sulfate rich and methane poor throughout the targeted drilling interval.

Deeply buried brine affects the subsurface environment at the shallow-water Peru shelf sediments. At equatorial Pacific open-ocean sites, the subsurface environment is affected by water flow through the underlying basaltic basement.

F1. Map showing general locations of Legs 138, 112, and 201 sites, p. 57.

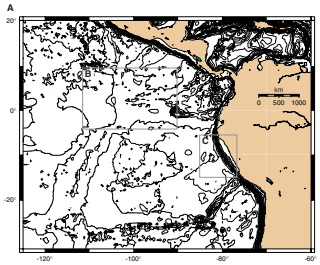

Scientific Objectives

The overarching objective of Leg 201 is to investigate the nature, extent, and biogeochemical consequences of prokaryotic activity in several different deeply buried marine sedimentary environments.

During Leg 201, we addressed several fundamental questions about the deeply buried biosphere:

1. Are different sedimentary geochemical regimes characterized by completely different prokaryotic activities and communities—or merely by shifts among the dominant species and different levels of community activity?
2. How does the transport of electron acceptors, electron donors, and, potentially, of prokaryotes through deep sediments affect sediment chemistry and community structure?
3. To what extent do past oceanographic conditions affect prokaryotic communities now active in deep-sea sediments?
4. How do biogeochemical processes of the deep subsurface biosphere affect the surface world?

Several aspects of these questions require extensive postcruise research to fully address. This reliance on postcruise research is necessary for at least two reasons. First, some experiments initiated during the cruise will take months (radiotracer experiments) or years (cultivation experiments) to complete. Second, some key studies, such as genetic assays of the prokaryotic communities and isotopic studies of biogeochemical fluxes, will be undertaken postcruise because they require technical facilities and expenditures of time beyond those available to a shipboard party.

Despite these limitations, other aspects of the above questions were successfully addressed during Leg 201. In particular, shipboard biogeochemical, geophysical, and sedimentological studies provide new understanding of the effects of interstitial water chemistry, sediment composition and structure, fluid flow, and past oceanographic conditions on metabolic diversity, prokaryotic activities, and the nature of metabolic competition in these subsurface environments. These shipboard studies improve our understanding of how deep subsurface biogeochemical processes affect both their local environments and the surface world.

Scientific Approaches

The study of deep subsurface prokaryotes and their activity is a methodological and experimental challenge at the frontiers of modern life and earth sciences. Leg 201 is the first deep-sea drilling expedition to be primarily focused on subsurface prokaryotic communities and their geochemical activities. Many of the studies carried out during this cruise were undertaken by ODP shipboard scientists for the first time. Many of these approaches had not been previously used to study the deep biosphere. A number of methods and concepts had to be further developed, refined, or even completely changed during the expedition. The scientific approaches were consequently chosen on the basis of extensive discussions and experiences of many colleagues and are still very much in the development phase. Some of these approaches may need further refinement before they are recommended for future routine application.

The research objectives of Leg 201 required shipboard scientists to address the following specific questions regarding the subseafloor sedimentary biosphere:

1. What are the physical-chemical conditions that support or limit microbial life at depth in marine sediments?
2. What are the prokaryotes that inhabit these thousand-year-old to multimillion-year-old sediments?
3. What are their metabolic activities, and how do these activities affect their chemical and physical environment?

To address these questions effectively, a very wide range of sedimentological, geophysical, geochemical, and microbiological analyses were undertaken during Leg 201. To maximize understanding of the interplay between subsurface prokaryotes and their environment, whenever possible, these diverse analyses were conducted on the same sediment samples or samples immediately adjacent to each other.

A full suite of standard sedimentary analyses was used to document the physical and compositional nature of subsurface environments explored during Leg 201. These included visual core descriptions, digital

color scanning and optical reflectance scanning of the split cores, and microscopic observation and/or X-ray diffraction analyses of individual sediment samples.

Core logging of magnetic susceptibility and intensity was used to identify environments of particular interest for Leg 201 objectives, such as pronounced biogeochemical fronts or lithostratigraphic boundaries. Core logs (magnetic susceptibility, gamma ray attenuation [GRA] bulk density, and natural gamma radiation [NGR]) were also used to correlate intervals of particular interest from hole to hole at the same site. Where possible, magnetic reversal logs were used to determine sediment age and correlate from hole to hole and site to site. NGR was measured both on cores in the laboratory and using wireline logs for in situ formation properties. Wireline logs (resistivity, NGR, and geophysical proxies for density and porosity) were also used to characterize the physical and compositional nature of subseafloor environments.

Analysis of the physical environment also included study of environmental properties such as temperature and pressure, which are important for the selection of cell properties and regulation of metabolic activity. Physical properties critical for quantifying transport processes, such as porosity and diffusivity, were analyzed in order to interpret the chemical gradients with respect to subsurface flow, chemical diffusion, and the availability of substrates for prokaryotes.

The detailed analysis of interstitial water chemistry was a major emphasis during Leg 201 and was probably more comprehensive than during any previous ODP leg. A broad spectrum of dissolved inorganic ions, gases, and organic solutes was measured with close vertical resolution throughout the sediment column at each site in order to identify potential substrates and products of microbial metabolism and provide the chemical data necessary to quantitatively model steady-state net rates of microbial activities.

Additional shore-based analyses of solid-phase geochemistry and interstitial water chemistry will enable mass balance calculations of burial rates and diagenetic transformations of organic compounds and mineral phases. Stable isotope analyses of carbon, hydrogen, oxygen, sulfur, nitrogen, and iron in both dissolved and solid chemical phases will serve as a complementary approach to interpret the biogeochemical alterations. The sensitivity of isotopic analyses allows inferences about processes that are too slow to detect with other experimental process studies. Furthermore, analyses of specific biomarkers and their isotopic signals will help to identify which prokaryotes were involved in these slow alterations in the past.

A variety of experiments were undertaken during Leg 201 to estimate in situ activities of specific samples. Most of these experiments relied on minute quantities of radioactive chemicals to trace rates of specific activities. Although specific activities are generally limited to a subset of the prokaryotic community, they typically serve a crucial role in the flow of energy and material through the entire community. Well-established ^{35}S, ^{14}C, and ^{3}H techniques were used to quantify within-sample rates of sulfate reduction, methanogenesis, and thymidine uptake. Innovative experiments with $^{3}H_2$ were used to trace hydrogen uptake and turnover. A few additional experiments included incubating samples with stable isotopes as tracers; some used ^{18}O to study oxygen exchange between water and phosphate, and others used ^{13}C to trace assimilation of carbon from acetate into biomass.

A wide variety of microbial cultivation experiments were initiated during Leg 201 to identify and quantify subseafloor prokaryotic populations. These included a large number of incubations that utilize selective media for enrichments in order to isolate and identify a broad spectrum of physiological types with respect to energy metabolism and temperature adaptation (general heterotrophs; fermenters; autotrophic and heterotrophic sulfate reducers, methanogens, and acetogens; iron and manganese reducers; anaerobic ammonium and methane oxidizers; and psychrophiles, mesophiles, and thermophiles). Serial dilution (MPN) cultivation experiments were initiated to enumerate those prokaryotes able to show growth and metabolic activity under nutrient-rich laboratory conditions. Homogenized sediment slurries were diluted in tenfold steps into liquid media, which should support the growth of specific physiological types of prokaryotes. In such experiments, the highest dilutions that still have growth are classically interpreted to indicate the MPN of these organisms (American Public Health Association, 1989). MPN counts typically provide only a minimum estimate of the true numbers of organisms that were viable in situ because many prokaryotes (perhaps the vast majority) are not cultivable with currently available methods. MPN cultivations also serve as starting material for enrichments and isolations of the prokaryotes. The isolation of prokaryotes from the highest dilutions with positive growth maximizes the chance of finding organisms that are quantitatively dominant and, therefore, geochemically most important.

As for many ODP legs over the past decade, total cell numbers of prokaryotes were determined during Leg 201 by direct microscopy of fluorescently stained cells (acridine orange direct count [AODC]). Similar counts of defined groups of prokaryotes will be done postcruise by using fluorescence in situ hybridization (FISH) to specifically stain cells that share genetic sequence information.

The genetic diversity and geographic continuity of subseafloor prokaryotic populations will be addressed by postcruise research. This research will largely rely on the recently developed approach of analyzing deoxyribonucleic acid (DNA) and ribonucleic acid (RNA) from entire communities in natural samples. This approach allows analysis of natural communities of prokaryotes that are unavailable in culture, either because cultivation attempts have not yet succeeded in providing suitable growth conditions or because cultivation-based approaches have limited capacity to deal with great prokaryotic diversity. DNA and RNA in Leg 201 sediment samples will be extracted by several participating groups, who will use them to analyze subseafloor prokaryotic diversity based on genetic sequence information. This will, for the first time, establish a database on the diversity of prokaryotes from the deep subsurface and the key genes of their energy metabolism.

PRINCIPAL RESULTS

The principal objective of Leg 201 was to document the nature, extent, and biogeochemical consequences of microbial activity and prokaryotic communities in several different deeply buried marine sedimentary environments. To maximize the scientific utility of Leg 201 results, biogeochemical, microbiological, physical property, and sedimentological sampling and analyses and downhole tool deployment and downhole logging were all closely integrated. Leg 201 physical property, sedimentology, and downhole studies provided detailed evidence

of the environmental factors that influence subseafloor microbial life and are in turn influenced by it. To build comprehensive records of net microbial activities and their consequences, the Leg 201 shipboard party conducted a broad range of biogeochemical studies. To develop comprehensive records of subseafloor prokaryotic communities, the shipboard party also undertook and initiated a multifaceted array of microbiological studies. The extent of biogeochemical and microbiological analyses on Leg 201 samples is unprecedented in ODP history.

Subseafloor Microbial Activities of Different Sedimentary Geochemical Regimes

During Leg 201, a variety of sediments (Fig. **F2**) were cored in both open-ocean and ocean-margin provinces in the eastern tropical Pacific Ocean. Neogene deep-sea clays and Paleogene nannofossil ooze were cored at Peru Basin Site 1231. Miocene to Holocene carbonate and siliceous oozes and chalk were cored at Sites 1225 and 1226. Miocene to Holocene biogenic oozes and terrigenous sediments of the shallow Peru shelf were cored at Sites 1227, 1228, and 1229. Organic-rich Miocene to Holocene sediments were cored at Site 1230 on the Peru slope, in the accretionary wedge just landward of the Peru Trench.

In situ data from Leg 201 demonstrate that comparable temperature ranges are found at all the sites, allowing direct comparisons of microbial activities and communities in very different environments under similar thermal conditions (Fig. **F3**). In situ temperatures of the organic-poor sediments of Sites 1225 and 1231 and the organic-rich Peru shelf Site 1230 are in the range preferred by psychrophilic prokaryotes (0°–10°C). In situ temperatures of the organic-rich Peru shelf sediments and throughout most of the sediment column at eastern equatorial Pacific Site 1226 are in the low end of the range preferred by mesophilic prokaryotes (which inhabit 10° to 35°C environments).

AODCs showed that prokaryotic cell concentrations of the Leg 201 sediments generally followed the well-established trend of exponential declines in cell concentration with subsurface depth. Cell counts are generally higher at the ocean-margin sites than at the open-ocean sites (Fig. **F4**). Cell concentrations progressively increase from Peru Basin Site 1231 to equatorial Pacific Site 1225 to eastern equatorial Site 1226 to Peru shelf Site 1227 to Peru shelf Site 1229 and Peru slope hydrate Site 1230. A similar difference between open-ocean and ocean-margin sites was noted in a recent survey of previously studied ODP sites (Parkes et al., 2000).

The geometric mean prokaryotic cell concentrations for all of the Leg 201 sites are close to, or even slightly below, the mean concentrations for all previously studied ODP sites (Fig. **F5**). This finding is somewhat surprising because so many of the Leg 201 sites contained organic-rich sediments, including the Peru shelf sites, Peru slope hydrate Site 1230, and eastern equatorial Site 1226. Because previously enumerated sites targeted a representative range of ODP sampled environments, the similarity of our results to the average for previously studied sites may reflect a collective ODP bias toward drilling at the ocean margins and away from drilling in such regions as the oceans' central gyres.

Interstitial water studies of the Leg 201 sites showed that net subseafloor microbial activity is much higher at the ocean-margin sites than at the open-ocean sites. For example, subseafloor concentrations of dissolved inorganic carbon (DIC = HCO_3^- + CO_2 + CO_3^{2-}) and ammonium

F2. Lithostratigraphic summary, Leg 201 sites, p. 59.

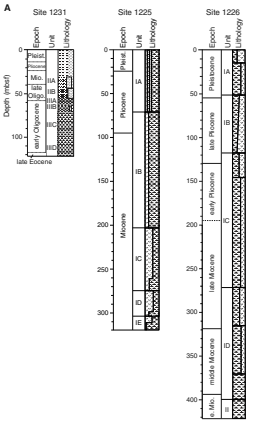

F3. Temperature profiles of Leg 201 sites, p. 61.

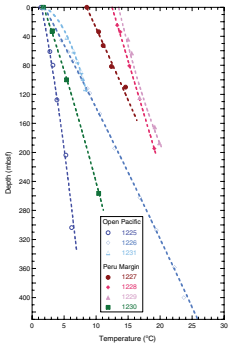

F4. Cell enumeration data, p. 62.

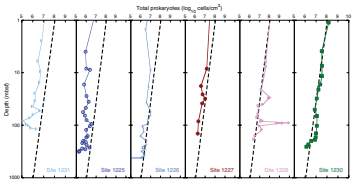

F5. Leg 201 cell counts compared to previously censused sites, p. 63.

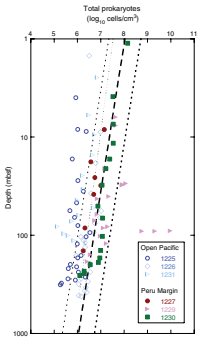

are much higher at ocean-margin Sites 1227, 1228, 1229, and 1230 than at open-ocean Sites 1231, 1225, and 1226 (Fig. F6). DIC and ammonium are generic products of microbial activity, regardless of the principal electron-accepting pathway. Consequently, the very high concentrations of those chemical species at the ocean-margin sites and the generally low concentrations at the open-ocean sites indicate that net respiration of organic carbon to carbon dioxide and net mineralization of organic nitrogen to ammonium is much higher in subseafloor sediments of the ocean margin than subseafloor sediments of the open ocean.

On a more precise level of comparison, the profiles of DIC show that the Leg 201 sites span a wide range of subsurface activity levels (Fig. F7). The lowest DIC concentration is present at clay-rich open-ocean Site 1231. DIC concentrations are visibly higher at equatorial Site 1225 and still higher at eastern equatorial Site 1226. Still higher DIC concentrations are present at the Peru shelf sites (1227, 1228, and 1229). The highest concentrations are present at Peru slope hydrate Site 1230, downslope of the shelf sites and directly beneath the Peru upwelling zone. Ammonium shows the same site-to-site progression as DIC. This site-to-site progression of increasing DIC and ammonium concentrations matches the progression of increasing cell concentrations seen in Figure F4. The similarity of these progressions suggests that subsurface cell concentrations are related to net subsurface microbial activity.

Leg 201 profiles of dissolved chemicals in interstitial waters also document the subseafloor occurrence of specific microbial processes. Despite the large apparent differences between net microbial activities of the ocean-margin sites and those of the open-ocean sites, all of the microbial processes that we inferred to occur in subsurface ocean-margin sediments also appear to occur in the subseafloor open-ocean sediments.

Downhole depletion of dissolved sulfate occurs at all of the Leg 201 sites (Fig. F8). The lowest magnitude of subseafloor depletion occurs at open-ocean Site 1231, where dissolved sulfate declines by <2 mM. The highest magnitude of subseafloor sulfate depletion occurs at the Peru slope hydrate Site 1230, where all of the sulfate diffusing downward from the seafloor disappears by 9 mbsf.

Concentration profiles of dissolved manganese (Fig. F8) and iron suggest that manganese and iron reduction also occur at all of the sites sampled during this cruise. Reduced manganese and iron are, respectively, products of manganese(IV) and iron(III) reduction. Consequently, concentration profiles of dissolved manganese and iron can be used to infer net manganese and iron reduction in subseafloor environments. Concentrations of dissolved manganese (Fig. F8) and iron are generally higher in the deeply buried open-ocean sediments than in the deeply buried ocean-margin sediments. By inference, manganese and iron reduction are overall more important for diagenesis in subseafloor open-ocean sediments. This finding is consistent with the general perception that manganese oxides and iron oxides are largely depleted at shallow sediment depths in shelf environments (Canfield et al., 1993).

Methane is a stable product of some microbial activities. It is a source of carbon and energy for other microbial activities. The presence of distinct minima and maxima in the subsurface profiles of dissolved methane at all Leg 201 sites indicates that methane is biologically created and destroyed in the subsurface realm of both the ocean-margin and open-ocean provinces (Fig. F9). Documentation of methane profiles at these open-ocean sites required Leg 201 scientists to develop new sam-

F6. Maximum DIC concentrations, Leg 201 sites, p. 64.

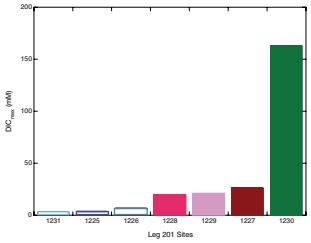

F7. DIC profiles, Leg 201 sites, p. 65.

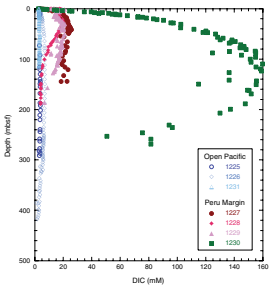

F8. Sulfate and manganese, Leg 201 sites, p. 66.

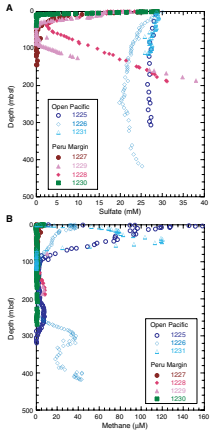

F9. Methane, Leg 201 sites, p. 67.

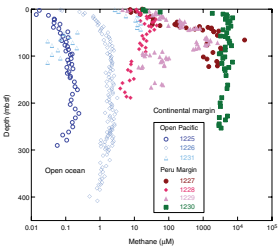

ple handling protocols and to accurately measure methane at extremely low concentrations. The discovery of methane at all Leg 201 sites strongly suggests that methanogenesis occurs in deeply buried sediments throughout the world ocean. This discovery builds on the recent observation that methane is commonly present in subseafloor sediments of the open ocean, despite the presence of high sulfate concentrations (D'Hondt et al., 2002). Unexpectedly, the Leg 201 studies also indicate that methanogenesis occurs in subseafloor realms of active manganese and iron reduction. This discovery echoes recent evidence that methanogenesis and iron reduction co-occur in the continental subsurface environment of a freshwater aquifer (Bekins et al., 2001). Even more unexpectedly, Leg 201 studies also showed that both ethane and propane are biologically created and destroyed in parallel with methane at both open-ocean and ocean-margin sites (see example from Site 1227 in Fig. **F10**).

Acetate and hydrogen are generally understood to be the most common products of microbial fermentation. They are also generally understood to be the most common energy sources in microbial respiration reactions. Consequently, they are expected to be key intermediates in subsurface microbial activities. Leg 201 studies showed that acetate, formate, and hydrogen are present throughout the subsurface environment at all sites. The properties that control subsurface concentrations of acetate, formate, and hydrogen, whether kinetic or thermodynamic, remain to be determined.

F10. Methane, ethane, and propane, Site 1227, p. 68.

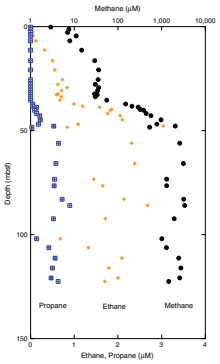

Influences of Subseafloor Flow and Brines on Microbial Activities and Sediment Chemistry Deep in the Sediment Column

Classic models of microbial activity in marine sediments assume that the oxidants (electron acceptors) that are used to support respiration by sedimentary prokaryotes are introduced to the sediment through the sediment/water interface. Sulfate is the most common electron acceptor in marine sediments. Oxygen and nitrate are the electron acceptors that yield the highest free energies. Sulfate, dissolved oxygen, and nitrate are all introduced to the subseafloor realm by diffusion from the overlying ocean. Leg 201 studies of open-ocean Sites 1225 and 1231 showed that nitrate and traces of oxygen also enter at least some deep-sea sediments by diffusing or advecting upward from waters flowing through the underlying basaltic crust (Fig. **F11**). In this manner, electron acceptors with high free-energy yields enter deep in open-ocean sediment columns. Conversely, downward diffusion from the sediment into the water flowing through the basement strips away products of microbial activity, such as methane, ammonium, and DIC. In both of these ways, chemical exchange between the sediment column and the underlying basement mirrors diffusive exchange across the sediment/ocean interface.

F11. Nitrate, Sites 1225 and 1231, p. 69.

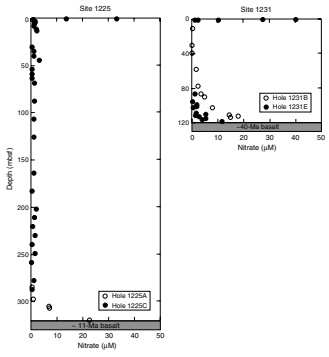

The discovery that nitrate and dissolved oxygen enter the sediment column from the formation waters of the underlying basalt has an additional interesting implication. It indicates that at least in some areas microbial activity within the basalt is insufficient to strip even the scarcest preferentially utilized electron acceptors from the water that flows through it.

At the Peru shelf sites, chemical species also enter the sediment sequences from below; however, at these sites, the chemicals diffuse up-

ward from underlying Miocene brine. At Site 1229, dissolved sulfate diffuses upward into methane-rich Pleistocene sediment. Downhole profiles of dissolved sulfate, methane, acetate, and barium show that chemical distributions at the lower (brine controlled) sulfate/methane interface mirror those of the overlying "normal" sulfate/methane interface (Fig. F12). Cell counts and the pronounced inflections in chemical profiles demonstrate that the subseafloor prokaryotic cell populations and activity are focused at the lower sulfate/methane interface. Dissolved barium profiles indicate that microbial activity at this lower interface directly influences sediment chemistry by causing the precipitation of barite immediately below the lower interface and the dissolution of barite immediately above it. Perhaps the most striking feature of this interface is its thousandfold increase in cell concentrations relative to the sediments that lie immediately above and below it (Fig. F12). The observed cell concentrations at this interface are an order of magnitude higher than the concentrations observed at the seafloor.

Effects of Past Oceanographic Conditions on Current Microbial Activities in Deep-Sea Sediments

In all of the sedimentary environments sampled during Leg 201, sedimentary properties and, by inference, past oceanographic conditions affect the current rates and sediment depths of several principal microbial activities. This point is most broadly demonstrated by the general correspondence between each site's geographic location (open ocean, equatorial upwelling, or coastal upwelling) and its current cell concentrations and concentrations of metabolic products (e.g., DIC and methane) (Figs. F5, F6, F7, F9).

At individual sites, the depths at which specific microbial activities are most pronounced are commonly directly related to sediment properties. These properties in turn were largely determined by oceanographic conditions at the time of the sediment's original deposition. For example, correspondences between dissolved iron concentration and magnetic susceptibility suggest that current subseafloor rates and foci of microbial iron reduction may be ultimately controlled by the availability of oxidized iron in mineral form. This relationship is illustrated at Site 1225, where the concentration of dissolved iron closely follows magnetic susceptibility (Fig. F13). At that site, the peak iron concentration is present in lithologic Subunit IC, where magnetic susceptibility is highest. These sediments were deposited during the middle–late Miocene "carbonate crash" of the equatorial Pacific (Farrell et al., 1995). Leg 201 magnetic reversal records suggest that the magnetic susceptibility of these sediments dates to the time of their original deposition. The overlying interval of near-zero magnetic susceptibility and very low dissolved iron concentration was deposited during the late Miocene "biogenic bloom" of the Indo-Pacific tropical ocean (Farrell et al., 1995).

Relationships between dissolved manganese concentrations, lithology, and physical properties similarly suggest that current rates and stratigraphic foci of microbial manganese reduction are contingent on oceanographic history. Such a relationship is seen at Site 1226, where the peak dissolved manganese concentration is present in the oldest sediments (Fig. F14). This sedimentary interval exhibits the lowest natural gamma radiation and, as shown by Leg 138 shipboard studies, the lowest average total organic carbon (TOC) concentration of this 16-m.y. sedimentary sequence (Shipboard Scientific Party, 1992a). This interval

F12. AODC and sulfate, barium, methane, and acetate, Site 1229, p. 70.

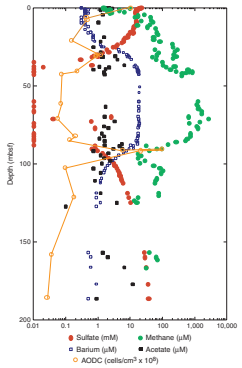

F13. Iron and magnetic susceptibility, Site 1225, p. 71.

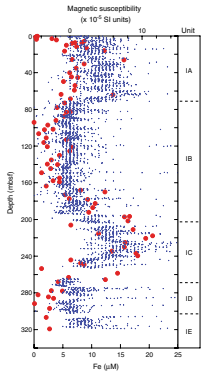

F14. Manganese and NGR, Site 1226, p. 72.

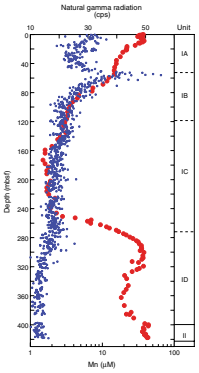

of low gamma radiation and low TOC was deposited at very slow rates over 8 m.y. (Shipboard Scientific Party, 1992a). The overlying interval of higher gamma radiation, higher TOC, and much lower dissolved manganese concentration was deposited during the late Miocene biogenic bloom (Shipboard Scientific Party, 1992a). These relationships suggest that manganese reducers now active in these sediments are utilizing oxidized manganese that accumulated during an interval of unusually low carbon accumulation from 8 to 16 m.y. ago.

Profiles of magnetic susceptibility and concentrations of dissolved iron, manganese, and sulfide suggest that current iron- and manganese-reducing activity may be similarly contingent on depositional history at the Peru shelf sites. For example, at Site 1229 the peak dissolved iron concentration and lowest dissolved sulfide concentration coincide with intervals of relatively high magnetic susceptibility at 87 mbsf and below 123 mbsf (Fig. **F15**). High magnetic susceptibility is present in intervals of terrigenous-dominated sediments deposited during intervals of low relative sea level. The peak iron concentration at 87 mbsf is within the well-developed methanogenic zone at this site (Fig. **F16**). The peak concentration below 123 mbsf lies within the underlying sulfate-reducing zone. In short, higher manganese and iron concentrations are consistently associated with relatively high susceptibility intervals at both open-ocean and ocean-margin sites. This association illustrates one way in which current rates and stratigraphic depths of an individual microbial process may depend on past ocean history.

At the Peru shelf sites, the lithologic context of anaerobic oxidation of methane (AOM) zones suggests another way that past ocean history may affect current microbial activity. At these sites, AOM and related processes predominantly occur in narrow subsurface zones that are associated with thin sedimentary intervals characterized by high grain density (Fig. **F17**), accompanied by high NGR, high resistivity, and low porosity. These thin low-porosity intervals are unusually rich in terrigenous sediment and are interpreted to have been deposited during times of low relative sea level. This lithologic association of AOM zones with high-density, low-porosity offlap sediments provides intriguing evidence that on the Peru shelf the position of AOM zones may be presently pinned within the sediment column by lithologic properties and, by extension, depositional history. More detailed determination of the extent to which physical and compositional properties control subseafloor biogeochemical zonations in this region will require further investigation.

A different aspect of the Peru shelf records provides evidence that geologically recent oceanographic changes may also affect the activity of subseafloor organisms at shallow burial depths. At Sites 1228 and 1229, a brief positive excursion in alkalinity, DIC, ammonium, and sulfide coincides with a brief negative excursion in dissolved sulfate at 2–3 mbsf (Fig. **F18**). This near-surface interstitial water anomaly indicates that the steady-state diffusion of biologically active chemicals past the upper sediment column was disrupted by late Pleistocene environmental change and has not yet fully recovered. There are at least three possible explanations for this anomaly. It may result from ongoing activity in a microbial "hotspot" at this shallow sediment depth, it may be a chemical relic of past microbial activity and is now relaxing back to a diffusional steady state, or it may be due to the recent establishment of an oxygen minimum at this water depth, causing the extinction of a bioirrigating benthos and a stimulation of sulfate reduction. The first

F15. Iron and magnetic susceptibility, Site 1229, p. 73.

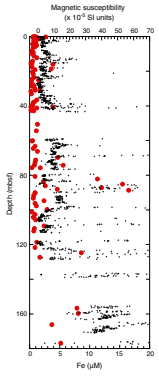

F16. Manganese, iron, and methane, Site 1229, p. 74.

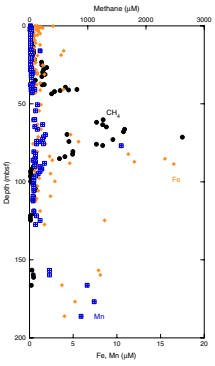

F17. Grain density, methane, and sulfate, Site 1227, p. 75

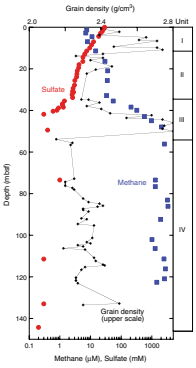

F18. Sulfate, Sites 1227, 1228, and 1229, p. 76.

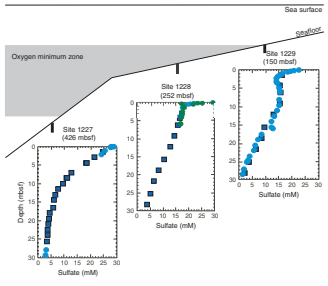

and third of these explanations imply that this anomaly is a fingerprint of current microbial activity.

Environmental Effects of the Subseafloor Biosphere

Chemical profiles of the Leg 201 sites provide consistent evidence of microbial influence on their sedimentary environment. This evidence is most clearly expressed at the ocean-margin sites, where microbial activity is highest. At these sites, the precipitation and dissolution of a number of minerals, including pyrite, barite, dolomite, and apatite, are catalyzed by microbial activities.

Dissolved barium, sulfate, and methane profiles provide a particularly clear illustration of the interplay between microbial activity and authigenic mineral formation and dissolution at these sites (1227, 1228, 1229, and 1230). The dissolved barium profiles at these sites are broadly similar to their methane profiles and are inversely related to their dissolved sulfate profiles (Fig. F19). The inverse relationship between sulfate and barium is inferred to be controlled by the solubility product of barite and the in situ activity of sulfate-reducing bacteria. Within the AOM zone, dissolved sulfate concentration declines toward 0 mM, barite dissolves, and the dissolved barium concentration rises. Diffusion of the dissolved barium past the AOM zone is suspected to sustain modern barite formation in the zone of dissolved sulfate. At sites with particularly high dissolved barium concentrations (such as Site 1230), a significant fraction of the sulfate diffusing toward the AOM zone may participate in this cycle of barite precipitation and dissolution before finally being reduced by microbial activity.

F19. Barium and sulfate, Site 1230, p. 77.

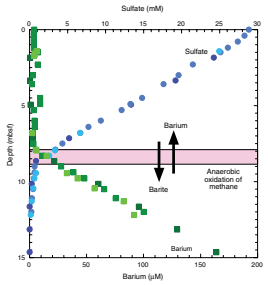

Structure of Subseafloor Microbial Communities

A broad range of microbiological studies was initiated during Leg 201 in order to study the diversity and population size of subsurface prokaryotic communities and to analyze the pathways and rates of their metabolic activities. These studies will not yield immediate results, partly because of the expected slow growth of deep subsurface prokaryotes and partly because the research requires special analytical equipment available only in shore-based laboratories.

A very large number of cultivation experiments and viable counts based on MPN methods were among the studies initiated on board. These cultivation experiments target a broad physiological spectrum of heterotrophic and autotrophic prokaryotes that utilize diverse electron acceptors and donors in their energy metabolism. Some experiments target chemoautotrophs using different electron donor/acceptor combinations. Others focus on heterotrophs using different electron acceptors for respiration. Others focus on methanogens and acetogens or fermenting or spore-forming prokaryotes. Still others target prokaryotes adapted to different monomeric or polymeric carbon sources, different temperature adaptations (psychrophilic, mesophilic, or thermophilic), and/or different pH, salinity, and pressure requirements. Some cultivation experiments focus on consortia depending on syntrophic degradation of organic substrates. Gradient cultures were initiated to screen for different substrate concentration requirements. Radiotracer MPN cultivations were inoculated for detection of minimal growth.

A wide range of other microbiological studies will be conducted postcruise. An extensive sampling scheme was developed for postcruise studies of prokaryotic populations using culture-independent molecu-

lar analyses. Molecular techniques based on 16S rRNA (ribosomal ribonucleic acid) gene sequence information will be used to analyze prokaryotic diversity and function. Sequence libraries for populations of different sediment depths and geochemical interfaces are expected to demonstrate differences related to the special conditions for life in the deep subsurface. Quantitative analyses of the prokaryotic communities will be done using, for example, FISH and real-time polymerase chain reaction. Secondary ion mass spectrometry (SIMS) will be used to analyze the stable carbon isotope composition of individual cells or cell clusters that are identified with nonspecific fluorescence stains or FISH probes. The potential metabolic activity of dominant members of these communities will be analyzed by sequencing functional genes for key enzymes, such as dissimilatory sulfite reductase and adenosine-5′-phosphosulfate reductase for bacterial sulfate reduction, coenzyme-M methyl reductase for methanogenesis, and formyl tetrahydrofolate synthase for acetogenesis. Finally, the carbon isotopic signature of biomarkers will be analyzed in order to identify the carbon substrate of the dominant prokaryotic populations.

It was an important goal of Leg 201 to identify and quantify the dominant microbial processes in the deep subsurface. To identify gross rates of microbial processes and rates that involve intermediate metabolites, experiments using radioactive tracers were conducted on the ship. Such use of radiotracers increases the sensitivity of process rate measurements by several orders of magnitude. The following microbial processes were analyzed at all relevant sites with samples from many depths and geochemical zones: sulfate reduction (^{35}S), methanogenesis (^{14}C) and acetogenesis (^{14}C), anaerobic methane oxidation (^{14}C), acetate (^{14}C) and hydrogen (^{3}H) turnover, and prokaryotic growth using thymidine (^{14}C) and leucine (^{3}H) incorporation. Most of these experiments were terminated by the end of the cruise. Their activities will be measured in shore-based laboratories after the cruise. The results of these experiments will be compared to net rates obtained by modeling of interstitial water chemical gradients.

Contamination Tests

The study of deep subsurface prokaryotic communities is highly dependent on rigorous contamination control. Contamination tests are necessary to assess the extent to which prokaryotes from the surface environment may have reached the microbiological sediment samples at any point. Contaminating prokaryotes may be introduced from drilling fluid during the coring operation, they may penetrate into cores from their contaminated periphery during the wireline trip, or they may be introduced during the subsequent sectioning and subsampling of sediment. Consequently, refinement of routine methods for testing and avoiding potential contamination was an important part of the microbiological work initiated during Leg 201 (see **House et al.,** this volume).

During the drilling operation at all sites, perfluorocarbon tracer (PFT) was fed in trace quantities into the seawater pumped through the drill string (Smith et al., 2000a, 2000b). This practice ensured that the core liner was bathed in a dissolved tracer that could later be analyzed at high sensitivity in retrieved cores and microbiological samples. The quantity of PFT detected in a sample provided an estimate of the maximal amount of seawater introduced into that sample. The PFT provides an upper-bound estimate of prokaryotic contamination, as it may penetrate by molecular diffusion through pore space inaccessible to prokary-

otes. To further evaluate the extent to which contaminating prokaryotes may have penetrated into a sample, fluorescent beads of approximate prokaryotic cell size were applied as an additional contamination tracer. A suspension of >10^{11} 0.5-µm-sized beads was released in the core cutting shoe at the critical moment of impact against the sediment. Microscopic counts of beads subsequently indicated whether samples used for microbiology had become "infected." This test may be more realistic with respect to the possibility of prokaryote-sized particles penetrating a sediment core. However, it is rather qualitative because the beads are not uniformly delivered to all surfaces of the core. Taken together, the two approaches provide a critical test on which to base confidence as to the noncontaminated nature of microbiological samples.

A summary of the extensive contamination tests for all Leg 201 sites is given in Figure F20 (this figure is based on the uncorrected data set and may include data points that were discarded as unreliable later [Site 1225]), which shows PFT and bead concentrations observed in selected samples. The two contamination indicators are positively correlated, thus improving confidence in the prediction of potential contamination by their combined use. The subset of samples presented in Figure F20 was chosen to reflect the wide range of tracer results observed during Leg 201. Out of the 154 PFT tests conducted on sediment samples, 62% had <0.1 µL seawater/g sediment potential contamination and 16% had no detectable contamination (<0.01 µL seawater/g sediment potential contamination). Out of 22 bead tests performed at all sites, >50% had no detectable beads. The centers of the cores, which were used for microbiological sampling, were compared to the periphery in contact with the core liner. The results show that core centers are much less contaminated than core peripheries (see House et al., this volume). Advanced hydraulic piston corer (APC) cores generally show far less potential contamination than the "biscuits" of sediment retrieved in extended core barrel (XCB) cores. The large scatter in all data shows that potential contamination is highly irregular from sample to sample. Consequently, contamination tests must be conducted specifically on the same sample that is used for a microbiological experiment in order to judge its contamination potential. It is not sufficient to rely on general experience with a specific coring/sampling technique or sediment type or to examine a sample from a different core portion.

Samples specifically used for isolations and viable bacterial counts during Leg 201 were generally proven by both PFT and bead tests to have very low or undetectable contamination. Through the extensive experience gained during the cruise, our confidence has strengthened that, with rigorous contamination controls and aseptic sampling techniques, deep subsurface samples can routinely be obtained without the introduction of microorganisms from the surface environment.

F20. PFT and bead contamination tests, p. 78.

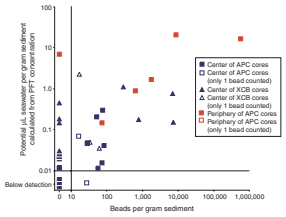

SITE SUMMARIES

Open-Ocean Sites

Peru Basin Site 1231

Background and Objectives

Site 1231 was selected for drilling in order to study the microbial activities and communities of the organic-poor sediments that character-

ize much of the world's open ocean. Before drilling at Site 1231, the nature of subseafloor microbial communities in open-ocean clays had never been assessed.

The principal objectives at this site were

1. To test by comparison with other sites drilled during this expedition whether microbial activities, microbial communities, and the nature of microbe-environment interactions are different in very organic-poor open-ocean sediments than in the more organic-rich sediments of the equatorial upwelling region and the coastal upwelling region and
2. To document the microbial activities, communities, and environmental context of an expanded manganese-reducing zone in very organic poor, relatively deeply buried marine sediments.

Site 1231 is in the Peru Basin at 4827 m water depth. The lithologies, age, and many geochemical characteristics of the targeted sediments were characterized by Leg 34 studies at nearby Site 321 (Shipboard Scientific Party, 1976). The total sediment thickness at Site 321 is 115 m. The sediment is composed of 58 m of late Oligocene to Holocene clay and 57 m of iron-rich late Eocene to early Oligocene nannofossil ooze (Shipboard Scientific Party, 1976). The lower 50 m of sediment at Site 321 is rich in iron and manganese (Dymond et al., 1976). Iron and manganese accumulation rates estimated for the sediments present below 49 mbsf are about an order of magnitude higher than those estimated for sediments above 49 mbsf (Boström et al., 1976). In analyses of six interstitial water samples, dissolved manganese was present at relatively higher concentrations in the upper 45 m of the sediment column (3.5–7.4 ppm) than in the lower 50 m (0–1 ppm) (Brady and Gieskes, 1976). Dissolved sulfate concentrations also appeared to be slightly higher in the upper 45 m (>28 mM) than in the lower 50 m (27 mM) (Brady and Gieskes, 1976). Little or no evidence for other postdepositional reactions was seen among major dissolved ions at Site 321. This finding led Brady and Gieskes (1976) to conclude that any reactions in these sediments occur at such slow rates that their chemical signature is annihilated by diffusional exchange with the top and bottom of the sediment column. Consequently, Site 1231 provided a challenging opportunity for assessing the microbial activities and communities of low-activity sediments typical of much of the open ocean.

The subsurface extent of key electron donors (hydrogen, acetate, and formate), electron acceptors with standard free-energy yields greater than that of sulfate (oxygen and nitrate), products of key metabolic reactions (dissolved iron), and other biologically important chemicals was not determined for Site 321.

Principal Results

At Site 1231, the DIC profile hovers slightly at or below 3.3 mM for most of the sediment column. It exhibits three slight exceptions to this relative constancy: it slightly increases from 2.8 mM near the sediment/water interface, it exhibits a small peak of ~3.7 mM centered at 55 mbsf, and it declines slightly to ~3.0 mM at the sediment/basement interface. These DIC concentrations are even lower than those at Site 1225 (3.0–4.0 mM). They are much lower than the DIC concentrations observed at the other Leg 201 sites. Dissolved ammonium concentrations are also generally lower at Site 1231 than at the other Leg 201 sites. As at Site 1225, concentrations of DIC, ammonium, and alkalinity peak in the

middle of the sediment column and decline toward both the sediment/ocean interface and the sediment/basement interface. The relatively low variability in the concentration profiles of these chemical species suggests that net microbial activity is lower at Site 1231 than at any other Leg 201 site. The midcolumn peaks in these profiles and their relatively low values near both the sediment/water and sediment/basement interfaces indicate chemical exchange from the sediment to the ocean and from the sediment to the basement.

The dissolved sulfate concentrations are >28 mM at the sediment surface and decrease linearly to 27 mM near the basement. The slight total downhole decrease in sulfate concentrations suggests that Site 1231 is characterized by lower sulfate-reducing activity than all of the other Leg 201 sites. Dissolved sulfide ($\Sigma H_2S = H_2S + HS^-$) is below the detection limit (0.0002 mM) throughout the entire sediment column.

Electron acceptors with higher standard free-energy yields than sulfate are present throughout most of the sediment column at Site 1231. Dissolved nitrate appears to be present in the uppermost meter and the lowermost 60 m of the sediment column (where it ranges from ≥15 µM at 114 mbsf to 2 µM at 77 mbsf). Dissolved oxygen similarly appears to be present in the top 0.6 m below the seafloor as well as the last 3.8 m of sediment above basaltic basement. The diffusion of oxygen and nitrate from the overlying ocean down into the sediment is readily predictable from deep-ocean chemistry. However, the first Leg 201 locations, Sites 1225 and 1226, provided the only previous precedent for upward transport of nitrate (and, at Site 1225, oxygen) into deeply buried sediment from the underlying basaltic crust. As at Site 1225, the introduction of dissolved nitrate high into the sediment column at Site 1231 indicates that nitrate-utilizing microbial activity is present but may proceed at a very low rate in the site's lowermost sediments. Also as at Site 1225, the presence of dissolved oxygen and nitrate in these deepest sediments suggests that microbial activity in the underlying basalt is insufficient to strip even the scarcest preferentially utilized electron acceptors from the water that flows through the basalt.

Dissolved manganese is present from 1 to 65 mbsf at Site 1231. Concentrations steadily rise from ~17 µM at 1.4 mbsf to a local peak of 78 µM at ~17 mbsf, decline briefly by a few micromolar, and then rise to sustain the highest concentration of 120 µM from 36 to 46 mbsf. Manganese concentrations below this peak steadily decline to essentially 0 µM at 68 mbsf. A relatively broad zone of generally high but variable dissolved iron concentrations (7–36 µM) spans the interval from 1 to 30 mbsf. A very small secondary peak in dissolved iron (5 µM) is centered near 74 mbsf. Two aspects of these broad patterns run counter to the general expectation that manganese reduction occurs at shallower depths than iron reduction in marine sediments. The first aspect is the broad co-occurrence of dissolved iron and manganese from 1 to 30 mbsf. The second aspect is the presence of the maximum dissolved iron concentration much closer than the maximum dissolved manganese concentration to the sediment/water interface. It appears likely that rates of manganese reduction in these sediments are limited by the availability of manganese oxides that supply dissolved manganese. Rates of iron reduction may be similarly limited by the presence and solubility of the minerals that supply dissolved iron.

As at other Leg 201 sites, the downhole distribution of microbial manganese and iron reduction at Site 1231 appears to be ultimately determined by lithology and depositional history. The peak intervals of dissolved manganese production are limited to the clays that lie be-

tween 11 and 55 mbsf. The maximum manganese concentration (120 µM) is present in the yellow volcanic-rich clay of Subunit IIA (31–44 mbsf). The secondary peak (78 µM) is centered in the green diatom-rich clay of Unit I (11–30 mbsf). Dissolved iron is similarly limited to the clay-rich portions of the upper sediment column. It exhibits a sharp maximum concentration (36 µM) a few meters below the seafloor in the radiolarian- and clay-rich diatom ooze of upper Unit I (0–11 mbsf). Most of the dissolved iron at Site 1231 is present in a broad maximum of 26 µM in the green clay of Unit I. Dissolved iron concentrations are consistently ≤5 µM in the nannofossil oozes that lie between 55 mbsf and the basaltic crust (114 mbsf). Dissolved manganese is consistently <1 µM over the same interval.

Although Site 1231 may be the microbially least active of the Leg 201 sites, its sediments still contain methane at concentrations of up to 15 µM. At this site, methane is limited to the upper clay-rich portion of the sediment column between 0 and 42 mbsf. This methane-bearing interval is completely within the interval of high dissolved manganese concentrations. Interestingly, this methane was only detected after prolonged incubation of headspace samples over a couple of days, whereas short 20-min incubation according to the standard ODP safety protocol showed only trace methane concentrations throughout the sediment column. The appearance of methane over time is currently interpreted as a release of sorbed methane. From sediments below 42 mbsf, no release of sorbed methane was observed and the concentrations remained at trace levels of <0.2 µM. The relationship of this sorbed methane to current microbial activity remains unknown.

Acetate concentrations range between 1 and 14 µM at Site 1231. Formate varies between 1 and 19 µM. Concentrations of both fatty acids are lowest in the top 3 m below seafloor (1–2 µM). They are slightly higher (3–6 µM) in the nitrate-reducing zone that spans the last 50 m above basement. Acetate and formate exhibit their highest concentrations (4–14 µM and 9–19 µM, respectively) at intermediate sediment depths (25–75 mbsf and 25–80 mbsf, respectively). These broad patterns suggest that at Site 1231 fatty acid concentrations may be lower in the sedimentary intervals that include electron acceptors with the highest energy yields. Curiously, the acetate and formate concentrations at this site are generally an order of magnitude higher than concentrations in sediments of the equatorial Pacific sites but are similar to those found at the Peru margin sites and in other very active coastal marine sediments. As noted in the site chapters, accurate understanding of the fatty acid distribution and its microbial relevance will require thorough postcruise analyses of microbial energetics in subseafloor environments.

Hydrogen concentrations are extremely high in the uppermost 35 m of the sediment column, with a peak value of 102 nM at 15 mbsf. This is the highest hydrogen concentration measured at any Leg 201 site. It exceeds the hydrogen concentration of near-surface iron-reducing sedimentary environments by >100-fold. The zone of high hydrogen coincides with the zone of iron reduction but does not show any direct correlation with distributions of fatty acids or methane. The presence of extremely high hydrogen concentrations at the site with the lowest organic carbon mineralization rates remains unexplained at this point. From 44 mbsf down to the basaltic basement, hydrogen concentrations are, in contrast, very low (0.05–0.22 nM).

Prokaryotic cell counts were conducted on samples from throughout the sediment column at Site 1231. These data show that mean cell concentrations are generally lower at this open-ocean site than at any pre-

viously enumerated ocean drilling site. Cell concentrations exhibit a distinct local concentration peak at 10–15 mbsf, the approximate depth of the Unit I zone of iron and manganese reduction.

Experiments on major microbial processes and on enumeration of viable prokaryotes were initiated at selected depths ranging from near the seafloor to the bottom of the drilled sediment column. The studied processes include methane and acetate formation and consumption, sulfate reduction, hydrogen oxidation, and rates of cell growth. The cultivation experiments include selective growth conditions for a wide range of autotrophic and heterotrophic prokaryotes ranging from psychrophilic to thermophilic. Cultivation experiments particularly focused on manganese- and iron-reducing bacteria throughout the column. Studies of sulfate-reducing bacteria in macrofaunal burrows were also initiated. Detailed microbiological sampling targeted sediment depths of particular biogeochemical interest, such as the midcolumn reduced manganese interface and the sediment/basalt interface.

The results from six Adara tool deployments define a temperature profile composed of two distinct intervals: a linear gradient of 90°C/km from 0 to 55 mbsf and a linear gradient of 35°C/km from 55 to 115 mbsf. The sediment/water interface temperature measured by a mudline Adara tool deployment is 1.7°C. The estimated temperature at the base of the drilled sediment column (115 mbsf) is 8.6°C. Throughout the entire drilled interval (0–121 mbsf), temperatures are in the psychrophilic range.

Trials were undertaken of two experimental tools at this site: the Davis-Villinger Temperature-Pressure Probe (DVTP-P) and the catwalk infrared (IR) camera. The single DVTP-P deployment indicated minor overpressure at 108 mbsf.

Equatorial Upwelling Sites

Site 1225

Background and Objectives

Sites 1225 and 1226 were selected as drilling targets because their microbial activities and cell counts were expected to be far below those in ocean-margin settings but above those in the lowest-activity open-ocean environments.

The principal objectives at Site 1225 were

1. To test by comparison with other sites drilled during this expedition whether microbial communities, activity, and survival strategies are different in this deeply buried, organic-poor environment than those in open-ocean sediments with more organic matter or shallower burial and
2. To examine how hydrologic flow in the underlying basement affects microbial communities, microbial activities, and microbial influence on environmental properties in organic-poor sediments with sulfate-rich interstitial waters.

Site 1225 is located in the eastern equatorial Pacific near the present-day boundary between the South Equatorial Current and the North Equatorial Countercurrent at 3760 m water depth. It lies in the sedimentary bulge created by the rain of biogenic debris from the relatively high productivity equatorial ocean. Geochemical studies of DSDP and ODP sites throughout this region have shown that seawater flows through the

basaltic basement that underlies the sediments throughout this region (Baker et al., 1991; Oyun et al., 1995). Anomalously low conductive heat flow occurs throughout the region (Von Herzen and Uyeda, 1963; Sclater et al., 1976), possibly because the large-scale flow of relatively cool seawater through the basalts depresses conductive heat flow (Oyun et al., 1995).

The lithologies, sediment age, and many geophysical characteristics of the target site were well characterized by earlier studies of nearby Site 851 (Mayer, Pisias, Janecek, et al., 1992; Pisias, Mayer, Janecek, Palmer-Julson, and van Andel, 1995). Those studies indicated that the site is representative of a large portion of the eastern equatorial Pacific region. The sediments of Site 851 have a continuous biostratigraphy with a minimal age of 11 Ma at the basaltic basement. The gross lithologic and physical properties of the carbonate and siliceous oozes and chalk at Site 851 are characteristic of sediments throughout the region (Mayer, Pisias, Janecek, et al., 1992). The interstitial water chemical profiles at Site 851 exhibit clear evidence of seawater flow through the underlying basalts (and perhaps the lower part of the sediment column) (Oyun et al., 1995; Spivack and You, 1997).

Cragg and Kemp (1995) documented the presence of prokaryotic cells and activity throughout the sediment column at Site 851. For the first few tens of meters below seafloor, counts of both total cells and dividing cells were low relative to counts from similar depths at sites from the Peru shelf and the Japan Sea (Cragg and Kemp, 1995). At greater depths, Site 851 cell counts approached the averaged values from all previously counted sites.

Leg 138 shipboard chemistry showed that concentrations of several dissolved chemical species (ammonium, strontium, and silica) and alkalinity peaked midway down the sediment column. In contrast, dissolved sulfate exhibited maximum values near the sediment/water interface and the basement/sediment interface (Mayer, Pisias, Janecek, et al., 1992). These patterns of sedimentary interstitial water concentration are inferred to result from low levels of biological activity throughout the sediment column, coupled with diffusive exchange with the overlying ocean and with water flowing through the underlying basalts (and perhaps the lower part of the sediment column) (Spivack and You, 1997). Geochemical modeling suggests that net microbial sulfate reduction in the upper half of the Site 851 sediment column corresponds to a respiration rate of 10^{-9} to 10^{-8} mol CO_2/cm^2/yr (D'Hondt et al., 2002). This rate of respiration is only the barest fraction of the rate of carbon dioxide reduction by photosynthesis in the overlying equatorial ocean (10^{-3} mol/cm^2/yr) (D'Hondt et al., 2002). The subsurface distribution of electron acceptors with higher standard free-energy yields (oxygen, nitrate, manganese oxide, and iron oxides) in this region was not determined for Site 851.

Principal Results

At Site 1225, concentrations of methane, ammonium, DIC, and alkalinity peak in the middle of the sediment column and decline toward both the sediment/ocean interface and the sediment/basement interface. In contrast, sulfate concentrations are lowest in the middle and lower part of the sediment column and nitrate and dissolved oxygen are present only at the ocean and basement interfaces. These profiles result from the balance between net subsurface microbial activities and small net fluxes of biologically utilized chemicals across the ocean/sediment and sediment/basement interfaces.

Interstitial water data also document dissolved oxygen penetration into the top 2 m of the sediment column, an interval containing nitrate in the top 1.5 m of the sediment, a peak concentration of dissolved manganese at 3.6 mbsf, a broad zone of relatively high dissolved iron centered at ~25 mbsf, and sinks for reduced manganese and dissolved iron at 100 mbsf. Sulfate concentrations decrease downhole by only ~7% from local bottom-water values; most of this decrease occurs in the upper ~60 m. This vertically extended sequence of successive interstitial water chemical zones closely resembles the centimeter- to decimeter-scale sequence seen in nearshore sediments (with depth-dependent transitions from a zone of oxygen reduction to successive zones of nitrate, manganese oxide, iron oxide, and sulfate reduction). These data are consistent with the hypothesis that subseafloor microbial communities preferentially utilize the available electron acceptor that yields the highest free energy of reaction.

In the lower portion of the sediment column, this vertical sequence of successive reduction zones is reversed as a result of water flow through the underlying basaltic basement. Diffusion of solutes from this basement water to the overlying sediment delivers nitrate to the lowermost 20 m of the sediment column (300 mbsf to basement) and possibly also dissolved oxygen to the lowermost meter of the column (319.3 mbsf to basement). This short interval of dissolved oxygen and nitrate is overlain by a broad zone of dissolved manganese centered near 250 mbsf and a broad peak of dissolved iron centered at ~230 mbsf. These dissolved nitrate and oxygen profiles show that electron acceptors yielding high free energies of reaction are introduced to at least some portions of the deep subseafloor biosphere by hydrologic processes. They also indicate that microbial activity in the underlying basalt is insufficient to strip even the scarcest preferentially utilized electron acceptors from the seawater that flows through the basalt at this site.

Dissolved hydrogen concentrations in incubations of Site 1225 sediments are generally in the range of 1–2 nM. Lovley and Goodwin (1988) and Hoehler et al. (2001) observed similar concentrations in experiments with near-surface aquatic sediments where sulfate reduction is the primary electron-accepting reaction. On the basis of their observations, Lovley and Goodwin (1988) hypothesized that hydrogen concentrations in aquatic environments are controlled by competition between different metabolic pathways. According to this hypothesis, prokaryotes using electron acceptors that yield higher free energies of reaction are able to operate at lower electron donor concentrations and thereby out-compete prokaryotes limited to electron acceptors that yield lower free energies of reaction. Documentation of these concentrations at Site 1225 suggests that even in low-activity subseafloor sediments, hydrogen concentrations may be controlled by the same thermodynamic competition between electron-accepting pathways as in high-activity sediments and can be predicted from the dominant pathway.

Methane is present at trace concentrations of <0.25 µM throughout the sediment column. This finding demonstrates the presence of methane in subseafloor sediments with sulfate concentrations that are very close to seawater values. The generation of methane in these sediments challenges models of microbial competition that are based on standard free energies. There are a number of possible reasons for the occurrence of methanogenesis in sulfate-rich sediments. For example, the methanogens and sulfate reducers may rely on different electron donors (e.g.,

the methanogens may utilize methylated amines and the sulfate reducers may rely on hydrogen and/or acetate) (Oremland and Polcin, 1982; Oremland et al., 1982b; King, 1984).

The steady-state maintenance of methane in the subseafloor sediments of Site 1225 indicates that if anaerobic methanotrophy occurs here, it does not drive methane concentrations below a few hundredths to tenths of micromolar. Concentrations are lowest near the sediment/ocean and sediment/basement interfaces, where methane may be oxidized by prokaryotes using electron acceptors that yield relatively high energies of reaction (such as nitrate or dissolved oxygen). The highest methane concentrations are present in the middle of the sediment column, where sulfate appears to be the principal terminal electron acceptor available. We hypothesize that the peak methane concentrations are held at the observed level (~0.15–0.25 µM) because sulfate-reducing methanotrophs cannot oxidize methane at lower concentrations under in situ conditions.

Concentrations of acetate and formate were <1 and <0.5 µM, respectively, throughout the sediment column. These concentrations are an order of magnitude lower than those measured in continental shelf sediments (Sørensen et al., 1981; Wellsbury and Parkes, 1995) and are also lower than in other deep sediment sites (Wellsbury et al., in press). These very low concentrations may be regulated by limiting energy yields or limited by the kinetics of active uptake by the anaerobic respiring prokaryotes. Since these results are among the first to demonstrate very low concentrations of short-chain fatty acids in cold, low-activity subsurface sediments, there is no database for comparison.

Comparison of Site 1225 physical property, sedimentology, and chemical records suggests that broad-scale patterns of past oceanographic change exert strong influence on present subseafloor metabolic activity. Concentrations of dissolved iron closely follow downhole variation in magnetic susceptibility and split-core reflectance, with peak concentrations of dissolved iron and solid-phase iron compounds (inferred from magnetic susceptibility) in the intervals from ~0 to 70 mbsf and 200 to 270 mbsf. The intact magnetic reversal record suggests that the magnetic phases were created during or shortly after sediment deposition. These intervening sediments are low in dissolved iron, are low in magnetic susceptibility, are characterized by the most intensely bioturbated intervals, and were deposited during a late Miocene–early Pliocene biogenic bloom that occurred throughout much of the global ocean (van Andel et al., 1975; Farrell et al., 1995; Dickens and Owen, 1999).

Four Adara tool deployments plus two deployments of the Davis-Villinger Temperature Probe (DVTP) defined a sediment/water interface temperature of 1.4°C and an estimated sediment/basement interface temperature of 7.0°C. The downhole temperature gradient curved slightly downward. The slight curvature appears to be best explained by a geologically recent decrease in basement temperature, perhaps a result of an increased rate of seawater flow through the basement. Throughout the sediment column, in situ temperatures were well within the range inhabited by psychrophilic prokaryotes.

Experiments on major microbial processes and experiments for enumeration of viable prokaryotes were initiated at selected depths ranging from near the mudline to near the basement, where samples were obtained within centimeters of the basalt. Subsamples for postcruise biomolecular assays and microbiological experiments were routinely taken from all of the distinct geochemical zones and lithologic subunits. Total

cell numbers were enumerated on board. These cell counts are very close to data obtained from nearby Site 851 and consequently demonstrate the high reproducibility of AODC tests in subseafloor microbial studies.

At this site, novel experiments with core temperatures and contamination tracers were undertaken to determine how handling of cores and samples for microbiological studies might be improved. Catwalk experiments with an IR camera were used to assess the effects of different core handling procedures on transient warming of the core and, consequently, on the survival of temperature-sensitive prokaryotes.

Site 1226

Background and Objectives

Site 1226 was selected as a drilling target because its microbial activity was expected to be intermediate between that in ocean-margin settings and that in the lowest-activity open-ocean environments.

The principal objectives at this site were

1. To test by comparison with other sites drilled during this expedition whether microbial communities and activities are different in this deeply buried environment than in open-ocean sediments with less organic matter and shallower burial;
2. To document the conditions under which methanogenesis occurs in sulfate-rich open-ocean sediments; and
3. To test how basement hydrologic flow affects microbial communities, microbial activities, and microbial effects on environmental properties in the sediments that overlie the basement.

Site 1226 (3297 m water depth) is located in the eastern equatorial Pacific, 300 km south of the Galapagos Islands, near the present-day boundary between the South Equatorial Current and the Peru Current. Near the sea surface in this region, the advection of water from the Peru Current results in relatively high nutrient levels and biological productivity (Chavez and Barber, 1987). According to its calculated backtrack path, this site has drifted eastward but has remained near its present latitude for most of its history (Pisias et al., 1995; Farrell et al., 1995). Sediment thickness at Site 1226 is 420 m. The oldest sediments immediately overlie basaltic basement and have a biostratigraphic age of 16.5 Ma (Shipboard Scientific Party, 1992a). As described in **"Principal Results,"** p. 23, in "Site 1225," geochemical studies of DSDP and ODP sites throughout this region have shown that seawater flows through the underlying basaltic basement (Baker et al., 1991).

The lithology, sediment age, and many geochemical and geophysical characteristics of the target site were well characterized by earlier studies of Site 846. The gross lithologic and physical properties of the carbonate and siliceous oozes and chalk at Site 846 are characteristic of sediments throughout the region (Shipboard Scientific Party, 1992a; Pisias, Mayer, Janecek, Palmer-Julson, and van Andel, 1995). Leg 138 studies showed that the region has undergone large variations in sediment accumulation over the course of its history. Accumulation of calcium carbonate and opal was unusually low at Site 846 during the Miocene "carbonate crash" of 11–7.5 Ma and was unusually high during the widespread Indo-Pacific "biogenic bloom" that occurred from ~7 to 4.5 Ma (Farrell et al., 1995). The organic carbon accumulation rate is

presently high and appears to have gradually increased throughout the Pleistocene (Shipboard Scientific Party, 1992a; Emeis et al., 1995).

Leg 138 shipboard chemical studies of Site 846 show that concentrations of several dissolved chemical species (methane, ammonium, strontium, and silica) and alkalinity peak part way down the sediment column. In contrast, dissolved sulfate, lithium, and calcium exhibit maximum values near the sediment/water interface and the basement/sediment interface (Shipboard Scientific Party, 1992a).

As at Sites 851 and 1225, these patterns of sedimentary interstitial water concentration are inferred to result from modest levels of biological activity throughout the sediment column, coupled with diffusive exchange with the overlying ocean and with seawater flowing through the underlying basaltic basement. The sediments of Site 846 have a higher organic carbon content than the sediments of Sites 851 and 1225. Organic carbon content at Site 846 ranges from 0.2% to 1.0% and is highest in the Pleistocene and upper Pliocene deposits. Accordingly, Site 846 exhibits steeper gradients than Sites 851 and 1225 in interstitial water chemical species that respond to prokaryotic mineralization processes, such as sulfate, ammonium, and methane. The distinctly higher concentrations of methane at Site 846 than at Site 851 are particularly intriguing because methanogenesis is generally understood to be suppressed by sulfate-reducing bacteria and methane may be oxidized in the presence of sulfate.

The subsurface distribution of key electron donors (hydrogen, acetate, and formate) and of electron acceptors with higher standard free-energy yields (oxygen, nitrate, manganese oxide, and iron oxides) was not determined for Site 846.

Principal Results

Site 1226 provides an excellent series of samples from the sediment/water interface down to basement, including good cores from the contact zone between sediment and basalt. The geochemical gradients that span the 420-m-thick sediment column are bounded at the sediment/seawater interface and the sediment/basement interface by comparable but opposite reduction-oxidation (redox) zonations. Sulfate reduction appears to be the predominant electron-accepting pathway at this site. A broad maximum of DIC and ammonium in the interstitial water demonstrates the mineralization of organic material throughout the sediment column at several-fold higher rates than at Site 1225. Concentrations drop steeply to near-seawater values at the sediment/water interface and less steeply toward seawater values at the contact with basement. Water flow through the basement thus provides an effective sink for sedimentary metabolic DIC.

As at Site 1225, the overall chemical zonations are consistent with thermodynamic control of electron acceptor use by subsurface prokaryotes. The data show that water flow through the underlying basaltic basement introduces electron acceptors with high free-energy yields to sediment hundreds of meters below the seafloor. Relative to Site 1225, however, these zonations are more compressed because of higher rates of prokaryotic activities. Oxygen was not detected at any sediment depth within the column at Site 1226, and any oxic surface layer of sediment must thus have been closer to the ocean interface than the depth of our first dissolved oxygen measurement in Hole 1226B, in Section 201-1226B-1H-1, 10 cm. Nitrate, however, was detected in core sections nearest to the sediment/water and sediment/basement interfaces. As at Site 1225, nitrate diffuses upward into the overlying sediment from wa-

ter flowing through the basement. However, at Site 1226 the diffusing nitrate barely penetrates into the sediment column before being reduced.

As the next electron acceptor in the classical redox sequence, the interstitial water distribution of manganese shows a more complex pattern. Dissolved manganese peaks just at the sediment/water interface and again 9 m below, followed by a steep drop to a zone of near-zero concentrations between 100 and 250 mbsf. Yet another distinct peak in manganese is present at 300 mbsf. At the bottom of the sediment column, manganese peaks again between 400 mbsf and the sediment/basement interface. The near-basement peak and the 300-mbsf peak together define a broad 160-m interval of unusually high dissolved manganese concentrations.

Comparison with the Leg 138 *Initial Reports* data indicates that the most deeply buried interval of high dissolved manganese is composed of hydrothermally influenced sediments immediately above the basement. The 300-mbsf peak is present in sediments that were deposited at low rates during the Miocene "carbonate crash." In contrast, the sediments that define the overlying interval of near-zero dissolved manganese concentrations were deposited at high rates during the 7- to 4.5-Ma "biogenic bloom" that occurred throughout much of the world ocean (Farrell et al., 1995). These results suggest that the availability of electron-accepting pathways to current subseafloor activity directly depends on broad-scale patterns of past oceanographic change. More detailed interpretation of these multiple zones of apparent manganese reduction and oxidation must await further solid-phase and interstitial water chemical analyses.

The zone of dissolved sulfide extends from just 5 m below the sediment/water interface to a depth of 280 mbsf, and the broad peak reaches 0.7 mM at ~100 mbsf. Throughout this sulfidic sediment column, iron is <10 µM but displays narrow peaks of ~40 µM just above and below the sulfide zone. This pattern reflects both the low equilibrium concentration of ferrous iron in sulfidic interstitial water and the presence of reducible iron near the sediment surface and in the deep sediment column, including a third iron peak at 380 mbsf. The interstitial water data identify a sink for both sulfide and manganese within an interface at 250–280 mbsf, where manganese may precipitate with sulfide.

Methane exhibits a broad peak at 100–250 mbsf with concentrations of 2–3 µM. Although this is still a trace level of biogenic methane, it is more than tenfold higher than at Site 1225. Sulfate is present at >80% of seawater concentration throughout the sediment column and indicates active sulfate reduction over the entire methane peak. The coexistence of methane and sulfate at these levels demonstrates the ability of methanogens to maintain an active metabolism in a high-sulfate environment where competition for energy substrates must be strong and where the methanogens may be limited to noncompetitive substrates (Oremland and Polcin, 1982; Oremland et al., 1982b). The results also show that sulfate-reducing bacteria in this environment are apparently unable to exploit methane beyond the existing low concentration.

Acetate and formate concentrations are low in the upper 0–100 m of sediment (<0.5 µM). At greater depths, their concentrations increase to 1–3 µM. This shift in concentrations appears to result from regulation mechanisms that are not yet understood for any sedimentary environment. The volatile fatty acids (VFAs), acetate and formate, are known to be important substrates for most anaerobic respiring bacteria and for

methanogens (Winfrey and Ward, 1983; Wellsbury and Parkes, 1995). The interstitial water concentrations of these intermediate fermentation products are regulated by a balance between production and consumption. Concentrations of both acetate and formate are usually found to be relatively higher in organic-rich marine sediments, where they appear to be a function of the rate of fatty acid production and of the energy-yielding metabolism of the consumers. For example, sulfate reducers are able to outcompete methanogens in their efficiency of substrate uptake and thereby drive acetate and formate concentrations to lower levels. However, control of VFA concentrations by such competition is difficult to reconcile with their increased concentrations in the deeply buried Site 1226 sediments that exhibit high dissolved manganese and iron concentrations.

Hydrogen was very low in incubated sediment samples from Site 1226, ranging from 0.1 to 0.8 nM. This is below the equilibrium concentration of a few nanomolar measured in the sulfate reduction zone of more active nearshore sediments (Hoehler et al., 1998) and is even below the concentrations measured at Site 1225, where prokaryotic activity is significantly lower than at Site 1226. According to theoretical calculations of the minimum energy yield required for prokaryotic respiration (Thauer et al., 1977; Schink, 1997) and also according to hydrogen data from a range of sedimentary environments, equilibrium concentration of hydrogen is maintained at the lowest limit that provides the lowest required energy yield of the hydrogen-metabolizing prokaryotes (Hoehler et al., 2001). Based on the dissolved sulfate, manganese, and iron data, sulfate reduction is the predominant respiration process throughout most of the sediment, with the other electron acceptors gaining relative significance near the top and bottom of the sediment column. However, the Site 1226 hydrogen incubation concentrations are lower than those in surface sediments, where sulfate reduction is the predominant process. This finding suggests that either the Site 1226 sulfate-reducing communities derive the canonical minimum energy yield at lower hydrogen concentrations than surface sulfate-reducing communities or they utilize hydrogen at energy yields below the previously accepted theoretical limit.

Experiments on samples from selected sediment depths were conducted on the major microbial processes, including methanogenesis, acetogenesis, sulfate reduction, hydrogen oxidation, and prokaryotic growth. Although most of these data will be available only postcruise, initial results show a time constant of hydrogen turnover on the order of a few days. Other substrates for microbial activities will have much longer turnover of months to years, and only the postcruise radiotracer results will demonstrate these rates. Total prokaryotic cell counts show 10^6–10^7 cells in the upper 100 m of the sediment column. This is an order of magnitude higher than at Site 1225, in accordance with the higher availability of organic material at Site 1226. Below 100 mbsf, the cell concentrations are rather similar at the two sites. A broad spectrum of prokaryotic MPN counts and enrichments was initiated at this site, ranging from heterotrophs to autotrophs and from psychrophiles to thermophiles. Samples were also taken for cultivation from pieces of basaltic rock recovered at the bottom of Hole 1226B. Because of the slow growth rate of the indigenous microorganisms, successful counts and cultures will expectedly require many months to years for growth and development.

Contamination tests are very important for all the microbiological work and were done continuously throughout drilling by injecting PFT

into the drilling water. In all cores that were used for microbiological experiments, counts, or isolations, a contamination test was also conducted with prokaryote-sized fluorescent microbeads released within the core catcher upon impact with the sediment (five tests at Site 1226). The detection limit of the PFT method is 0.02 µL drilling fluid (seawater)/g sediment. The results show low to nondetectable contamination in most piston (APC) cores (<0.1 µL drilling fluid/g sediment) but significant potential contamination in XCB cores where the sediment was also visibly disturbed. Subsampling of XCB cores was done here with a reduced sampling program from intact biscuits of sediment. Slurry samples used for an extensive program of microbiology and process studies all (apart from one) have nondetectable contamination when using the PFT method and nondetectable or extremely low contamination using the bead method.

Eight Adara tool deployments and four deployments of the DVTP define a sediment/water interface temperature of 1.7°C and an estimated sediment/basement interface temperature of 24.4°C. An accurate linear temperature gradient of 54°C/km was determined through the 420-m-thick deposit. As the sediment depth increases, temperatures thus shift from the psychrophilic microorganism range to the mesophilic range. Deployment of the corresponding pressure tool (DVTP-P) showed ambient hydrostatic pressure.

As at Site 1225, most cores from the first deep hole (Hole 1226B) were logged on the catwalk with an IR camera for postcruise analysis of the IR logging utility. In order to continue building a temperature database suitable for assessing the microbiological effectiveness of catwalk core handling strategies and for determining microbial cultivation strategies, the IR camera was also used to immediately log temperature gradients across cut section ends.

Ocean-Margin Sites

Peru Shelf Sites

Site 1227

Background and Objectives. Site 1227 was one of three Leg 201 sites selected for drilling on the continental shelf of Peru. These shelf sites were collectively selected to provide records of microbial activities, communities, and geochemical consequences in organic-rich ocean-margin sediments.

The principal objectives at this site were

1. To test by comparison with other sites drilled during this expedition whether microbial communities, microbial activities, and the nature of microbe-environment interactions are different in organic-rich ocean-margin sediments than in open-ocean sediments with less organic matter and
2. To test how the presence of sulfate-depleted subsurface brine affects microbial communities, microbial activities, and microbial influence on environmental properties in organic-rich, sulfate-depleted sediments.

Site 1227 (427 m water depth) is in the immediate vicinity of Leg 112 Site 684, in a small fault-bounded sediment pond in the Trujillo Basin on the Peru continental shelf. The Trujillo Basin lies within the Peru up-

welling zone, and its sediments are correspondingly rich in organic carbon. The TOC content of Site 684 sediment samples ranges between 1.2% and 10.6%, (Shipboard Scientific Party, 1988c). The average TOC concentration of these samples is approximately an order of magnitude higher than the average concentration at open-ocean Site 846 (Leg 201 Site 1226) (Shipboard Scientific Party, 1988c, 1992a). It is about two orders of magnitude higher than the TOC content of open-ocean Site 851 (Leg 201 Site 1225) (Shipboard Scientific Party, 1988c, 1992b).

Geochemical studies of Leg 112 sites show that brine is present below the seafloor in the Trujillo and Salaverry Basins (Suess, von Huene, et al., 1988). The composition of the brine differs from site to site, perhaps because of differences in its degree of dilution and the nature of its interaction with the surrounding sediments (Suess, von Huene, et al., 1988). Detailed chemical analyses indicate that this brine is of marine origin and is early Miocene in age (Kastner et al., 1990). The Leg 112 *Initial Reports* volume suggested that it enters the younger sediment column by diffusion from interstitial brine in underlying Miocene sediments (Suess, von Huene, et al., 1988). Kastner and colleagues (1990) inferred that it is emplaced by stratigraphically bounded advection from north to south. The sulfate depletion of the brine at Site 1227 presumably results from bacterial sulfate reduction closer to the brine's source (e.g., deeper in the sediment column). Whatever the brine's mode of emplacement, Site 1227 provides an opportunity to study how the presence of sulfate-depleted brine affects subseafloor life in organic-rich sediments. Consequently, it provides an excellent standard of comparison for Sites 1228 and 1229, which are affected by the intrusion of sulfate-rich brine into, respectively, sulfate-rich and sulfate-depleted sediments.

Leg 112 shipboard chemistry suggests that the concentrations of methane at Site 684 increase by at least three orders of magnitude (from 10^2 to 10^5 µL/L) over the first 50 to 60 mbsf and remain between 10^4 and 10^5 µL/L to at least 100 mbsf. Ethane and butane concentrations also increase downhole to maximum concentrations at ~60 mbsf (Shipboard Scientific Party, 1988c). In contrast, the concentrations of dissolved sulfate decline from a near-seawater value to zero over the uppermost 30 or 40 mbsf (Shipboard Scientific Party, 1988c). These profiles of dissolved hydrocarbons and sulfate indicate that the hydrocarbons and the sulfate are simultaneously destroyed by sulfate-reducing prokaryotic communities at ~40 mbsf.

Concentrations of several dissolved chemical species increase steadily to the base of the hole (ammonium, chloride, calcium, and magnesium). The increases in dissolved chloride, calcium, and magnesium provide evidence of the brine diffusing upward into the sediment column. Alkalinity exhibits a maximum value at ~40 mbsf, where the rate of anaerobic oxidation of methane appears to be greatest. The magnesium/calcium ratio peaks at 12 mbsf and steadily declines to the base of the hole, presumably as a result of dolomitization throughout the methane-rich sedimentary interval (Shipboard Scientific Party, 1988c).

All of these patterns of sedimentary interstitial water concentrations are inferred to result from relatively high levels of biological activity throughout the sediment column, coupled with diffusive exchange with the overlying ocean and with the brine introduced at depth. The subsurface extent of key electron donors (hydrogen, acetate, and formate) and electron acceptors with standard free-energy yields greater than that of sulfate (oxygen, nitrate, manganese oxide, and iron oxides) was not determined for Site 684.

Principal Results. Interstitial water studies at Site 1227 define one of the most highly resolved chemical records in ODP history. An important objective with these profiles is to identify and quantify zones of prokaryotic activity based on reactive interstitial water species. A deep brine dominates the profiles of conservative seawater ions at this site, including chloride, which increases (with a linear gradient of 5 mM/m down to 70 mbsf and of 3 mM/m below that) to reach twice seawater chlorinity at 120 mbsf. Downhole depletion of sulfate at a relatively shallow depth, DIC concentrations as high as 25 mM, ammonium rising to 23,000 µM at 150 mbsf, and very high concentrations of methane all indicate that prokaryotic activity is much higher at this ocean-margin site than at open-ocean Sites 1225 and 1226. Dissolved sulfate concentrations rapidly decline in the upper 15 mbsf from a seawater value of 29 mM to 5 mM. Concentrations then decline more slowly to 0 mM at ~40 mbsf. Concentrations of dissolved hydrogen sulfide rise rapidly over the same 0- to 40-mbsf interval, from 0.04 mM at 0.24 mbsf to 9 mM at 39–40 mbsf. The convex-upward shape of both the sulfate and sulfide profiles from the sediment/water interface to ~40 mbsf indicates that bacterial sulfate reduction occurs throughout the interval. Sulfide concentrations steadily decline over the sulfate-poor remainder of the drilled section to <0.3 mM at 150 mbsf.

From 1 to 31 mbsf, dissolved barium concentrations rise slightly, from 0 to 1.9 µM. Over the next several meters, barium concentrations rise at an increasingly steep rate, climbing from 9 µM at 38 mbsf to 170 µM at 43 mbsf. Concentrations then rise steadily to 350 µM at ~150 mbsf. Dissolved sulfate and barium are both present throughout the entire interval of non-zero sulfate. Throughout this interval, the concentrations of dissolved barium and dissolved sulfate appear to be related by the solubility product of barite. Upward diffusion of barium from 43 to 38 mbsf appears to sustain modern barite formation in this Peruvian shelf sediment. The barite is visible as lighter bands in the sediment column and was confirmed by X-ray diffraction. At slightly greater depth (~42 mbsf), dissolved sulfate concentrations decline toward 0 mM, barite begins to dissolve, and dissolved barium concentrations rise. The narrow barium peak centered at 43 mbsf is inferred to mark the principal depth of current barite dissolution.

A similarly well-defined sulfate/methane interface coincides with the dissolved sulfide peak at ~40 mbsf. Dissolved methane concentrations slowly rise from 7 µM at 1 mbsf to 55 µM at 35 mbsf. From 40 to 56 mbsf, methane concentrations then rapidly rise to 2×10^3 µM at 56 mbsf and hover in the range of 10^3 µM for the remainder of the drilled sediment column. The disappearance of almost all methane at the depth of sulfate depletion indicates that most of the methane diffusing upward through this sediment column is ultimately destroyed by anaerobic methanotrophy. The presence of methane at a low concentrations throughout the overlying sediment column indicates, as at open-ocean Sites 1225 and 1226, that methane can be maintained at a background level of several micromolar in subseafloor sediments, despite the potential for methane oxidation by sulfate reduction.

Like methane, ethane and propane are detected throughout most of the sediment column. Ethane is present throughout the sediment column below ~1 mbsf, and propane is present throughout the column below ~11 mbsf. Concentrations of ethane decline sharply at the 40-mbsf top of the anaerobic methanotrophy zone (from 2 to 0.7 µM). Concentrations of propane decline more gradually (from 3 to 0 µM) in parallel with methane across the same interval. These distributions demonstrate

that ethane and propane are biologically consumed in the anaerobic methanotrophy zone at this site. Concentrations of all three hydrocarbon species exhibit small distinct peaks in the upper part of the sulfate-rich zone. These small peak occurrences demonstrate that methane, ethane, and propane are all biologically produced in sulfate-rich sediments at this site. Methanogenesis occurs at 1 mbsf, whereas ethanogenesis and propanogenesis occur at ~10 mbsf. Most of the methane, ethane, and propane produced in these sulfate-rich sediments are consumed within a few meters (~5 mbsf for methane and 15–25 mbsf for ethane and propane). Trace concentrations of ethane (10^{-1} µM) persist throughout the sulfate-rich sediments at this site. This persistence indicates that ethane can be maintained at a very low background level in sulfate-rich sediments, despite its potential for oxidation by sulfate reduction.

In most incubation samples from Site 1227, hydrogen concentrations are between 0.2 and 0.5 nM. These concentrations closely resemble those observed at open-ocean Site 1226. Samples from the first few meters of the sediment column exhibit significantly higher hydrogen concentrations (0.9–2.4 nM). These concentrations are consistent with observation in shallower nearshore sediments (Hoehler et al., 1998). However, similar concentrations in samples from 93 and 113 mbsf are a factor of five to ten lower than those observed in nearshore methanogenic sediments. As for Site 1226, further investigation will be needed to determine whether or not these results indicate that the Site 1227 methanogenic and sulfate-reducing communities utilize hydrogen at free-energy yields lower than the generally accepted theoretical limit for actively growing cells.

The VFAs, formate and acetate, are important intermediates in the anaerobic pathways of organic matter degradation and were analyzed throughout the sediment column. Acetate concentrations range between 0 and ~10 µM and generally increase from the surface sediment down to the base of the drilled sediment column (~150 mbsf). Formate concentrations vary considerably throughout the sediment column (between 0 and ~5 µM) but exhibit no mean trend over the sampled sediment column. The average acetate and formate concentrations of this site are an order of magnitude higher than concentrations in sediments of the equatorial Pacific sites and are similar to concentrations found in very active coastal marine sediments. These results suggest that relative substrate concentrations of different sites may be related to the activity levels of the principal prokaryotic processes, although the absolute process rates are orders of magnitude lower in the open-ocean sediments than in the coastal sediments.

Concentrations of dissolved manganese and iron are, respectively, 0–6 and 0–30 µM at Site 1227. The peak manganese concentration from Site 1227 (6 µM) is a factor of 27 lower than that of equatorial Pacific Site 1225 and a factor of 7 lower than that of equatorial Pacific Site 1226. The peak iron concentration from Site 1227 (30 µM) is a factor of 1.3 greater than that at Site 1225 and a factor of 1.5 lower than that at Site 1226. There are at least two possible explanations why the dissolved iron and manganese concentrations are low at Site 1227 relative to the open-ocean sites. Either the ferrimagnetic material at this ocean-margin site is not an effective source of bioavailable manganese and iron oxides, or dissolved manganese and iron are scavenged and precipitated much more quickly at this site. Stratigraphic relationships between magnetic susceptibility and dissolved sulfide concentrations suggest that these dissolved metals are scavenged by sulfide precipitation at

Site 1227. A relatively steep decline in sulfide concentrations from 40 to 75 mbsf is associated with the prominent magnetic susceptibility peak from 40 to 50 mbsf. The ultimate sink for sulfide diffusing deeper into the column is associated with the other most prominent magnetic susceptibility peak at this site (which begins at ~140 mbsf).

A pronounced peak in the values of almost every physical property measured at this site spans the interval from 40 to 50 mbsf. These physical properties include magnetic susceptibility, GRA bulk density, grain density, *P*-wave velocity, NGR, thermal conductivity, and axial formation factor. Smaller peaks in the values of most of these properties are present in the uppermost 20 m of the sediment column. The bulk porosity profile mirrors the variability in other physical properties at this site; its downhole record is nearly the exact inverse of the bulk density and grain density records. These variations in physical properties result from variations in the bulk lithology of the sediment column. The porosity lows and high values in other physical properties are present in sandier intervals of the sediment column.

The 40- to 50-mbsf interval is composed of sandy silt, rich in glauconite, dolomite, quartz, feldspar, pyrite, and shell fragments. It grades upward into dolomite-bearing clayey silt, rich in diatoms and nannofossils. It directly overlies clay- and nannofossil-bearing diatom ooze. Traces of bioturbation are much more abundant in the 40- to 50-mbsf interval than in the overlying and underlying sediments. The primary front of active anaerobic methanotrophy occurs at the top of this 40- to 50-mbsf sandy interval. The successive fronts of barite precipitation and barite dissolution are present in the same interval. Peak concentrations of dissolved iron, manganese, silica, and phosphate are also present in this interval. Secondary peaks in the dissolved concentrations of iron, manganese, silica, and phosphate are present between 0 and 20 mbsf and are similarly associated with relatively coarse-grained sediments. These relationships suggest that several principal activities of the subsurface biosphere (including anaerobic methanotrophy, iron and manganese reduction, ethanotrophy, and propanotrophy) are pinned in a narrow stratigraphic interval by physical properties and sediment composition at this site. Its mineral composition and its traces of relatively intensive bioturbation indicate that the physical and compositional properties of this interval are primarily determined by the nature of the sediment when it was first deposited on the seafloor. However, to some extent, these properties may have been modified by the postdepositional microbial activities that still occur in them today. Density and porosity can be affected by biologically mediated precipitation and dissolution of authigenic minerals, such as barite, dolomite, and apatite. Magnetic susceptibility may be diminished by biologically mediated dissolution of solid-phase iron oxides and subsequent iron reduction. To a much lesser extent, magnetic susceptibility may also be enhanced by massive biologically induced precipitation of reduced iron and manganese. More detailed determination of the extent to which physical and compositional properties control the microbial activities at this site and the extent to which those activities control the physical and compositional properties will require further investigation.

Preliminary cell counts of eight samples from Site 1227 suggest that sedimentary cell concentrations at most sediment depths are slightly higher at this ocean-margin site than at equatorial Pacific Site 1225. Based on the same few data, at most sediment depths, cell concentrations from Site 1227 may be roughly equivalent to those of open-ocean Site 1226. This data set will be expanded by postcruise analyses.

Experiments on major microbial processes and on enumeration of viable prokaryotes were initiated at selected depths ranging from near the mudline to the bottom of the drilled sediment column. The studied processes include methane and acetate formation and consumption, sulfate reduction, hydrogen oxidation, and rates of cell growth. The cultivation experiments include selective growth conditions for a wide range of autotrophic and heterotrophic prokaryotes ranging from psychrophilic to thermophilic. Specific sampling was targeted to the sulfate/barium interface to study the possible attack of sulfate-reducing bacteria and methane-oxidizing archea on sulfate bound in barite.

One Adara and two DVTP deployments combined with the Leg 112 data define a linear gradient of 49°C/km, with a sediment/water interface temperature of 8.6°C and an estimated temperature at 160 mbsf of 16.4°C. Throughout the sediment column, temperatures are in the low mesophilic range.

Trials were undertaken of three experimental tools at this hole: the pressure coring sampler (PCS), the DVTP-P, the Fugro percussion corer (FPC), and the APC-Methane (APC-M) tool.

Site 1228

Background and Objectives. Site 1228 was one of three Leg 201 sites selected for drilling on the continental shelf of Peru. These shelf sites were collectively selected to provide records of microbial activities, communities, and geochemical consequences in organic-rich ocean-margin sediments.

The principal objectives at this site were

1. To test by comparison with other sites drilled during this expedition whether microbial communities, microbial activities, and the nature of microbe-environment interactions are different in organic-rich ocean-margin sediments than in open-ocean sediments with less organic matter and
2. To test how the presence of sulfate-bearing subsurface brine affects microbial activities, microbial communities, and microbial influence on environmental properties in organic-rich, sulfate-rich sediments.

Site 1228 is in the immediate vicinity of Leg 112 Site 680. As described in **"Principal Results,"** p. 32, in "Site 1227," geochemical studies of Leg 112 sites show that brine is present below the seafloor in the Trujillo and Salaverry Basins (Suess, von Huene, et al., 1988). Interestingly, at Site 680 the deep brine source of sulfate prevents the interstitial water concentration of sulfate from becoming depleted at any depth. Site 1228 therefore provides an opportunity to study how the introduction of sulfate-bearing brine affects subseafloor life in organic-rich, sulfate-rich sediments. Consequently, it provides an excellent standard of comparison for Sites 1227 and 1229, which are, respectively, affected by the intrusion of sulfate-free brine and sulfate-rich brine into organic-rich, sulfate-depleted sediments.

Site 1228 is located at 252 m water depth on the outer shelf edge in the middle of the modern oxygen minimum zone of the Peruvian high-productivity upwelling system. At this depth on the Peru shelf, an oxidized sediment zone is practically absent at the sediment/water interface and sulfate reduction is the predominant mineralization process to the very surface (Rowe and Howarth, 1985; Fossing, 1990; Parkes et al., 1993). The organic content is high at Site 680 (3%–10% TOC), and sul-

fate reduction rates are still detectable with radiolabeled sulfate in samples taken from as deep as 80 mbsf (Parkes et al., 1990).

The lithologic and physical properties at Site 680 change strongly through the 200-m-deep interval drilled during Leg 112 (Shipboard Scientific Party, 1988a). The sediment mainly consists of diatom mud in the upper 50 m of the Pleistocene deposit. Below 50 mbsf, the terrestrial component of the mud is higher but the sediment is primarily biogenic. The lower part of the sediment column consists of a coarse-grained phosphate and feldspar gravel interpreted as drilling artifacts overlying coarse-grained sand cemented by dolomite (Shipboard Scientific Party, 1988a). Dolomite is the primary authigenic phase, but calcite and apatite are also common.

Shipboard chemical analyses from Leg 112 indicate that concentrations of methane at Site 680 are in the range of 10–100 µL/L (0.4–4 µM) in the upper 100 m of the sediment column. Methane was not analyzed at greater depths at Site 680. Concentrations of dissolved sulfate decline from a near-seawater value to a minimum of 6 mM over the uppermost ~50 mbsf and then rise toward higher values in the underlying sediment as a result of diffusion from the underlying sulfate-rich brine (Shipboard Scientific Party, 1988a). A peak sulfide concentration is present between 20 and 40 mbsf (Mossman et al., 1990). Sulfide concentrations were not measured in deeper portions of the underlying brine-affected interval.

Chloride concentrations increase steadily to the base of the hole, and ammonium steadily increases to at least 80 mbsf. Alkalinity exhibits a maximum value at 20 mbsf. Concentrations of calcium and magnesium exhibit minimum values at 5 and 20 mbsf, respectively, and then increase steadily to the base of the hole. The magnesium/calcium ratio peaks at ~5 mbsf and also steadily declines to the base of the hole (Shipboard Scientific Party, 1988a; Kastner et al., 1990).

These downhole profiles of dissolved chemical concentrations are inferred to result from relatively high levels of biological activity throughout the sediment column, coupled with diffusive exchange with the overlying ocean water and with a sulfate-bearing brine introduced at depth. Prokaryotic cell counts and activities were studied to a depth of 9.1 mbsf at Site 680. Nearly 10^9 cells/mL were present in all samples analyzed. In MPN cultivation studies, 10^1 to 10^5 cells/mL were found to be viable (Cragg et al., 1990; Parkes et al., 1990). The subsurface extent of key electron donors (hydrogen, acetate, and formate) and electron acceptors with standard free-energy yields greater than that of sulfate (oxygen, nitrate, manganese oxide, and iron oxides) was not determined for Site 680.

Principal Results. Continuous APC coring from the seafloor to 200 mbsf enabled high-quality sampling for geochemistry and microbiology throughout the drilled sediment column of Site 1228. Because of the overall predominance of sulfate reduction in the highly sulfidic sediment and the presence of sulfate throughout the sediment column, there were no distinct chemical interfaces to target in the sampling scheme for Site 1228. Concentrations of chloride range linearly from a typical seawater concentration at 0 mbsf to twice the seawater concentration at 200 mbsf. This linear profile demonstrates the long-term stability of brine diffusion and provides a reference for all other interstitial water constituents. Analyzed nonconservative species that are affected by microbial activity in the subsurface included sulfate, DIC, and ammonium. Interstitial water analyses at high depth resolution show un-

expected details with implications for both the rates of long-term processes and for more recent changes.

Sulfate reduction in the upper 50 m of the sediment column is not sufficient to deplete sulfate at depth. The overall sulfate distribution shows a steep drop in concentrations over the first few meters below the sediment/water interface, a sigmoidal curve in dissolved sulfate concentrations over the following 10 m, a decrease to 2.5 mM at 38 mbsf, and then a continuous increase to 30 mM at 200 mbsf. The sigmoidal curve of the first 10 m indicates that the near-surface distribution of sulfate reduction and/or transport processes changed strongly in geologically recent time and that diffusion through the sediment column has not yet fully adjusted to a new steady state. The continuous increase in sulfate concentrations from 40 to 200 mbsf results from upward diffusion of the underlying sulfate-rich brine.

The depth profiles of DIC and ammonium closely match the described sulfate distribution. The overall DIC profile reveals a distinct DIC maximum of 19 mM at 2 mbsf, a decline to 15 mM, a rise to a second, broader maximum of 20 mM at 25 mbsf, and then a gradual downhole decrease to 4 mM. Ammonium similarly increases from ~2000 µM near the sediment surface to a local maximum of 2600 µM at 2 mbsf, declines slightly, and then increases gradually to 5000 µM downhole. Comparison to Site 680 biochronostratigraphic data (Shipboard Scientific Party, 1988a) suggests that the sediment that contains the DIC and ammonium maxima may have been deposited a few tens of thousands of years ago. These near-surface interstitial water anomalies indicate that steady-state diffusion of biologically active chemicals past the upper sediment column was disrupted by late Pleistocene environmental change and has not yet fully recovered. The exact nature of these changes will be analyzed when a more complete data set becomes available.

Concentrations of manganese and iron in the interstitial water are extremely low (<0.1 µM) down to ~60–80 mbsf. Below this depth, they increase gradually to ~10 µM (manganese) and 50 µM (iron) at 200 mbsf. The source of these dissolved metals at depth may be either diffusion from below or in situ manganese or iron reduction in the lower sediment column.

In contrast to most other ocean-margin sites, including Site 1227, a sulfate/methane interface is absent from the sediment of Site 1228. Methane concentrations remain low throughout the 200-m sediment column, reaching a maximum of only 8 µM. Yet, the distribution of methane clearly reflects the sulfate distribution, with a maximum coinciding with the sulfate minimum and a general inverse correlation between sulfate and methane concentrations throughout the sediment column. These results indicate that even at a concentration above 9% of its seawater level (minimum = 2.5 mM; seawater = 28.9 mM), sulfate regulates the ability of methane-oxidizing consortia to take up methane and maintain low background concentrations. In this respect, Site 1228 provides a unique opportunity to analyze the energetics of anaerobic oxidation of methane and to test current theories of the limiting parameters for this key microbial process.

Acetate and formate are important fermentation products as well as substrates for sulfate-reducing bacteria. Their concentrations in this organic-rich shelf sediment are tenfold higher than those in deep-sea sediments of the tropical Pacific (Sites 1225 and 1226) but only about one-half their concentrations at Peru shelf Site 1227. The Site 1228 data show considerable scatter with depth. Acetate concentrations fall

mostly in the range of 1–4 µM and formate concentrations in the range of 0.5–3 µM. The higher concentrations of both fatty acids are present below 100 mbsf. These concentrations are regulated by uptake mechanisms that are not yet fully understood.

Interestingly, the depth of the distinct sulfate minimum at ~40 mbsf is present in an interval of strong lithologic and physical change. At this depth, the sediment shifts from a diatomaceous silt of predominantly hemipelagic origin to older quartz- and feldspar-bearing silt with a more abundant terrestrial component. At 43 mbsf, there is a distinct minimum in porosity and maxima in density, thermal conductivity, and magnetic susceptibility. It is intriguing to speculate that such a physical boundary may temporarily lock the position of biogeochemical zonations in the sediment column.

The temperature gradient in the Site 1228 sediment column was defined from two discrete temperature measurements taken with the DVTP. The results were combined with Leg 112 data to define a linear temperature gradient of 34°C/km and a heat flow of 32 mW/m^2. This heat flow estimate is lower than the 46 mW/m^2 estimated for Site 680 by the Leg 112 Shipboard Scientific Party (1988a) and confines the previous broad estimate of 20–70 mW/m^2 for this site (Yamano and Uyeda, 1990). The temperature increases down through the sediment column from an estimated annual mean of 12.5°C at the seafloor to an extrapolated 19.3°C at 200 mbsf. These temperatures are all within the low mesophilic range for prokaryotes.

Samples were taken for total counts, viable (MPN) counts, and isolations of prokaryotes from selected depths throughout the sediment column. Because of the short transfer time between Sites 1227, 1228, and 1229, the AODCs of total prokaryotic cell numbers at Site 1228 will be conducted postcruise. A large number of MPN samples and isolation incubations target a broad physiological spectrum of heterotrophic and autotrophic prokaryotes that utilize diverse electron acceptors and donors in their energy metabolism. The selective influence of increased salinity and brine composition is also targeted in some incubations. The expected slow growth of deep subsurface prokaryotes will require long postcruise incubation of samples before definite results are obtained from these experiments. This is also the case for the many experiments on microbial processes measured by radiotracer techniques on samples taken from throughout the entire sediment column.

Because the absence of prokaryotic cell contamination from drilling and sampling operations is critical for the isolation of indigenous prokaryotes and measurement of their activities, a PFT tracer was continuously added to the drill water. Tracer samples were taken on the catwalk or in the laboratory from all core sections and subsamples used for microbiology. It was demonstrated that PFT concentrations are typically higher at the periphery than at the sampled center of whole-round core segments. The microbiology subsamples had PFT concentrations below or near the detection limit. This limit corresponds to the potential introduction of 0.01 µL seawater/g sediment. Such seawater introduction could maximally introduce 5 cells/g, based on the mean cell density in seawater (5×10^{-8} cells/L). An additional contamination test uses fluorescent microbeads dispersed on impact at the head of the core barrel. At Site 1228, this test consistently indicates that contamination is unlikely. This method releases 2×10^{11} prokaryote-sized beads at the most sensitive position during drilling, and the tests on microbiological samples showed no beads or, at most, one bead in the >60 microscopic fields of view routinely scanned. The extensive contamination tests ap-

plied at this site thus confirm the high quality of microbiology samples that can be taken by careful techniques from APC cores without visible disturbance.

Site 1229

Background and Objectives. Site 1229 was one of three Leg 201 sites selected for drilling on the continental shelf of Peru. These shelf sites were collectively selected to provide records of microbial activities, communities, and geochemical consequences in organic-rich ocean-margin sediments.

The principal objectives at this site were

1. To test by comparison with other sites drilled during this expedition whether microbial communities, microbial activities, and the nature of microbe-environment interactions are different in organic-rich ocean-margin sediments than in open-ocean sediments with less organic matter;
2. To test how the occurrence of sulfate-bearing subsurface brine affects microbial communities, microbial activities, and microbial influence on sediment chemistry in organic-rich, sulfate-depleted, methane-rich sediments; and
3. To provide multiple opportunities for recovering and identifying the sulfate-reducing methanotrophic communities of deeply buried marine sediments.

Site 1229 is located on the Peru shelf in 150.5 m water depth. It is in the immediate vicinity of Leg 112 Site 681. As described in **"Principal Results,"** p. 32, in "Site 1227," geochemical studies of Leg 112 sites show that brine is present below the seafloor in the Trujillo and Salaverry Basins (Suess, von Huene, et al., 1988). Site 1229 provides an opportunity to study how the occurrence of sulfate-bearing brine affects subseafloor life in organic-rich, sulfate-depleted, methane-rich sediments. Consequently, it provides an excellent standard of comparison for Sites 1227 and 1228, which are, respectively, affected by the intrusion of sulfate-free brine into organic-rich, sulfate-depleted sediments and the intrusion of sulfate-rich brine into sediments with sulfate-bearing interstitial waters.

Shipboard chemical analyses from Leg 112 indicate that concentrations of methane at Site 681 increase from 10^2 to 10^5 µL/L in the first 40 m of the sediment column and decline from 10^5 to 10^2 µL/L between 73 and 100 mbsf (Shipboard Scientific Party, 1988b). In contrast, the concentrations of dissolved sulfate decline to 0 mM over the first ~30 mbsf, remain at or near 0 mM until 75 mbsf, and then increase steadily with greater depths (Shipboard Scientific Party, 1988b). This downhole pattern of sulfate concentrations indicates active sulfate reduction at depths above 30 mbsf and at depths below ~75–100 mbsf. The downhole pattern of methane concentrations indicates that methane is created at depths of 60–70 mbsf and diffuses to the overlying and underlying zones of active sulfate reduction, where both sulfate and methane are destroyed.

Chloride concentrations increase steadily to the base of the hole. Ammonium concentrations decline slightly from the sediment/water interface to 12 mbsf, increase from 12 to 80 mbsf, and then begin to decline again. Alkalinity also declines from the sediment/water interface to 12 mbsf, increases to a subsurface maximum at 32 mbsf, and then declines again with depth. Calcium and magnesium concentrations ex-

hibit minimum values at ~30 mbsf and then increase steadily to the base of the hole. The magnesium/calcium ratio exhibits a broad peak from ~0 to 40 mbsf and then steadily declines to the base of the hole (Shipboard Scientific Party, 1988b).

These downhole profiles of dissolved chemical concentrations are collectively inferred to result from high levels of biological activity and biologically driven solid-phase alteration throughout the sediment column, coupled with diffusive exchange with the overlying ocean and with a sulfate-bearing brine introduced at depth. AODCs show that prokaryotic cells are present in samples taken from as deep as 80 mbsf at Site 681 (Cragg et al., 1990). Viable prokaryotes were found and potential activity rates were identified in the same samples (Cragg et al., 1990). The subsurface extent of key electron donors (hydrogen, acetate, and formate) and electron acceptors with standard free-energy yields greater than that of sulfate (oxygen, nitrate, manganese oxide, and iron oxides) was not determined for Site 681.

Principal Results. An important objective for Site 1229 is to identify and quantify zones of microbial activity based on reactive interstitial water species. Toward this end, we established a highly resolved chemical record throughout the drilled sediment column. Profiles of conservative ions provide evidence of diffusive mixing between seawater diffusing downward from the sediment/water interface and a brine diffusing upward from older sediments. For example, concentrations of dissolved chloride increase linearly from 559 mM at the sediment/water interface to 1208 mM at the base of the drilled sediment column (186 mbsf). Peak concentrations of biologically affected chemical species, such as ammonium (5800 µM) and dissolved inorganic carbon (22 mM), indicate that rates of subseafloor microbial activity are much higher at this ocean-margin site than at open-ocean Sites 1225 and 1226. These peak concentrations also suggest that the subseafloor microbial activity at Site 1229 is slightly greater than that at Site 1228 (which lies just seaward of Site 1229) and perhaps is slightly less than that at Site 1227 (which is situated 310 km to the north on the Peru shelf).

As at Site 1228, the concentration profiles of several biologically affected chemical species exhibit a pronounced anomaly just below the seafloor (at 2–3 mbsf). This anomaly at Site 1229 consists of a brief positive excursion in alkalinity, DIC, ammonium, and sulfide, with a cooccurring negative excursion in dissolved sulfate. The same anomaly is also apparent in the ammonium and alkalinity profiles of Site 681 (Shipboard Scientific Party, 1988b). As described in **"Principal Results,"** p. 36, in "Site 1228," this near-surface interstitial water anomaly indicates that the steady-state diffusion of biologically active chemicals past the upper sediment column was disrupted by late Pleistocene environmental change and has not yet fully recovered. There are least three possible general explanations of this anomaly. It may result from ongoing activity in a microbial "hotspot" at this shallow sediment depth, it may be a chemical relic of past microbial activity (now relaxing back to a diffusional steady state), or it may be a result of the recent establishment of an oxygen minimum at this water depth, causing the extinction of a bioirrigating benthos and a stimulation of sulfate reduction in the uppermost 2 m of sediment.

The most striking biogeochemical feature of this site is the reversal of the biogeochemical zonation at depth. This reversal is immediately apparent in the dissolved sulfate profile. The sulfate concentrations de-

cline from a seawater value of 29 mM at the sediment surface to 0 mM at ~35 mbsf. They remain at 0 mM from 35 to 88 mbsf and then steadily rise from 0 to 38 mM at 186 mbsf. The sulfate that sustains microbial reduction over the uppermost 35 mbsf of the sediment column ultimately diffuses downward from the overlying ocean. The sulfate that sustains microbial reduction below 88 mbsf is inferred to diffuse upward from the underlying brine. Both intervals of sulfate reduction are marked by local maxima in the concentrations of dissolved sulfide, with a broad peak from ~20 to 40 mbsf and a sharper peak at ~90 mbsf.

The sulfate profile is mirrored by the dissolved methane profile. Dissolved methane concentrations are <100 µM from 0 to 20 mbsf, hold steady at a few hundred micromolar from 20 to 35 mbsf, and then rise to values of ~2000 µM (exceeding 1 bar partial pressure) between 65 and 75 mbsf. Methane then steadily declines to <100 µM at 93 mbsf and remains in the range of 100 µM or less to the base of the sampled sediment column. As at Site 1227, the disappearance of almost all methane at the depths of sulfate depletion indicates that most of the methane in this sediment column is ultimately destroyed by anaerobic methanotrophy. As observed at all previously drilled Leg 201 sites, the Site 1229 methane and sulfate profiles indicate that methane can be maintained in subseafloor sediments at background concentrations that are inversely related to the co-occurring dissolved sulfate concentrations.

The dissolved iron and manganese concentration profiles demonstrate that net reduction of iron and manganese oxides occurs in the methanogenic zone. The principal foci of net manganese and iron reduction are at slightly different depths, with iron reduction peaking at 75–90 mbsf and manganese reduction just above and below that interval. The presence of methanogenesis in iron- and manganese-reducing environments may result from a limited availability of mineral-supplied electron acceptors relative to electron donors. In these organic-rich sediments, electron donors may be supplied to the microbial community faster than mineral dissolution can supply dissolved reducible manganese and iron. Relatively high concentrations of manganese and iron in the lower sulfate zone could be due to either in situ mineral reduction or to diffusion from the underlying brine-rich sediment.

The dissolved barium profile is broadly similar to the methane profile. Dissolved barium concentrations are <2 µM from 0 to 24 mbsf. Concentrations of barium in interstitial water then rapidly rise to 18 µM at 40 mbsf and remain near 19 µM until almost 80 mbsf. They then decline steeply to 2 µM at ~100 mbsf and are <2 µM for the remainder of the drilled sediment column. As at Site 1227, the inverse relationship between sulfate and barium is inferred to be controlled by the solubility product of barite. Upward diffusion of barium past 35 mbsf and downward diffusion of barium past 90 mbsf is suspected to sustain modern barite formation at, respectively, ~24 and 100 mbsf. Similarly, the shoulders of the barium peak at ~40 and 80 mbsf are inferred to mark the principal depths of current barite dissolution at this site.

Prokaryotic cell counts were done at 10-m intervals throughout the upper sediment column and across both sulfate/methane interfaces. These data show that mean sedimentary cell concentrations are severalfold higher at this ocean-margin site than at the Leg 201 open-ocean sites and may be slightly higher than mean concentrations at nearby Site 1227. The most striking features of the shipboard cell counts are the thousandfold increase in cell concentrations in the lower zone of overlapping sulfate and methane concentrations and the tenfold in-

crease in cell concentrations in the upper zone of overlapping concentrations. The maximum cell concentrations observed in the lower sulfate/methane zone are actually an order of magnitude higher than the concentrations observed at the sediment/water interface. Given the coarse spacing of these samples and their positions relative to the chemically defined sulfate/methane overlap zones, the peak cell concentrations observed in the upper sulfate/methane zone may greatly underestimate the peak concentrations in that zone.

Acetate and formate concentrations exhibit strong local maxima of ~6 µM in both of the sulfate/methane interface zones. These maxima are centered at 37 and 90 mbsf. As with the cell counts, these local maxima are higher than the local maxima exhibited by both acetate (~2 µM) and formate (3 µM) at the sediment/water interface. Throughout most of the remaining record at this site, concentrations of both species are between 1 and 2 µM. As at Site 1227, the concentrations of both species reach their highest values near the base of the drilled sediment column (~15 µM). These results are intriguing because these volatile acids are important substrates for both sulfate reducers and methanogens. Hydrogen is another important electron donor in anaerobic communities. Almost all hydrogen concentrations measured at this site were <0.5 nM, and most were <0.2 nM. These concentrations resemble those observed at open-ocean Site 1225 and ocean-margin Site 1227. As noted in **"Principal Results,"** p. 23, in "Site 1225" and **"Principal Results,"** p. 32, in "Site 1227," these concentrations are much lower than expected from experiments with sulfate-reducing and methanogenic communities of surface sediments. The accurate interpretation of these acetate, formate, and hydrogen concentrations must await postcruise analyses of prokaryotic energetics in subseafloor environments.

The cell concentration data and sulfate and methane gradients demonstrate that the subseafloor prokaryotic population and activity are locally strongly focused at the sulfate/methane overlap zone defined by the upward-diffusing sulfate-bearing brine and the downward-diffusing seawater sulfate. The dissolved barium profile indicates that microbial activity in this zone directly influences sediment chemistry by mediating the precipitation and dissolution of barite. In these effects on subsurface biological activities and biogeochemical cycles, this brine-caused sulfate/methane interface mirrors the effects of the overlying "normal" sulfate/methane interface. Postcruise microbiological studies will be required to demonstrate whether or not the microbial community supported by the brine-induced interface is locally unique or the same as that supported by the overlying interface.

The upper sulfate-rich zone at Site 1229 lies entirely within lithostratigraphic Subunit IA, a stratigraphic interval of primarily hemipelagic sediments (0–40 mbsf). The underlying methane-rich zone is largely limited to lithostratigraphic Subunit IB, which is the upper portion of a longer interval (40–138 mbsf) of mixed terrigenous and hemipelagic sediments. The AOM zones that separate the upper and lower sulfate-rich zones from the intervening methane-rich zone are associated with brief sedimentary intervals characterized by high grain density, high NGR, high resistivity, and low porosity. These brief low-porosity intervals are unusually rich in terrigenous sediment and are interpreted to have been deposited during the two most recent lowstands of four onlap/offlap cycles that define the 40- to 138-mbsf interval.

In short, as at Site 1228, the upper sulfate-reducing interval at Site 1229 is composed of predominantly hemipelagic sediments, the

strongly methanogenic zone is rich in terrigenous sediment relative to the overlying sulfate-reducing zone, and the intervening AOM zone is present just above an interval of low-porosity, high-density lowstand sediments. The lower AOM zone at Site 1229 is present within a similar interval of high-density, low-porosity lowstand sediments. The lithologic association of AOM zones with high-density, low-porosity lowstand sediments at Sites 1229, 1228, and 1227 provides intriguing evidence that, on the Peru shelf, the position of AOM zones is currently pinned within the sediment column by lithologic properties and, by extension, depositional history.

As at Site 1227, stratigraphic patterns of magnetic susceptibility and dissolved manganese, iron, and sulfide concentrations indicate similar control of other microbial processes by depositional history at Site 1229. Magnetic susceptibility is generally much higher in the methanogenic zone and in the lower sulfate-reducing zone than in the overlying sulfate-reducing zone. This circumstance suggests that mineral sources of reducible iron and manganese are more abundant in the terrigenous-dominated sediments of the lower sulfate-reducing zone and the mixed terrigenous and hemipelagic sediments of the methanogenic zone than in the mostly hemipelagic sediments of the upper sulfate-reducing zone. The relatively high magnetic susceptibility of the intervals with more strongly terrigenous sediments is consistent with our finding that dissolved manganese and iron concentrations are generally higher in the lower methanogenic zone and the underlying sulfate-reducing zone than in the upper sulfate-reducing zone. The presence of higher manganese and iron concentrations and lower sulfide concentrations in these relatively high-susceptibility intervals in turn provides strong evidence that the current rates and stratigraphic foci of iron reduction, manganese reduction, and sulfide precipitation depend strongly on depositional history.

Experiments on major microbial processes and on enumeration of viable prokaryotes were initiated at selected depths ranging from near the mudline to the bottom of the drilled sediment column. The studied processes include methane and acetate formation and consumption, sulfate reduction, hydrogen oxidation, and rates of cell growth. The cultivation experiments include selective growth conditions for a wide range of autotrophic and heterotrophic microorganisms ranging from psychrophilic to thermophilic. Detailed microbiological sampling targeted the top of the sediment column and both the upper and lower sulfate/methane overlap zones.

The results from one DVTP deployment were combined with temperature data from Site 681 to define a linear gradient of 35.5°C/km for this site. The mean sediment/water interface temperature defined by this gradient is 13.4°C. The temperature defined for the base of the drilled sediment column (193 mbsf) is 20.2°C. Throughout this interval (0–193 mbsf), temperatures are in the low mesophilic range.

Trials were undertaken of four experimental tools at this hole: the PCS, the DVTP-P, the APC-M tool, and the FPC.

Peru Slope Hydrate Site

Site 1230

Background and Objectives. Site 1230 was the single hydrate-bearing site selected for drilling during Leg 201. The principal objectives at this site were

1. To determine if and how hydrate-bearing sequences differ in microbial activities, microbial communities, and the nature of microbe-environment interactions from nearby methane-rich sequences that lack hydrates (Sites 1227 and 1229) and nearby sulfate-rich sequences with low methane concentration (Site 1228) and
2. To provide a Peru margin microbial and biogeochemical counterpoint to hydrate-rich sites in other regions of the world ocean (such as Leg 164's northwest Atlantic Blake Ridge and Leg 204's northeast Pacific Hydrate Ridge).

Site 1230 is located on the lower slope of the Peru Trench in 5086 m water depth. Sediments of this area are part of the accretionary wedge just landward of the Peru Trench (Suess, von Huene, et al., 1988). The lithologies, sediment age, and many geochemical and geophysical characteristics of the target site were well characterized by Leg 112 studies of nearby Site 685 (Shipboard Scientific Party, 1988d). The upper 200 m of Pleistocene to Holocene sediment is a clay-rich diatomaceous mud, partly accreted by downslope transport from the shelf. At ~ 200 mbsf, a stratigraphic hiatus of ~4.5 m.y. separates the slope deposit from upper Miocene diatom ooze (Shipboard Scientific Party, 1988d). Authigenic carbonates and phosphates are sparse, whereas pyrite framboids are abundant throughout the section (Shipboard Scientific Party, 1988d). Calculated sedimentation rates are high; they average 250 m/m.y. for the Miocene sequence and 100 m/m.y. for the Pleistocene section (Shipboard Scientific Party, 1988d). These high rates are consistent with sedimentation in a lower-slope basin or trench axis.

The surface waters over Site 1230 are part of the Peru upwelling system and are biologically highly productive. The organic carbon content of the sediment is high at Site 685 (Shipboard Science Party, 1988d). Methane concentrations were observed to rise above 1 bar by 11.6 mbsf and remain in the range of 10^4–10^5 µL/L throughout the cored sediment column down to 432 mbsf (Kvenvolden et al., 1990). Concentrations of ethane and butane generally increase downhole from 1 to 100 µL/L, and the methane/ethane ratio decreases from 10^5 to 10^3. The Leg 112 Scientific Party found visual evidence of methane hydrate at 99 and 164 mbsf in the form of small pieces of dark gray hydrate (Shipboard Scientific Party, 1988d; Kvenvolden and Kastner, 1990). The samples looked like rounded pieces of mudstone but felt cold and showed bubbling foam. Based on this information, Site 1230 provides an excellent opportunity for assessing the nature of microbial communities and their activities in hydrate-bearing sediments rich in organic material and under high hydrostatic pressure.

Concentrations of dissolved sulfate declined to 0 mM between the first and second core analyzed at Site 685 (between 3 and 18.1 mbsf) (Shipboard Scientific Party, 1988d). Chloride concentrations range between 525 and 555 mM. The maximum concentration is associated with the most shallow sulfate-free sample (18.1 mbsf) and was suggested by the Leg 112 Shipboard Scientific Party to lie just above hydrate at the top of the hydrate stability field. Salinity, alkalinity, dissolved ammonium, phosphate, and magnesium concentrations rise to maximum values in the interval of 107–134 mbsf, decline sharply between 165 and 235 mbsf, and then decrease gradually to the base of the hole at ~450 mbsf. The maxima in alkalinity (156 mM), ammonium (31,760 µM), and phosphate (826 µM) were the highest then known from deep-ocean drilling (Shipboard Scientific Party, 1988d). Downhole

variation in chloride and calcium concentrations is generally opposite to the variation in these other chemical species. The pH drops below 7 at 133 mbsf and remains below 7 to the base of the hole (Shipboard Scientific Party, 1988d).

These patterns of interstitial water chemistry are inferred to result from high levels of biological activity throughout the sediment column, coupled with hydrate formation and diffusive exchange with the overlying ocean. The subsurface extent of key electron donors (hydrogen, acetate, and formate) and electron acceptors with standard free-energy yields greater than that of sulfate (oxygen, nitrate, manganese oxide, and iron oxides) was not determined for Site 685.

Principal Results. The biogeochemical zonation of Site 1230 is more typical of an upper-slope sediment than a typical deep-sea sediment; its uppermost sediment contains a narrow suboxic zone, and sulfate depletion occurs at <9 mbsf. Oxygen and nitrate are not detectable at the top of the mudline core. Dissolved manganese is present in the uppermost 0.5 m of sediment but is near the detection limit (<1 µM) throughout the remaining sediment column. Dissolved iron is likewise low (mostly 1–3 µM) in the upper 25 m of the sediment. Below the narrow suboxic zone, sulfate reduction is the dominant mineralization process down to the bottom of the sulfate zone at 8–9 mbsf. The sulfate gradient is nearly linear and indicates that most of the net sulfate reduction takes place at the sulfate/methane interface (Iversen and Jørgensen, 1985; Niewöhner et al., 1998; Borowski et al., 1996, 2000).

Methane builds up steeply beginning at the sulfate boundary, and it reaches >1 bar partial pressure by 11 mbsf. Below that depth, methane concentrations in recovered cores fluctuate around a few millimolar, which is the usual pattern in supersaturated cores with gas escape upon depressurization. At Site 1230, however, nine successful deployments of the PCS at depths ranging from 22 to 277 mbsf allowed the methane concentration profile from the entire sediment column to be accurately determined. The PCS recovered a full 1-m core in most deployments. Its highest internal pressure was 8086 psi in a core recovered from 254.6 mbsf. At 254.6 mbsf, 8086 psi is equivalent to 105% of hydrostatic pressure. The overpressure is caused by dissolving gas hydrate resulting from warming during the wireline trip (Dickens et al., 2000). The total amount of methane retrieved by the PCS reached 400,000 µM methane at 157 mbsf. This greatly exceeds methane solubility at the ambient temperature and hydrostatic pressure but is consistent with the presence of several percent gas hydrate in the sediment pore space.

The presence of gas hydrate was also monitored by rapid IR scanning of the recovered cores. Immediately after retrieval, each core was brought to the catwalk and scanned along the core liner surface with a digital IR camera. Our purpose was to detect the cooling effect caused by rapid gas hydrate dissolution. This approach was successful, as core segments with negative temperature anomalies of about –5°C proved to harbor gas hydrate. Hydrate was recovered from ~82 and ~148 mbsf as small pieces mixed with sediment. The recovered hydrate probably represented only a small fraction of the in situ hydrate because of rapid dissolution and loss in the expanding cores. Samples from four additional horizons (123, 142, 150, and 200 mbsf) probably contained disseminated gas hydrate, based on observed fizzing and scanned temperature anomalies as low as –3.2°C. Downhole sonic and resistivity logs suggest broad intervals of possible hydrate presence. Preliminary comparison of inferred hydrate distributions and PCS methane data sug-

gests that the interstitial concentrations of dissolved methane build up to reach the phase boundary of hydrate formation at ~50 mbsf. The dissolved concentrations may remain at this phase boundary at depth, with intervals of hydrate formation determined by the lithology and physical properties of the sediment.

The depth distribution of chloride in the interstitial water also provided evidence of hydrates, which release freshwater by dissolution during the wireline trip of the sediment core. Chloride shows a distinct gradient with a peak at 18 mbsf. This subsurface peak is presumably a remnant of the last glacial salinity excursion. It is accentuated by a drop in chlorinity below 18 mbsf that is probably due to freshening by hydrate dissolution. Within the methane zone, the drop in chlorinity is 10–27 mM and the concentrations show strong depth fluctuations with minimum values that appear to coincide with depths of hydrate occurrences (e.g., at 82 mbsf).

Ethane and propane are present at 1–2 ppm concentrations throughout the methane-rich zone down to ~140 mbsf. Their concentrations increase three- to fivefold over the next 70 m. Their distribution profiles suggest that ethane and propane are products of organic carbon degradation in the methanogenic zone.

Interstitial water analyses at Site 1230 provide clear evidence of very high microbial activity with extreme accumulations of products from organic degradation processes. Alkalinity and DIC increase steeply with depth from near seawater values at the sediment/water interface to a broad maxima of 155 mM at 100–150 mbsf, deep in the methanogenic zone. These concentrations are among the highest ever measured in marine sediments. Below this maximum, the concentrations drop again with depth. Ammonium likewise builds up extreme concentrations of 35,000 to 40,000 µM from 100 to 150 mbsf.

Below the interface of counter-diffusing sulfate and methane, there is a second diffusive interface between hydrogen sulfide and iron at 25 mbsf. The hydrogen sulfide produced from sulfate reduction reaches a peak concentration of 9.4 mM at the bottom of the sulfate zone. From there it decreases steeply both upward and downward, reaching zero near the sediment/water interface and at 25 mbsf. Iron is abundant (5–57 µM) in the interstitial water of the methane zone from 200 to 25 mbsf, where it meets the hydrogen sulfide and is inferred to precipitate as ferrous sulfide and pyrite.

A diffusive interface between sulfate and barium is encountered at 8–9 mbsf. Barium concentrations are only a few micromolar in the sulfate zone but increase steeply below that zone to plateau at 400 µM between 50 and 150 mbsf. At 250 mbsf the barium concentration approaches 1000 µM, which may be the highest interstitial water concentration of barium ever recorded in deep-sea sediments. The narrow depth interval of coexisting barium and sulfate appears to be a zone of barite precipitation. We infer their concentrations to be determined by the solubility product of barite in that zone. Consequently, the shallow sulfate zone is an effective barrier against upward diffusion of dissolved barium. Barium fronts associated with the sulfate boundary have also been observed in sediments of the Gulf of California and the South Atlantic Ocean (Brumsack, 1986; Kasten et al., 2001). Based on data from Leg 112, von Breymann et al. (1990) concluded that the deepest sites have the highest dissolved and solid-phase barium concentrations because detritus sedimenting through a deepwater column scavenges barium from seawater and enriches the sediment in barium.

Acetate and formate are generated as fermentation products and are used as substrates by sulfate-reducing or methanogenic prokaryotes. These VFAs are present at much higher concentrations at Site 1230 than at any other site studied during Leg 201. The acetate level is 5–20 µM in the sulfate reduction zone and reaches 230 µM in the methane zone at 145 mbsf. This acetate concentration is fivefold higher than at the most active sites on the Peru shelf and is even 10- to 100-fold higher than at the other deep-sea sites. Formate remains mostly at 5–10 µM throughout the sediment column. Hydrogen concentrations are low, in the 0.1- to 1.5-nM range.

The interstitial water at Site 1230 has a distinct yellow color that is not present at any other Leg 201 site. We presume this color is probably due to dissolved organic matter. The intensity of the color, which was measured spectrophotometrically, increases steeply from zero at the sediment/water interface to a broad maximum between 25 and 150 mbsf. Below that depth, it drops again to reach 15%–20% of the maximum value at 250 mbsf.

Prokaryotic cell concentrations in the organic-rich Pleistocene to Holocene sediments are near the average of previously studied subseafloor sediments in the upper 60 m of the sediment column. They are about threefold above average in the next 150 m. However, in the older accretionary wedge sediments below 216 mbsf, the cell density abruptly drops fourfold, from 7.9×10^6 to 1.9×10^6 cells/cm^3. This shows that the concentration of subseafloor prokaryotic cells at Site 1230 is closely related to sediment age rather than sediment depth. The factor that ultimately regulates cell concentrations may be the availability of energy substrates for prokaryotic metabolism.

Samples were taken at regular depth intervals through the entire sediment column for DNA and FISH-SIMS analysis, measurements of sulfate reduction rates, hydrogen turnover, methanogenesis rates, acetate turnover, thymidine incorporation, and prokaryote lipid biomarkers. Samples for cultivations and viable counts (MPN) target specific depths and geochemical zones, including the sulfate/methane interface and the hydrate-rich methane zone. Contamination tests with PFT and fluorescent beads show that the potential seawater contamination of Site 1230 microbiological samples is low or undetectable. The only case of detectable bead contamination in a slurry used for Site 1230 microbial cultivations is based on two beads counted in 100 microscopic fields of view scanned. By the experience accumulated during this leg, our confidence has strengthened that, with rigorous contamination controls and aseptic sampling techniques, deep subsurface samples can routinely be obtained without the introduction of microorganisms from the surface environment.

Four successful temperature measurements (two Adara tool deployments and two DVTP deployments) over a depth interval of 0–255 mbsf defined a geothermal gradient of 34.3°C/km at Site 1230, with a mudline temperature of 1.7°C and an estimated temperature of 11.2°C at 278 mbsf. The estimated local heat flux is 28 mW/m^2. This is similar to the heat flux calculated by Yamano and Uyeda (1990) at Site 685 from wireline logging data over 75–150 mbsf. Based on a downhole measurement of overpressure, upward interstitial water advection of ~1 cm/yr may occur at this site.

OPERATIONAL HIGHLIGHTS

Improved Recovery and Optimized Core Handling Procedures

According to our precruise operational strategy, all sites occupied during Leg 201 were previously cored during either ODP or DSDP expeditions. Each site was selected to define specific yet contrasting biogeochemical and sedimentary environments to address the fundamental questions regarding microbial communities and activities outlined in our cruise objectives. One outstanding operational result was the improved quality of core recovered relative to previous expeditions as a result of technological advancements in tools and modified coring and core handling techniques. At each site occupied, APC coring was pushed to significantly greater depths than achieved during previous occupations, thus providing cores with much less drilling disturbance than XCB cores (Table T1). This recovery was critical to meeting our geochemical and microbiological objectives, inasmuch as drilling disturbance that is endemic to XCB cores would have radically increased the potential of contamination of the cores with surface seawater.

T1. Operations summary, p. 79.

At many of our sites where subseafloor temperatures are well below ambient surface temperatures, thermal equilibration of the cores was a concern. With the cooperation of the rig floor personnel and technical staff, two shipboard strategies were developed to combat excessive core warming. Instead of the standard operational protocol of sleeving core barrels on the rig floor while a core barrel was deployed, the core was delivered to the catwalk as soon as the drill pipe was secure. This process required additional time and effort to reopen the drill string and deploy the next core barrel after core handling, but it minimized as much as possible the amount of time cores were exposed to ambient temperatures (consistently 25° to 27°C during the entire expedition). Subsections of cores intended for microbiological sampling were then transferred to either the hold refrigerator or the core locker, which were both regulated to 4°C. All microbiological subsampling was performed in the 4°C refrigerators, thus ensuring that organisms adapted to low subseafloor temperatures were protected from overheating.

Pressure Coring System

Discussions with the ODP Engineering Development Team prior to Leg 201 led to an agreement to deploy the redesigned PCS at least twice in a functional test mode at each of our first sites and to use the outcome of those tests to plan an operational strategy for further deployments at intervals of scientific interest during coring at subsequent sites. This program resulted in 17 deployments of the tool at six sites, most of them recovering core under pressure (Table T2). In addition, a specific experiment was designed at Site 1230, where a methane concentration profile was derived from multiple deployments (see "Downhole Tools," p. 31, in the "Site 1230" chapter).

T2. Summary of PCS operations, p. 80.

Fugro Percussion Corer

By agreement between ODP and developers of the third-party pressure coring device termed FPC, two engineers from Fugro Engineers B.V. joined the *JOIDES Resolution* at our shallow-water sites (1227, 1228, and

1229). We incorporated functional tests of the tool into our operational strategy, planning minimally six but potentially as many as nine tool deployments (an average of three per site) to provide the Fugro engineers data from which to derive an operational strategy for ODP Leg 204. Seven deployments were realized (Table T3) before the tool was damaged beyond our ability to repair at sea. However, we believe the intent and goals of the agreed deployment strategy were met and even exceeded during our operations.

T3. Summary of FPC operations, p. 81.

In Situ Temperature and Pressure Measurements

Downhole temperature profiles were augmented at six of our seven sites using the DVTP. In situ pressure measurements were attempted at all seven of the sites using the DVTP-P. The DVTP was deployed 18 times and returned a usable temperature profile in 12 cases. The DVTP-P was deployed 10 times. However, because of a series of mechanical malfunctions, shallow-water drill string behavior, and inhospitable formation conditions, only one record was considered reliable. Even this record did not have the characteristic spike and decay pattern recorded during previous deployments of the tool.

APC-Methane Tool

The APC-M tool was deployed at six of our seven sites. Data from these deployments will be evaluated postcruise, but initial observations suggest the electronics package was damaged in one of the early runs and data quality in subsequent deployments was compromised.

Perfluorocarbon Tracer

Perfluorocarbon tracer was pumped continuously throughout all coring operations during Leg 201 to monitor the potential of drilling fluid (surface seawater) contamination in cores sampled for microbiological studies. The tracer was metered into the circulation fluid system at a constant concentration (per Smith et al., 2000b) regulated by the shipboard rig instrumentation software. Results of analyses of PFT contamination are reported in "Microbiology" in each site chapter in this volume. In 21.7 days of coring operations, we consumed 22 canisters of PFT. For future operations with microbiological objectives, this consumption rate should be considered in precruise planning.

Fluorescent Microspheres

In addition to PFT, which indicated the potential for drilling fluid contamination in cores, fluorescent microspheres were deployed on individual cores to indicate whether or not microbe-sized particles might have infiltrated samples. The microspheres (in a suspension of deionized water) were transferred into a plastic bag that was installed in the core catcher. After several of the bags failed to rupture, the attachment geometry was modified by wedging both ends of the plastic bag into a shim above the core catcher and stretching the bag across the throat of the core barrel. The modified attachment geometry resulted in confirmed delivery of the microspheres on every subsequent deployment. Microspheres were deployed on 53 cores during Leg 201. For future reference, most of these were with dilute suspensions with six aliquots of diluted microspheres prepared from each bottle of concentrate. Early

deployments included undiluted suspensions, but we chose to use dilutions starting at our second site in order to conserve stock for later deployments. Stock on board at the beginning of Leg 201 was 24 bottles of concentrated microspheres; we used 22 bottles and could have used significantly more. Details of potential contamination as a result of these deployments are presented in "Microbiology" in each site chapter in this volume.

Thermal Infrared Camera

In preparation for Leg 204, a thermal imaging IR camera was tested at many of the sites occupied during Leg 201. During hydrogen sulfide alert status, camera operation was suspended because of restrictions on the number of personnel allowed on the catwalk and the potential of cable and air hose entanglement. The camera performed well (see "Physical Properties" in each site chapter) and provided a unique data set for Leg 201. However, future deployments of this system should include a less intrusive and less labor-intensive operational protocol.

Microbiological Rate Studies

For the first time in the history of ODP, radiotracer experiments were conducted in a van dedicated to this purpose. Routine monitoring during the expedition confirmed that work surfaces within the van remained free of contamination and, furthermore, that no contaminating radioactivity was carried outside of the van to other parts of the vessel.

REFERENCES

American Public Health Association, 1989. Estimation of bacterial density. *In* Clesceri, L.S., Greenberg, A.E., and Trussell, R.R. (Eds.), *Standard Methods for the Examination of Water and Wastewater* (17th ed.): Washington D.C. (American Public Health Association), 977–980.

Baker, P.A., Stout, P.M., Kastner, M., and Elderfield, H., 1991. Large-scale lateral advection of seawater through oceanic crust in the central equatorial Pacific. *Earth Planet. Sci. Lett.,* 105:522–533.

Bale, S.J., Goodman, K., Rochelle, P.A., Marchesi, J.R., Fry, J.C., Weightman, A.J., and Parkes, R.J., 1997. *Desulfovibrio profundus* sp. nov., a novel barophilic sulfate-reducing bacterium from deep sediment layers in the Japan Sea. *Int. J. Syst. Bacteriol.,* 47:515–521.

Bekins, B.A., Cozzarelli, I.M., Godsy, E.U., Warren, E., Essaid, H.I., and Tuccillo, M.E., 2001. Progression of natural attenuation processes at a crude oil spill site II. Controls on spatial distribution of microbial populations. *J. Contam. Hydrol.,* 53:387–406.

Boetius, A., Ravenschlag, K., Schubert, C.J., Rickert, D., Widdel, F., Gieseke, A., Amann, R., Jørgensen, B.B., Witte, U., and Pfannkuche, O., 2000. Microscopic identification of a microbial consortium apparently mediating anaerobic methane oxidation above marine gas hydrate. *Nature,* 407:623–626.

Borowski, W.S., Hoehler, T.M., Alperin, M.J., Rodriguez, N.M., and Paull, C.K., 2000. Significance of anaerobic methane oxidation in methane-rich sediments overlying the Blake Ridge gas hydrates. *In* Paull, C.K., Matsumoto, R., Wallace, P.J., and Dillon, W.P. (Eds.), *Proc. ODP, Sci. Results,* 164: College Station, TX (Ocean Drilling Program), 87–99.

Borowski, W.S., Paull, C.K., and Ussler, W., III, 1996. Marine pore-water sulfate profiles indicate in situ methane flux from underlying gas hydrate. *Geology,* 24:655–658.

————, 1999. Global and local variations of interstitial sulfate gradients in deep-water, continental margin sediments: sensitivity to underlying methane and gas hydrates. *Mar. Geol.,* 159:131–154.

Boström, K., Joensuu, O., Valdés, S., Charm, W., and Glaccum, R., 1976. Geochemistry and origin of East Pacific sediments sampled during DSDP Leg 34. *In* Yeats, R.S., Hart, S.R., et al., *Init. Repts. DSDP,* 34: Washington (U.S. Govt. Printing Office), 556–574.

Brady, S., and Gieskes, J.M., 1976. Interstitial water studies, Leg 34. *In* Yeats, R.S., Hart, S.R., et al., *Init. Repts., DSDP,* 34, Washington (U.S. Govt. Printing Office), 625–628.

Brumsack, H.-J., 1986. The inorganic geochemistry of Cretaceous black shales (DSDP Leg 41) in comparison to modern upwelling sediments from the Gulf of California. *In* Summerhayes, C.P., and Shackleton, N.J. (Eds.), *North Atlantic Palaeoceanography.* Spec. Publ.—Geol. Soc. London, 21:447–462.

Canfield, D.E., Jørgensen, B.B., Fossing, H., Glud, R.N., Gundersen, J., Ramsing, N.B., Thamdrup, B., Hansen, J.W., Nielsen, L.P., and Hall, P.O.J., 1993. Pathways of organic carbon oxidation in three continental margin sediments. *Mar. Geol.,* 113:27–40.

Chavez, F.P., and Barber, R.T., 1987. An estimate of new production in the equatorial Pacific. *Deep-Sea Res. Part A,* 34:1229–1243.

Cragg, B.A., Harvey, S.M., Fry, J.C., Herbert, R.A., and Parkes, R.J., 1992. Bacterial biomass and activity in the deep sediment layers of the Japan Sea, Hole 798B. *In* Pisciotto, K.A., Ingle, J.C., Jr., von Breymann, M.T., Barron, J., et al., *Proc. ODP, Sci. Results.,* 127/128 (Pt. 1): College Station, TX (Ocean Drilling Program), 761–776.

Cragg, B.A., and Kemp, A.E.S., 1995. Bacterial profiles in deep sediment layers from the eastern equatorial Pacific Ocean, Site 851. *In* Pisias, N.G., Mayer, L.A., Janecek,

T.R., Palmer-Julson, A., and van Andel, T.H. (Eds.), *Proc. ODP, Sci. Results,* 138: College Station, TX (Ocean Drilling Program), 599–604.

Cragg, B.A., Parkes, R.J., Fry, J.C., Herbert, R.A., Wimpenny, J.W.T., and Getliff, J.M., 1990. Bacterial biomass and activity profiles within deep sediment layers. *In* Suess, E., von Huene, R., et al., *Proc. ODP, Sci. Results,* 112: College Station, TX (Ocean Drilling Program), 607–619.

D'Hondt, S., Rutherford, S., and Spivack., A.J., 2002. Metabolic activity of the subsurface biosphere in deep-sea sediments. *Science,* 295:2067–2070.

Dickens, G.R., 2000. Methane oxidation during the Late Palaeocene Thermal Maximum. *Bull. Soc. Geol. Fr.,* 171:37–49.

Dickens, G.R., O'Neil, J.R., Rea, D.K., and Owen, R.M., 1995. Dissociation of oceanic methane hydrate as a cause of the carbon isotope excursion at the end of the Paleocene. *Paleoceanography,* 10:965–971.

Dickens, G.R., and Owen, R.M., 1999. The latest Miocene–early Pliocene biogenic bloom: a revised Indian Ocean perspective, *Mar. Geol.,* 161:75–91.

Dickens, G.R., Wallace, P.J., Paull, C.K., and Borowski, W.S., 2000. Detection of methane gas hydrate in the pressure core sampler (PCS): volume-pressure-time relations during controlled degassing experiments. *In* Paull, C.K., Matsumoto, R., Wallace, P.J., and Dillon, W.P. (Eds.), *Proc. ODP, Sci. Results,* 164: College Station, TX (Ocean Drilling Program), 113–126.

Dymond, J., Corliss, J.B., and Stillinger, R., 1976. Chemical composition and metal accumulation rates of metalliferous sediments from Sites 319, 320, and 321. *In* Yeats, R.S., Hart, S.R., et al., *Init. Repts. DSDP,* 34: Washington (U.S. Govt. Printing Office), 575–588.

Emeis, K.-C., Doose, H., Mix, A., and Schulz-Bull, D., 1995. Alkenone sea-surface temperatures and carbon burial at Site 846 (eastern equatorial Pacific Ocean): the last 1.3 m.y. *In* Pisias, N.G., Mayer, L.A., Janecek, T.R., Palmer-Julson, A., and van Andel, T.H. (Eds.), *Proc. ODP, Sci. Results,* 138: College Station, TX (Ocean Drilling Program), 605–613.

Farrell, J.W., Raffi, I., Janecek, T.C., Murray, D.W., Levitan, M., Dadey, K.A., Emeis, K.-C., Lyle, M., Flores, J.-A., and Hovan, S., 1995. Late Neogene sedimentation patterns in the eastern equatorial Pacific. *In* Pisias, N.G., Mayer, L.A., Janecek, T.R., Palmer-Julson, A., and van Andel, T.H. (Eds.), *Proc. ODP, Sci. Results,* 138: College Station, TX (Ocean Drilling Program), 717–756.

Fossing, H., 1990. Sulfate reduction in shelf sediments in the upwelling region off Central Peru. *Cont. Shelf Res.,* 10:355–367.

Getliff, J.M., Fry, J.C., Cragg, B.A., and Parkes, R.J., 1992. The potential for bacteria growth in deep sediment layers of the Japan Sea, Hole 798B—Leg 128. *In* Pisciotto, K.A., Ingle, J.C., Jr., von Breymann, M.T., Barron, J., et al., *Proc. ODP, Sci. Results,* 127/128 (Pt. 1): College Station, TX (Ocean Drilling Program), 755–760.

Hesselbo, S.P., Grocke, D.R., Jenkyns, H.C., Bjerrum, C.J., Farrimond, P., Bell, H.S.M., and Green, O.R., 2000. Massive dissociation of gas hydrate during a Jurassic oceanic anoxic event. *Nature,* 406:392–395.

Hinrichs, K.-U., 2001. A molecular recorder of methane hydrate destabilization. *Geochem. Geophys. Geosyst.,* 2 (Article), 2000GC000118.

Hinrichs, K.-U., Hayes, J.M., Sylva, S.P., Brewer, P.G., and DeLong, E.F., 1999. Methane consuming archaebacteria in marine sediments. *Nature,* 398:802–805.

Hoehler, T.M., Alperin, M.J., Albert, D.B., and Martens, C.S., 1994. Field and laboratory studies of methane oxidation in anoxic marine sediment: evidence for a methanogen-sulfate reducer consortium. *Global Biogeochem. Cycles,* 8:451–463.

————, 1998. Thermodynamic control on hydrogen concentrations in anoxic sediments. *Geochim. Cosmochim. Acta,* 62:1745–1756.

————, 2001. Apparent minimum free energy requirements for methanogenic Archaea and sulfate-reducing bacteria in an anoxic marine sediment, *FEMS Microbio. Ecol.,* 38:33–41.

Holland, H.D., 1984. *The Chemical Evolution of the Atmosphere and Oceans:* Princeton, NJ (Princeton Univ. Press).

Iversen, N., and Jørgensen, B.B., 1985. Anaerobic methane oxidation rates at the sulfate–methane transition in marine sediments from Kattegat and Skagerrak (Denmark). *Limnol. Oceanogr.,* 30:944–955.

Jørgensen, B.B., 1978. A comparison of methods for the quantification of bacterial sulfate reduction in coastal marine sediments. III. Estimation from chemical and bacteriological field data. *Geomicrobiol. J.,* 1:49–64.

Kasten, S., Haese, R.R., Zabel, M., Ruhlemann, C., and Schulz, H.D., 2001. Barium peaks at glacial terminations in sediments of the equatorial Atlantic Ocean—relicts of deglacial productivity pulses? *Chem. Geol.,* 175:635–651.

Kastner, M., Elderfield, H., Martin, J.B., Suess, E., Kvenvolden, K.A., and Garrison, R.E., 1990. Diagenesis and interstitial-water chemistry at the Peruvian continental margin—major constituents and strontium isotopes. *In* Suess, E., von Huene, R., et al., *Proc. ODP, Sci. Results,* 112: College Station, TX (Ocean Drilling Program), 413–440.

Kennett, J.P., Cannariato, K.G., Hendy, I.L., and Behl, R.J., 2000. Carbon isotopic evidence for methane hydrate instability during Quaternary interstadials. *Science,* 288:128–133.

Kieft, T.L., Fredrickson, J.K., Onstott, T.C., Gorby, Y.A., Kostandarithes, H.M., Bailey, T.J., Kennedy, D.W., Li, S.W., Plymale, A.E., Spadoni, C.M., and Gray, M.S., 1999. Dissimilatory reduction of Fe(III) and other electron acceptors by a *Thermus* isolate. *Appl. Environ. Microbiol.* 65:1214–1221.

King, G.M., 1984. Utilization of hydrogen, acetate, and noncompetitive substrates by methanogenic bacteria in marine sediments, *Geomicrobiol. J.,* 3:275–306.

Knoblauch, C., Jørgensen, B.B., and Harder, J., 1999. Community size and metabolic rates of psychrophilic sulfate-reducing bacteria in Arctic marine sediments. *Appl. Environ. Microbiol.,* 65:4230–4233.

Kvenvolden, K.A., 1993. Gas hydrates: geological perspective and global change. *Rev. Geophys.,* 31:173–187.

Kvenvolden, K.A., Frank, T.J., and Golan-Bac, M., 1990. Hydrocarbon gases in Tertiary and Quaternary sediments offshore Peru—results and comparisons. *In* Suess, E., von Huene, R., et al., *Proc. ODP, Sci. Results,* 112: College Station, TX (Ocean Drilling Program), 505–515.

Kvenvolden, K.A., and Kastner, M., 1990. Gas hydrates of the Peruvian outer continental margin. *In* Suess, E., von Huene, R., et al., *Proc. ODP, Sci. Results,* 112: College Station, TX (Ocean Drilling Program), 517–526.

Lanoil, B.D., Sassen, R., La Duc, M.T., Sweet, S.T., and Nealson, K.H., 2001. Bacteria and Archea physically attached with Gulf of Mexico hydrates. *Appl. Environ. Microbiol.,* 67:5143–5133.

Lonergan, D.J., Jenter, H.L., Coates, J.D., Phillips, E.J.P., Schmidt, T.M., and Lovley, D.R., 1996. Phylogenetic analysis of dissimilatory Fe(III)-reducing bacteria. *J. Bacteriol.,* 178:2402–2408.

Lovley, D.R., and Goodwin, S., 1988. Hydrogen concentrations as an indicator of the predominant terminal electron-accepting reactions in aquatic sediments, *Geochim. Cosmochim. Acta,* 52:2993–3003.

Mayer, L., Pisias, N., Janecek, T., et al., 1992. *Proc. ODP, Init. Repts.,* 138 (Pt. 1): College Station, TX (Ocean Drilling Program).

Mossmann, J.-R., Aplin, A.C., Curtis, C.D., and Coleman, M.L., 1990. Sulfur geochemistry at Sites 680 and 686 on the Peru margin. *In* Suess, E., von Huene, R., et al., *Proc. ODP, Sci. Results,* 112: College Station, TX (Ocean Drilling Program), 455–464.

Niewöhner, C., Henson, C., Kasten, S., Zabel, M., and Schultz, H.D., 1998. Deep sulfate reduction completely mediated by anaerobic methane oxidation in sediments of the upwelling area off Namibia. *Geochim. Cosmochim. Acta,* 62:455–464.

Oremland, R.S., Culbertson, C., and Simoneit, B.R.T., 1982a. Methanogenic activity in sediment from Leg 64, Gulf of California. *In* Curray, J.R., Moore, D.G., et al., *Init. Repts. DSDP,* 64 (Pt. 2): Washington (U.S. Govt. Printing Office), 759–762.

Oremland, R.S., Marsh, L.M., and Polcin, S., 1982b. Methane production and simultaneous sulfate reduction in anoxic salt marsh sediments. *Nature,* 296:143–145.

Oremland, R.S., and Polcin, S., 1982. Methanogenesis and sulfate reduction: competitive and noncompetitive substrates in estuarine sediments. *Appl. Environ. Microbiol.,* 44:1270–1276.

Orphan, V.J., House, C.H., Hinrichs, K.-U., McKeegan, K.D., and De Long, E.F., 2001. Methane consuming archea revealed by directly coupled isotopic and phylogenetic analysis. *Science,* 293:484–487.

Oyun, S., Elderfield, H., and Klinkhammer, G.P., 1995. Strontium isotopes in pore waters of east equatorial Pacific sediments: indicators of seawater advection through oceanic crust and sediments. *In* Pisias, N.G., Mayer, L.A., Janecek, T.R., Palmer-Julson, A., and van Andel, T.H. (Eds.), *Proc. ODP, Sci. Results,* 138: College Station, TX (Ocean Drilling Program), 813–819.

Parkes, R.J., Cragg, B.A., Bale, S.J., Getliff, J.M., Goodman, K., Rochelle, P.A., Fry, J.C., Weightman, A.J., and Harvey, S.M., 1994. A deep bacterial biosphere in Pacific Ocean sediments. *Nature,* 371:410–413.

Parkes, R.J., Cragg, B.A., Fry, J.C., Herbert, R.A., and Wimpenny, J.W.T., 1990. Bacterial biomass and activity in deep sediment layers from the Peru margin. *Philos. Trans. R. Soc. London A,* 331:139–153.

Parkes, R.J., Cragg, B.A., Getliff, J.M., Harvey, S.M., Fry, J.C., Lewis, C.A., and Rowland, S.J., 1993. A quantitative study of microbial decomposition of biopolymers in Recent sediments from the Peru Margin. *Mar. Geol.,* 113:55–66.

Parkes, R.J., Cragg, B.A., and Wellsbury, P., 2000. Recent studies on bacterial populations and processes in marine sediments: a review. *Hydrogeol. Rev.,* 8:11–28.

Pilson, M.E.Q., 1998. *An Introduction to the Chemistry of the Sea:* Upper Saddle River (Prentice Hall).

Pisias, N.G., Mayer, L.A., Janecek, T.R., Palmer-Julson, A., and van Andel, T.H. (Eds.), 1995. *Proc. ODP, Sci Results,* 138: College Station, TX (Ocean Drilling Program).

Pisias, N.G., Mayer, L.A., and Mix, A.C., 1995. Paleoceanography of the eastern equatorial Pacific during the Neogene: synthesis of Leg 138 drilling results. *In* Pisias, N.G., Mayer, L.A., Janecek, T.R., Palmer-Julson, A., and van Andel, T.H. (Eds.), *Proc. ODP, Sci. Results,* 138: College Station, TX (Ocean Drilling Program), 5–21.

Ravenschlag, K., Sahm, K., Knoblauch, C., Jørgensen, B.B., and Amann, R., 2000. Community structure, cellular rRNA content and activity of sulfate-reducing bacteria in marine Arctic sediments. *Appl. Environ. Microbiol.,* 66:3592–3602.

Rowe, G.T., and Howarth, R., 1985. Early diagenesis of organic matter in sediments off the coast of Peru. *Deep-Sea Res.,* 32:43–55.

Schink, B., 1997. Energetics of syntrophic cooperation in methanogenic degradation. *Microbiol. Mol. Biol. Rev.,* 61:262–280.

Sclater, J.G., Crowe, J., and Anderson, R.N., 1976. On the reliability of ocean heat flow averages. *J. Geophys. Res.,* 81:2997–3006.

Shipboard Scientific Party, 1976. Site 321. *In* Yeats, R.S., Hart, S.R., et al., *Init. Repts. DSDP,* 34: Washington (U.S. Government Printing Office), 111–153.

————, 1988a. Site 680. *In* Suess, E., von Huene, R., et al., *Proc. ODP, Init. Repts.,* 112: College Station, TX (Ocean Drilling Program), 249–304.

————, 1988b. Site 681. *In* Suess, E., von Huene, R., et al., *Proc. ODP, Init. Repts.,* 112: College Station, TX (Ocean Drilling Program), 305–362.

————, 1988c. Site 684. *In* Suess, E., von Huene, R., et al., *Proc. ODP, Init. Repts.,* 112: College Station, TX (Ocean Drilling Program), 525–596.

————, 1988d. Site 685. *In* Suess, E., von Huene, R., et al., *Proc. ODP, Init. Repts.,* 112: College Station, TX (Ocean Drilling Program), 597–704.

————, 1992a. Site 846. *In* Mayer, L., Pisias, N., Janecek, T., et al., *Proc. ODP, Init. Repts.,* 138 (Pt. 1): College Station, TX (Ocean Drilling Program), 265–333.

————, 1992b. Site 851b. *In* Mayer, L., Pisias, N., Janecek, T., et al., *Proc. ODP, Init. Repts.,* 138 (Pt. 2): College Station, TX (Ocean Drilling Program), 891–965.

————, 1999. Leg 180 summary. *In* Taylor, B., Huchon, P., Klaus, A., et al., *Proc. ODP, Init. Repts.,* 180: College Station, TX (Ocean Drilling Program), 1–77.

Smith, D.C., Spivack, A.J., Fisk, M.R., Haveman, S.A., Staudigel, H., and ODP Leg 185 Shipboard Scientific Party, 2000a. Methods for quantifying potential microbial contamination during deep ocean coring. *ODP Tech. Note,* 28 [Online]. Available from the World Wide Web: <http://www-odp.tamu.edu/publications/tnotes/tn28/INDEX.HTM>. [2002-03-30]

————, 2000b. Tracer-based estimates of drilling-induced microbial contamination of deep sea crust. *Geomicrobiol. J.,* 17:207–219.

Sørensen, J., Christensen, D., and Jørgensen, B.B., 1981. Volatile fatty acids and hydrogen as substrates for sulfate-reducing bacteria in anaerobic marine sediment. *Appl. Environ. Microbiol.,* 42:5–11.

Spivack, A.J., and You, C.F., 1997. Boron isotopic geochemistry of carbonates and pore waters, Ocean Drilling Program Site 851. *Earth Planet. Sci. Lett.,* 152:113–122.

Suess, E., von Huene, R., et al., 1988. *Proc. ODP, Init. Repts.,* 112: College Station, TX (Ocean Drilling Program).

————, 1990. *Proc. ODP, Sci. Results,* 112: College Station, TX (Ocean Drilling Program).

Tarafa, M.E., Whelan, J.K., Oremland, R.S., and Smith, R.L., 1987. Evidence of microbiological activity in Leg 95 (New Jersey Transect) sediments. *In* Poag, C.W., Watts, A.B., et al., *Init. Repts. DSDP,* 95: Washington (U.S. Govt. Printing Office), 635–640.

Teske, A., Hinrichs, K.-U., Edgcomb, V., de Vera Gomez, A., Kysela, D., Sylva, S.P., Sogin, M.C., and Jannasch, H.W., 2002. Microbial diversity of hydrothermal sediments in the Guaymas Basin: evidence for anaerobic methanotrophic communities. *Appl. Environ. Microbiol.,* 68:1994–2007.

Thauer, R.K., Jungermann, K., and Decker, K., 1977. Energy conservation in chemotrophic anaerobic bacteria. *Bacteriol. Rev.,* 41:100–180.

Thierstein, H.R., and Störrlein, U., 1991. Living bacteria in Antarctic sediments from Leg 119. *In* Barron, J., Larsen, B., et al., *Proc. ODP, Sci. Results,* 119: College Station, TX (Ocean Drilling Program), 687–692.

Valentine, D.L., and Reeburgh, W.S., 2000. New perspectives on anaerobic methane oxidation. *Environ. Microbiol.,* 2:477–484.

van Andel, T.H., Heath, G.R., and Moore, T.C., Jr., 1975. Cenozoic history and paleoceanography of the central equatorial Pacific Ocean: a regional synthesis of Deep Sea Drilling Project data. *Mem.—Geol. Soc. Am.,* 143.

Vargas, M., Kashefi, K., Blunt-Harris, E.L., and Lovley, D.R., 1998. Microbial evidence for Fe(III) reduction on early Earth. *Nature,* 395:65–68.

von Breymann, M.T., Emeis, K.-C., and Camerlenghi, A., 1990. Geochemistry of sediments from the Peru upwelling area: results from Sites 680, 682, 685, and 688. *In* Suess, E., von Huene, R., et al., *Proc. ODP, Sci. Results,* 112: College Station, TX (Ocean Drilling Program), 491–503.

Von Herzen, R.P., and Uyeda, S., 1963. Heat flow through the Pacific Ocean floor. *J. Geophys. Res.,* 68:4219–4250.

Wellsbury, P., Mather, I.D., and Parkes, R.J., in press. Geomicrobiology of deep, low organic carbon sediments in the Woodlark Basin, Pacific Ocean. *FEMS Microbiol. Ecol.*

Wellsbury, P., and Parkes, R.J., 1995. Acetate bioavailability and turnover in an estuarine sediment. *FEMS Microbiol. Ecol.,* 17:85–94.

Whelan, J.K., Oremland, R., Tarafa, M., Smith, R., Howarth, R., and Lee, C., 1986. Evidence for sulfate-reducing and methane producing microorganisms in sediments from Sites 618, 619, and 622. *In* Bouma, A.H., Coleman, J.M., Meyer, A.W., et al., *Init. Repts. DSDP,* 96: Washington (U.S. Govt. Printing Office), 767–775.

Whitman, W.B., Coleman, D.C., and Wiebe, W.J., 1998. Prokaryotes: the unseen majority. *Proc. Nat. Acad. Sci. U.S.A.,* 95:6578–6583.

Winfrey, M.R., and Ward, D.M., 1983. Substrates for sulfate reduction and methane production in intertidal sediments. *Appl. Environ. Microbiol.,* 45:193–199.

Yamano, M., and Uyeda, S., 1990. Heat-flow studies in the Peru Trench subduction zone. *In* Suess, E., von Huene, R., et al., *Proc. ODP, Sci. Results,* 112: College Station, TX (Ocean Drilling Program), 653–661.

Yeats, R.S., Hart, S.R., et al., 1976. *Init. Repts DSDP,* 34: Washington (U.S. Govt. Printing Office).

Figure F1. A. Map showing general locations of drill sites occupied during Legs 138 (rectangle B) and 112 (rectangle C). (Continued on next page.)

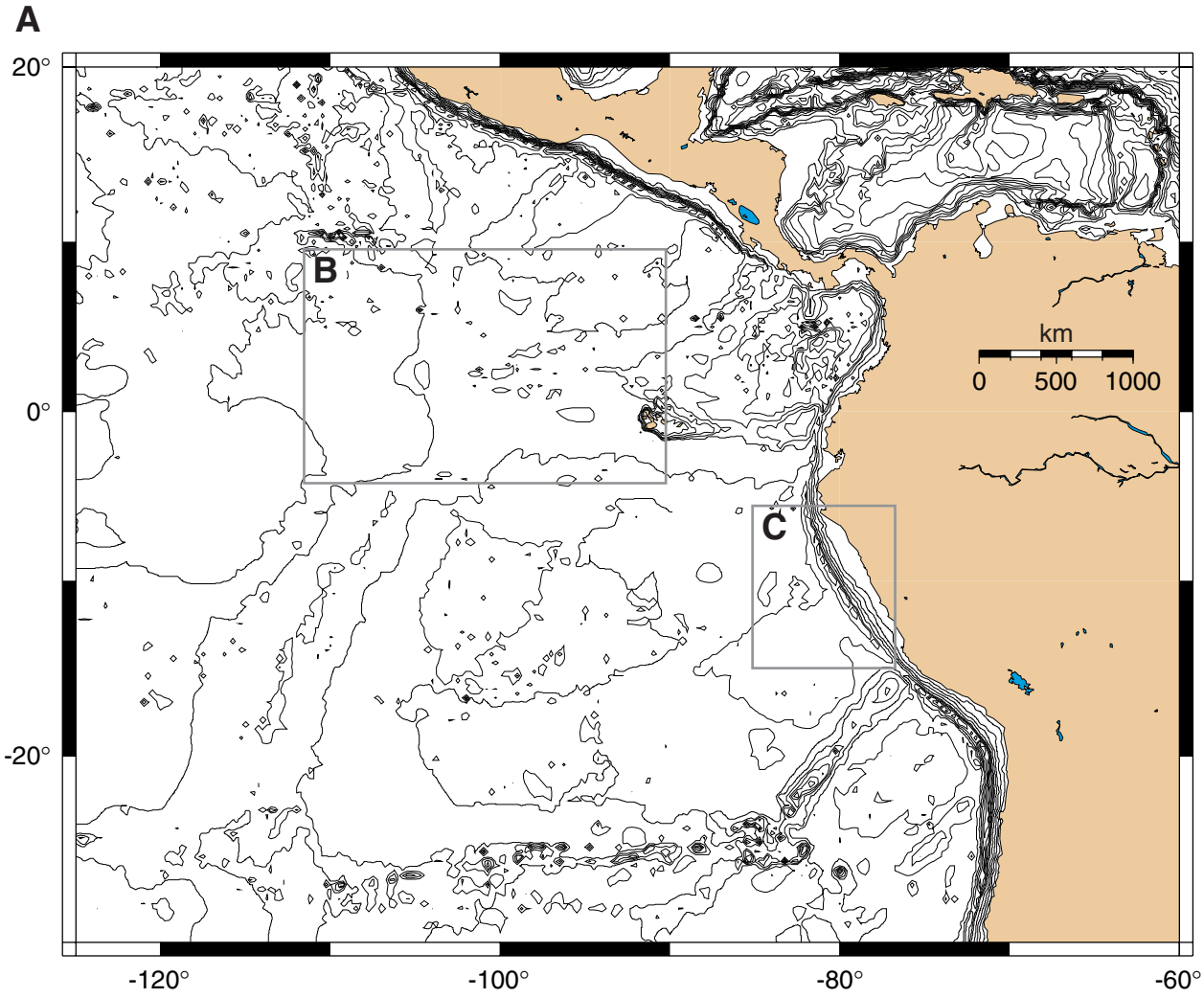

Figure F1 (continued). B. Detail map of equatorial Pacific primary sites with nomenclature. Previous ODP designations are in parentheses. **C.** Detail map of Peru margin primary sites and nomenclature. Previous DSDP/ODP site designations are in parentheses.

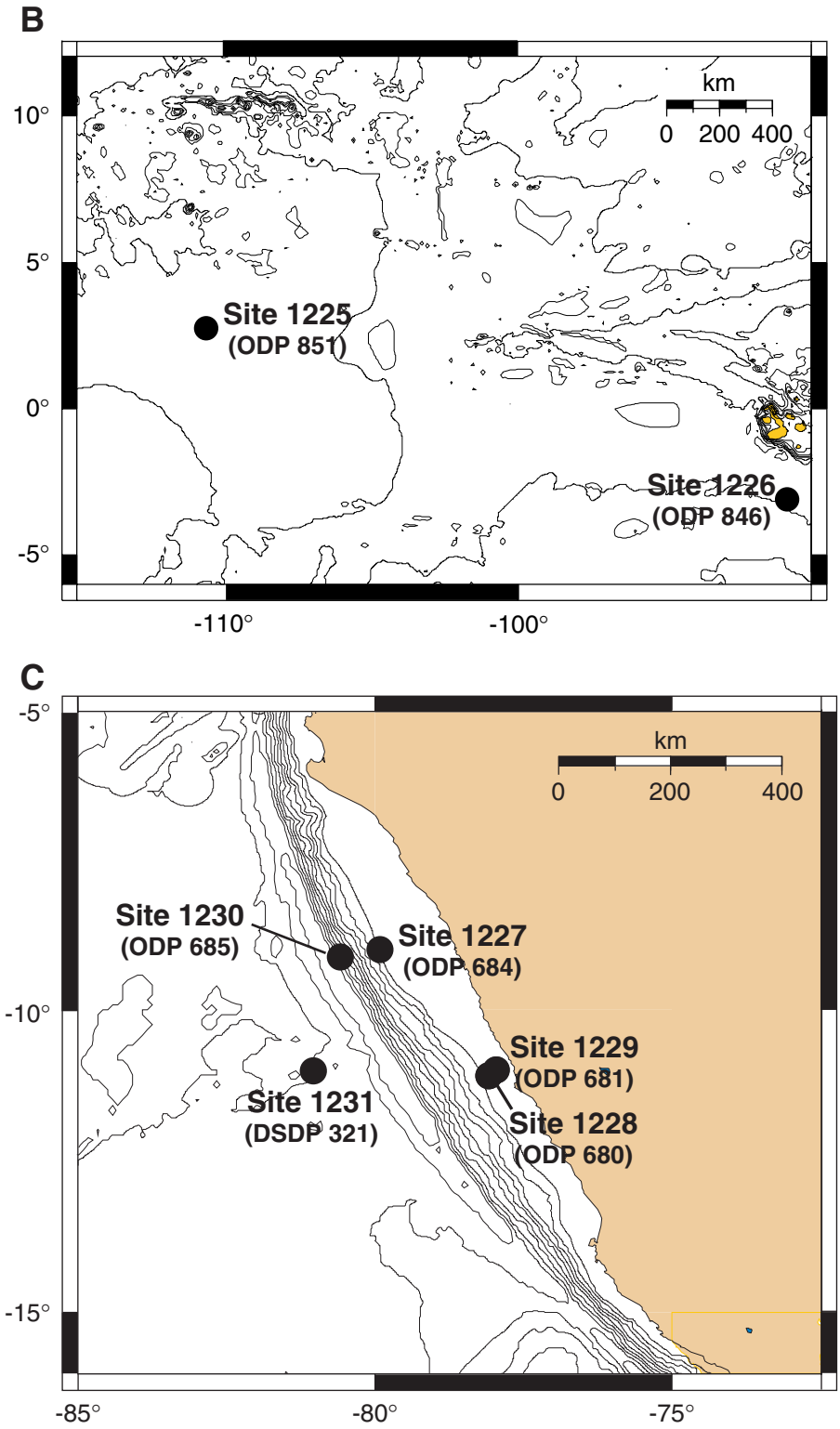

Figure F2. Lithostratigraphic summary. **A.** Open-ocean Leg 201 sites. (Continued on next page.)

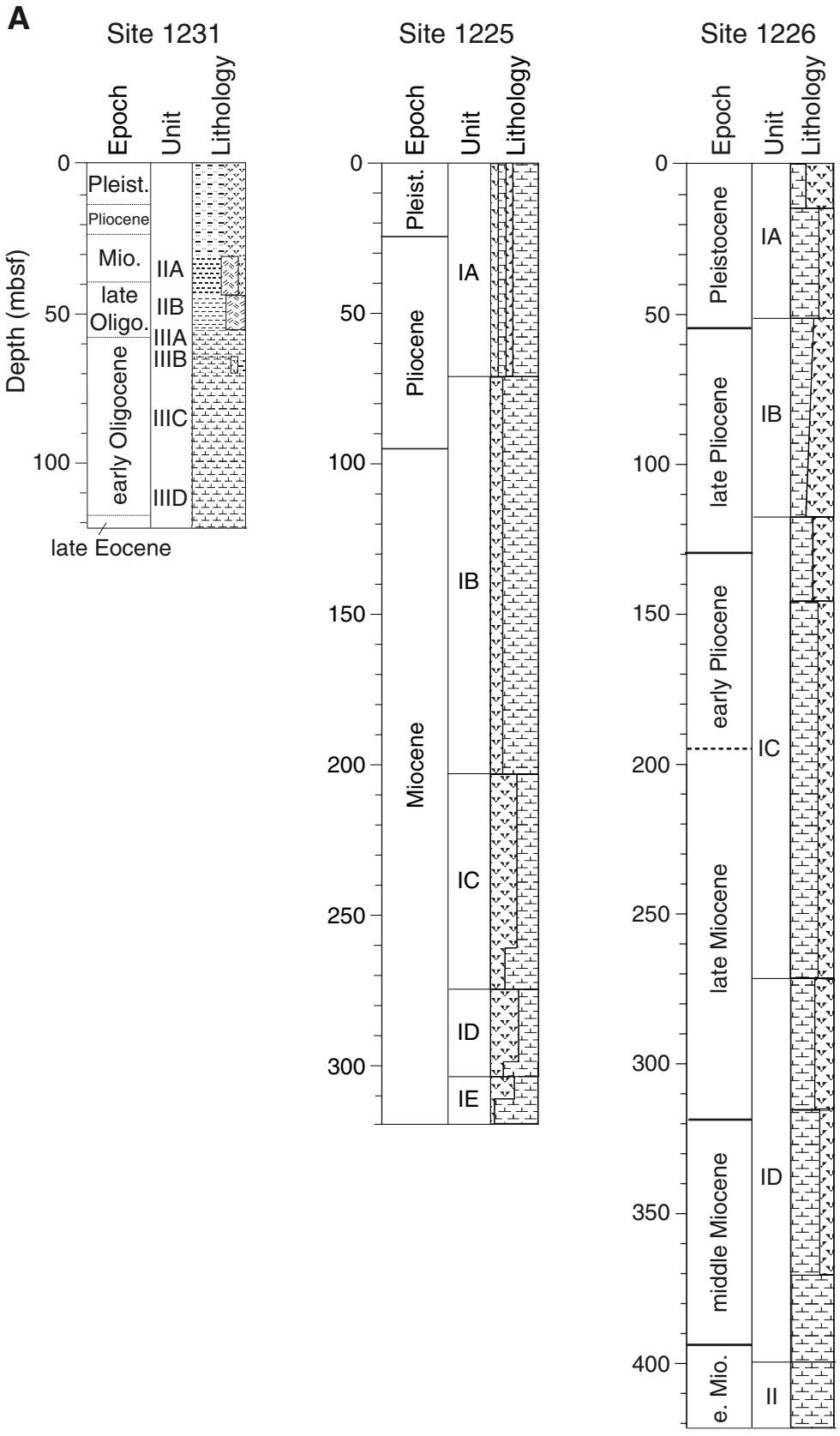

Figure F2 (continued). B. Ocean-margin Leg 201 sites.

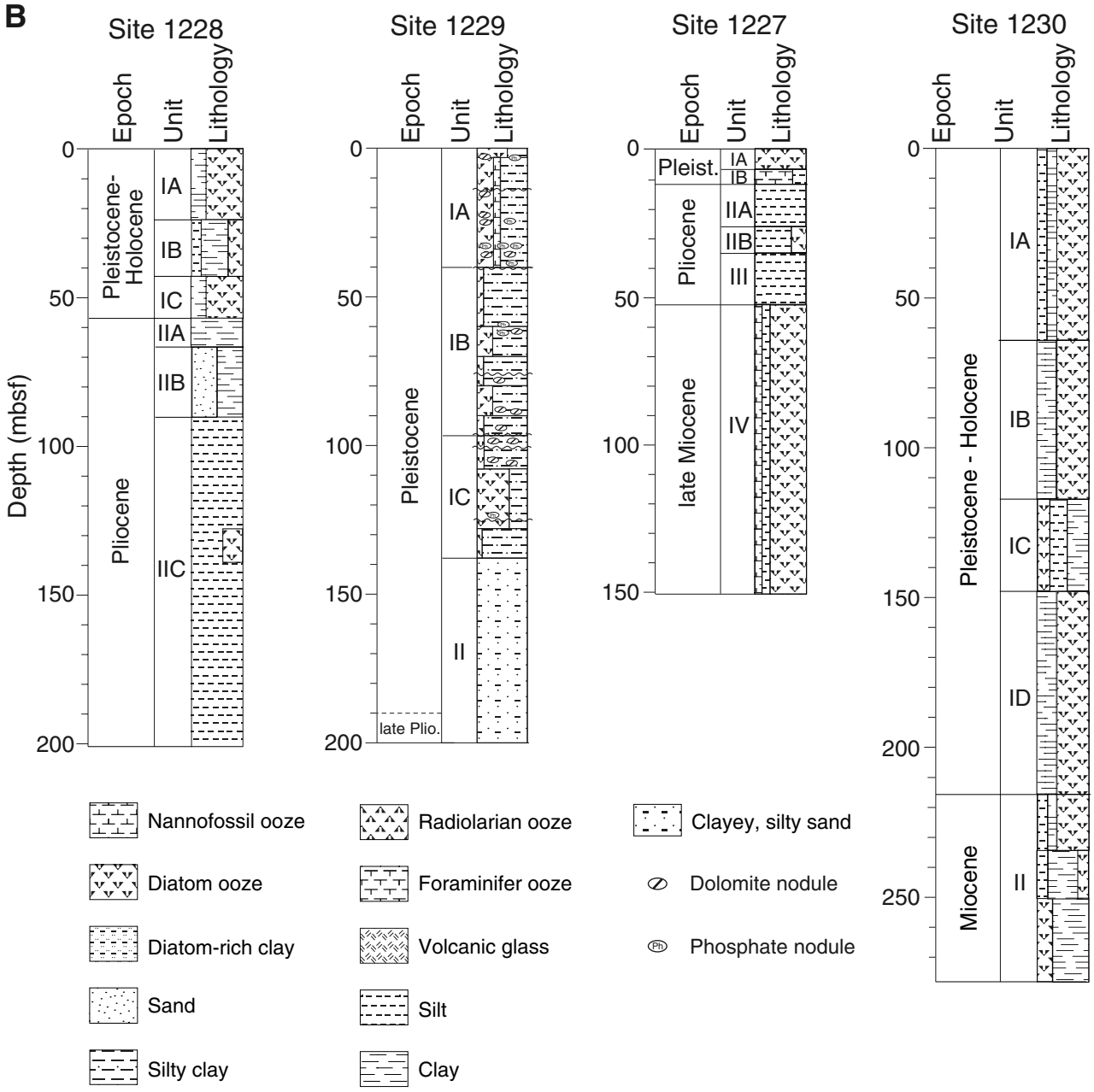

Figure F3. Downhole temperature profiles of Leg 201 sites. Symbols = measured downhole and seafloor temperatures. Dashed lines = least-square fits illustrating differences in gradients and offset of shelf sites resulting from higher seafloor temperatures.

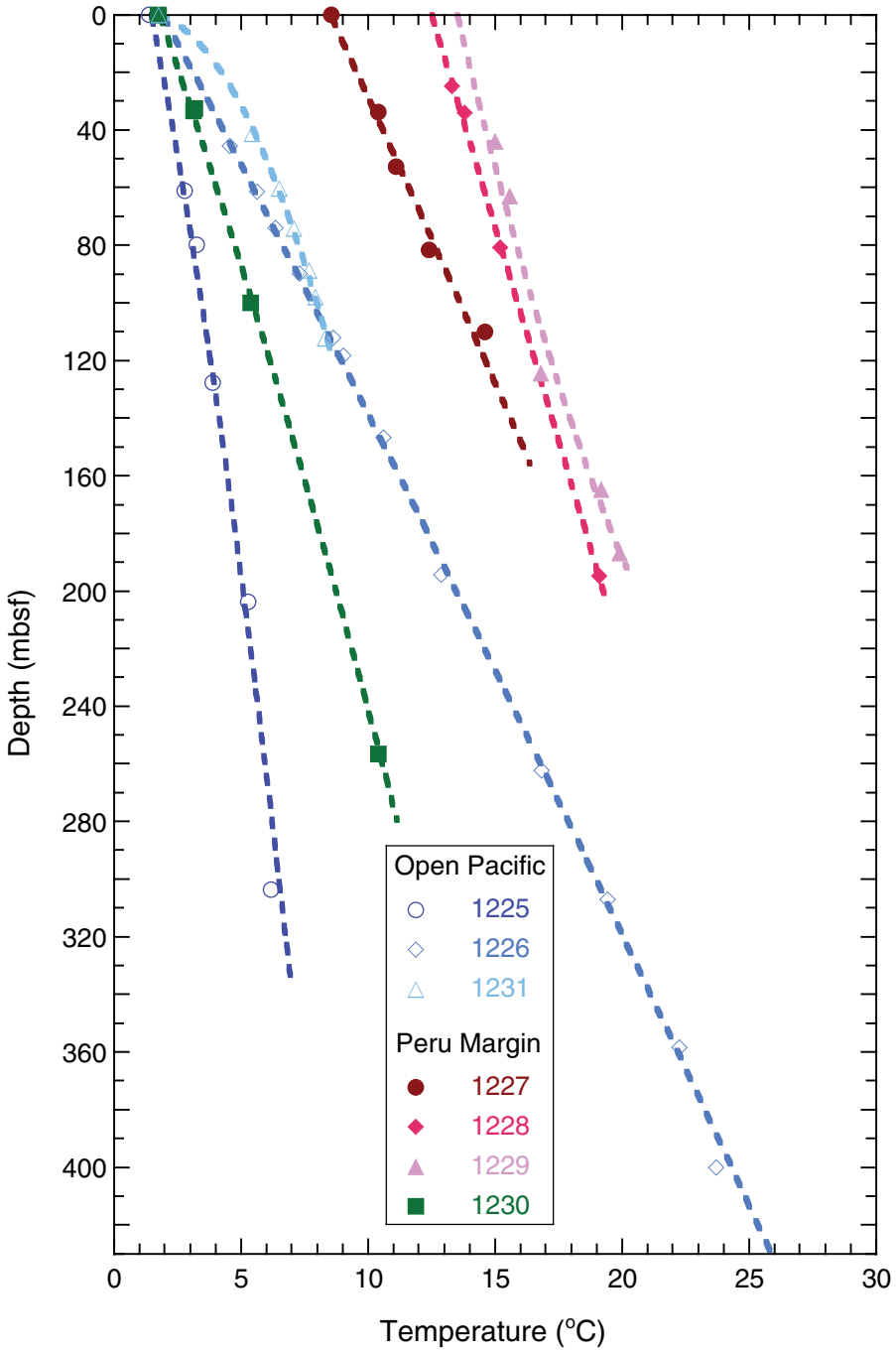

Figure F4. Cell enumeration data. Dashed line = geometric mean cell concentrations of previously censused ODP sites.

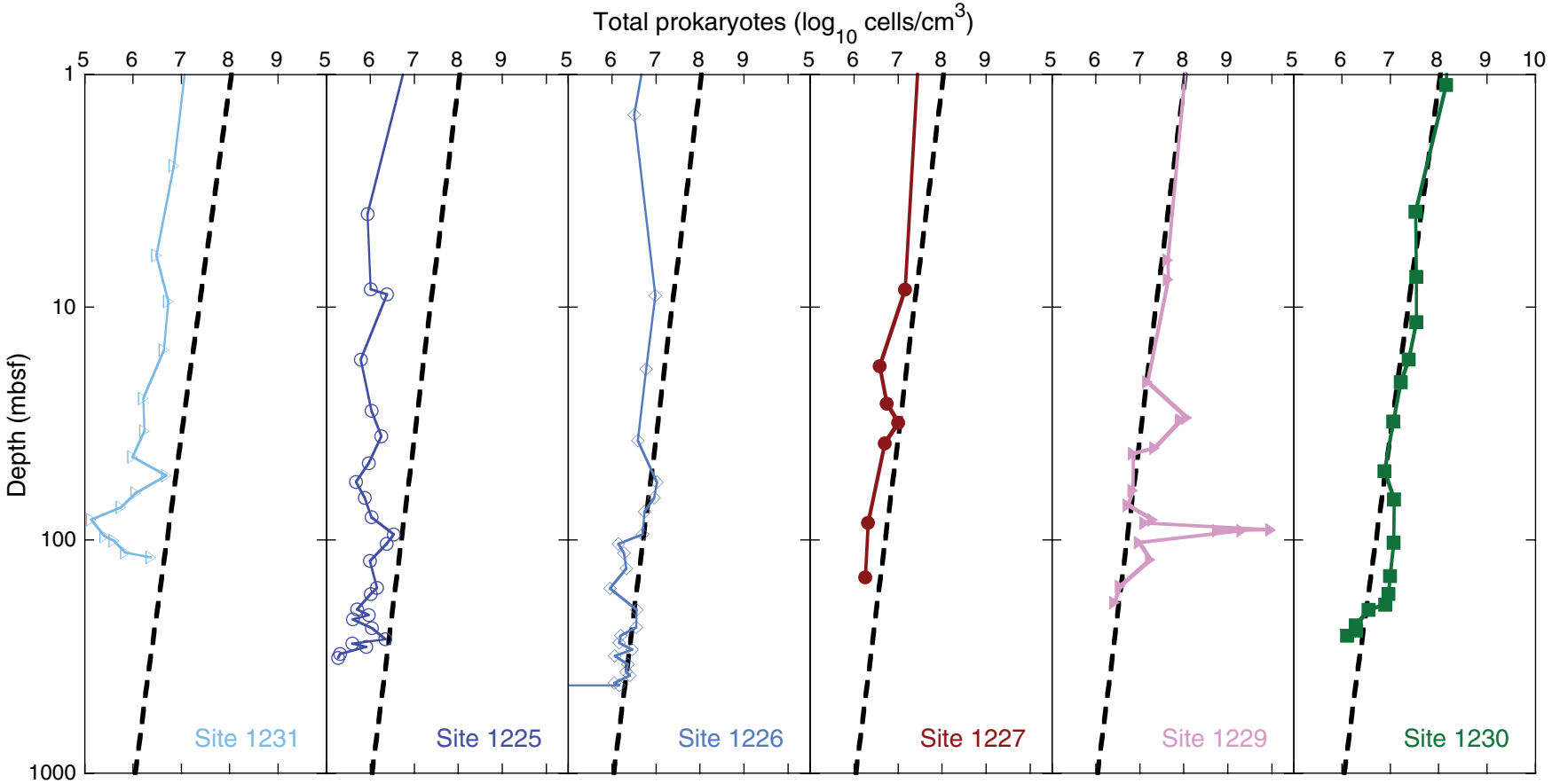

Figure F5. Cell enumeration data for Leg 201 sites compared to previously censused sites. Heavy dashed line = geometric means of cell concentrations at previously censused ODP sites. Heavy dotted lines = 2-σ envelope of cell concentrations at previously censused sites. Light dotted line = geometric means of all Leg 201 cell counts (y = 7.5316 – 0.55795 log (x); r^2 = 0.25).

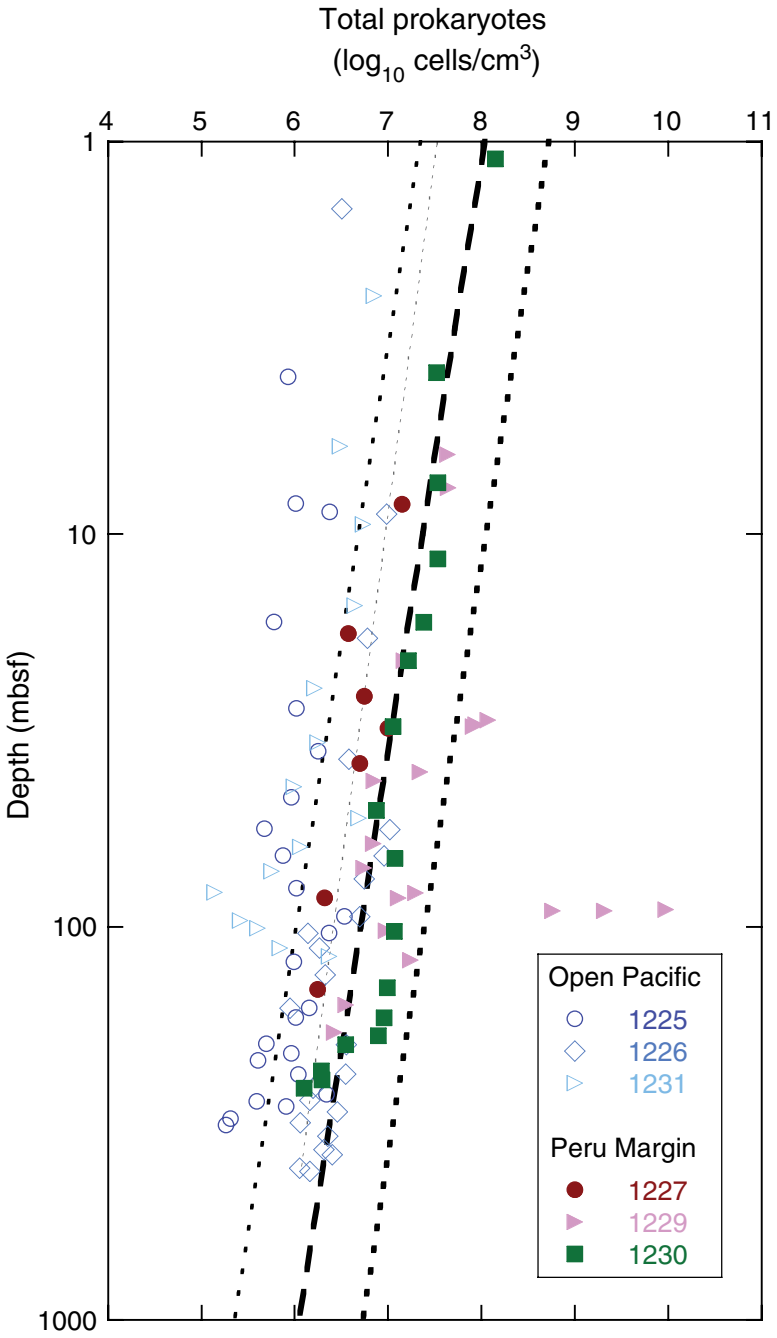

Figure F6. Histogram of maximum dissolved inorganic carbon (DIC) concentrations at Leg 201 sites.

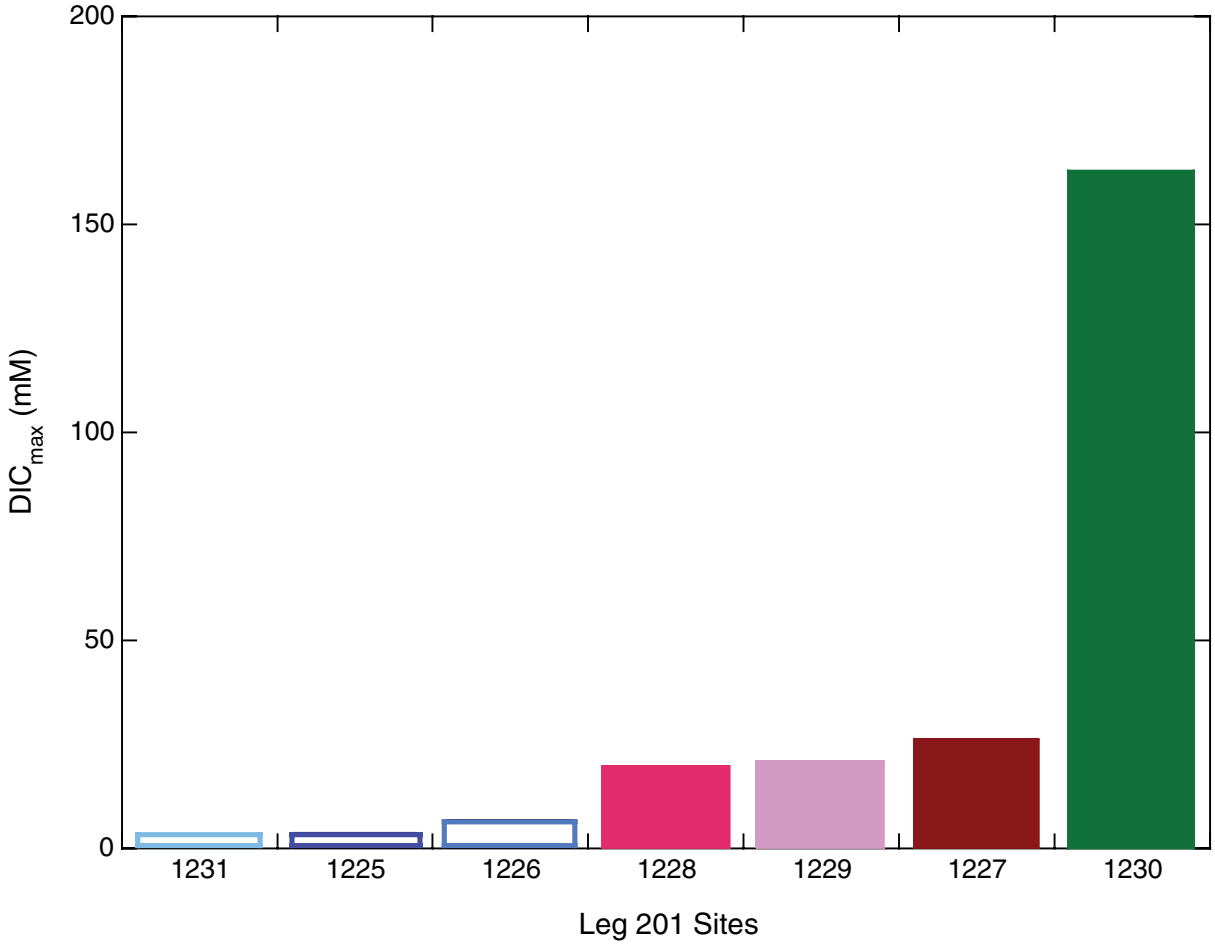

Figure F7. Dissolved inorganic carbon (DIC) profiles of Leg 201 sites.

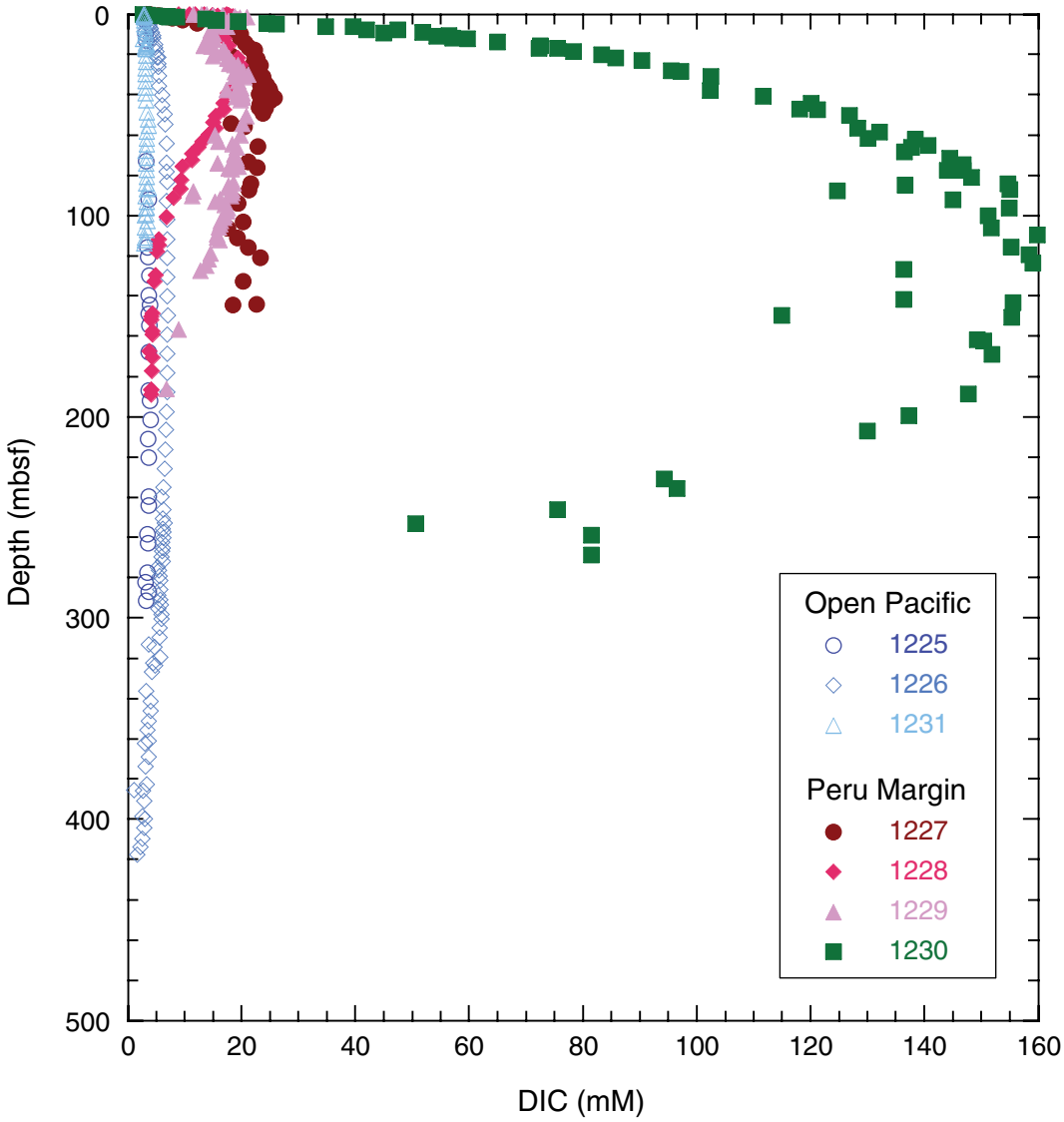

Figure F8. A. Dissolved sulfate profiles of Leg 201 sites. **B.** Dissolved manganese profiles of Leg 201 sites.

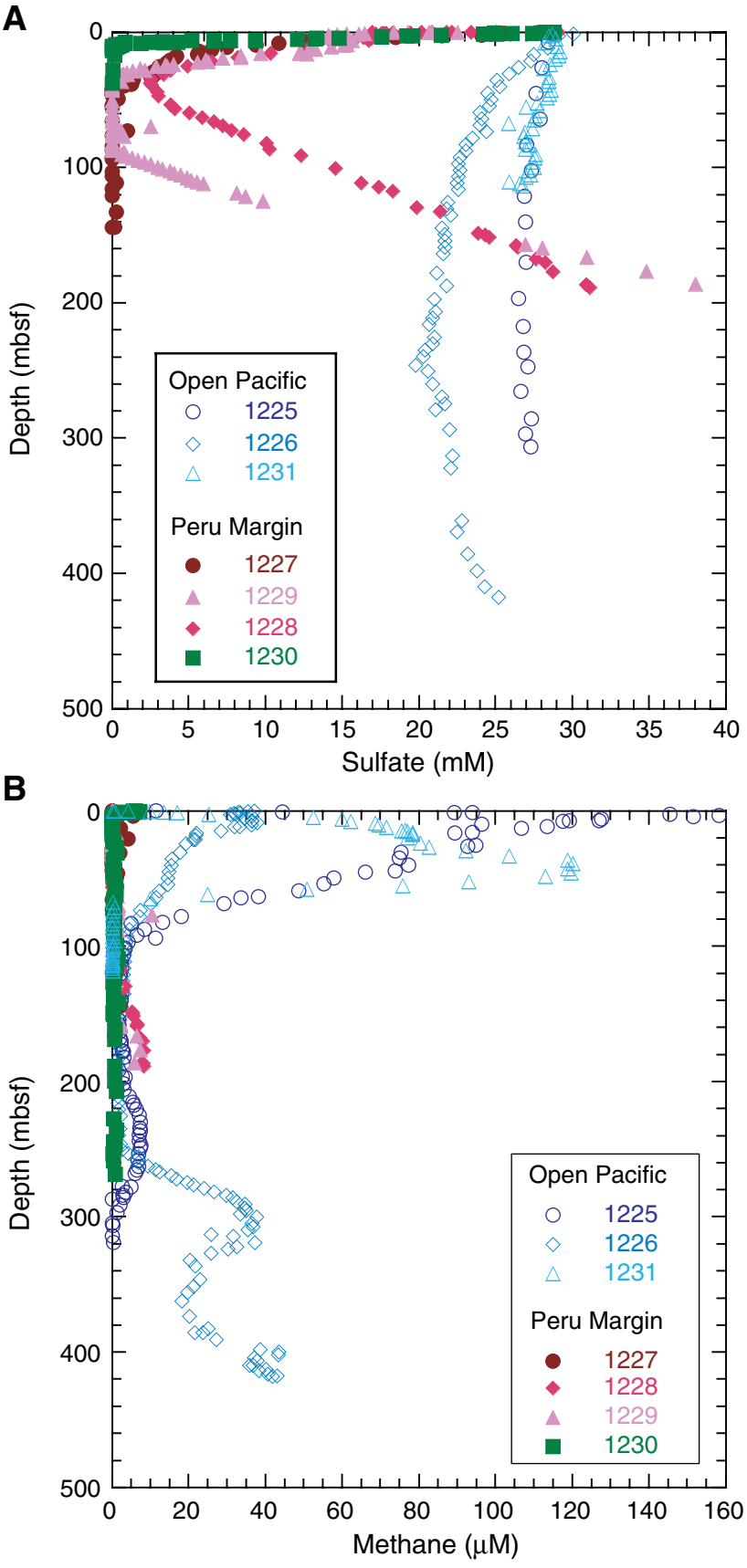

Figure F9. Methane concentration profiles of Leg 201 sites.

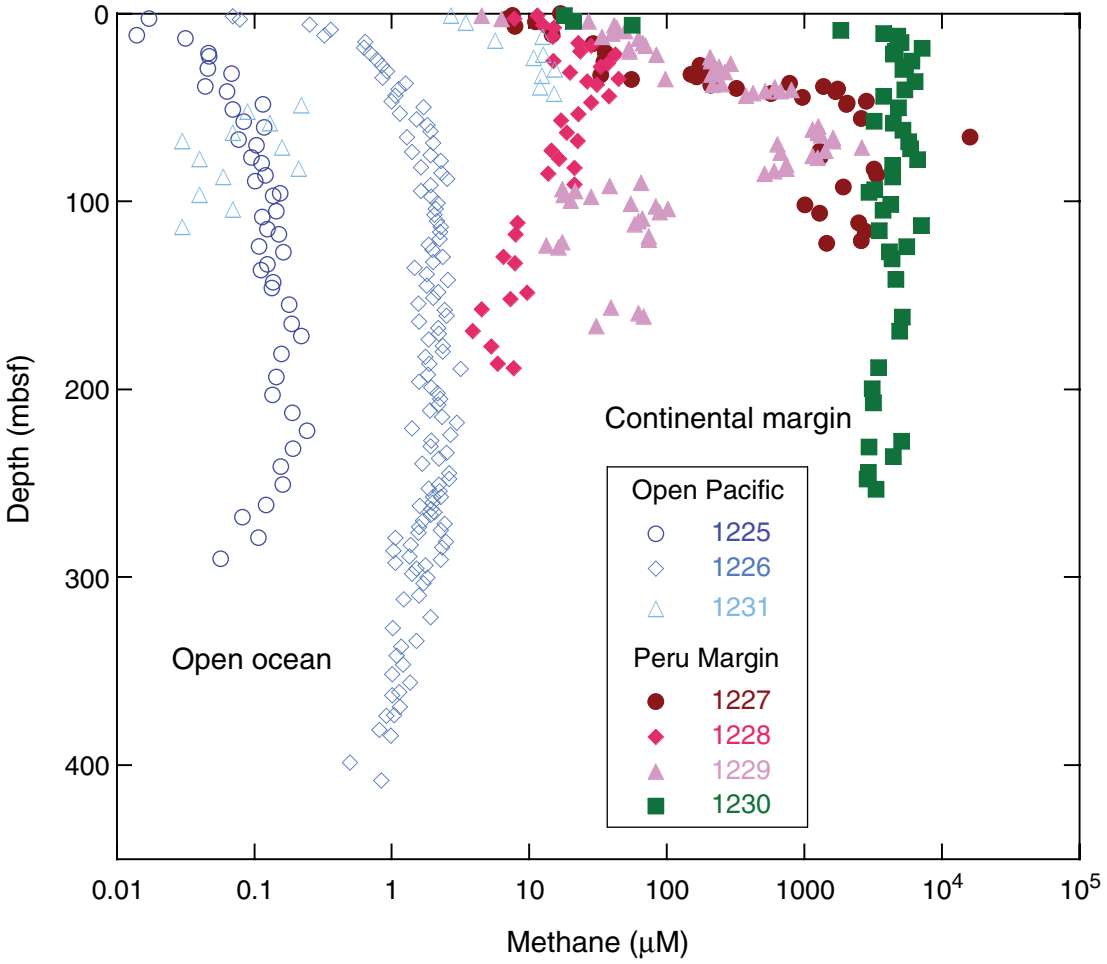

Figure F10. Methane, ethane, and propane concentrations of Peru shelf Site 1227.

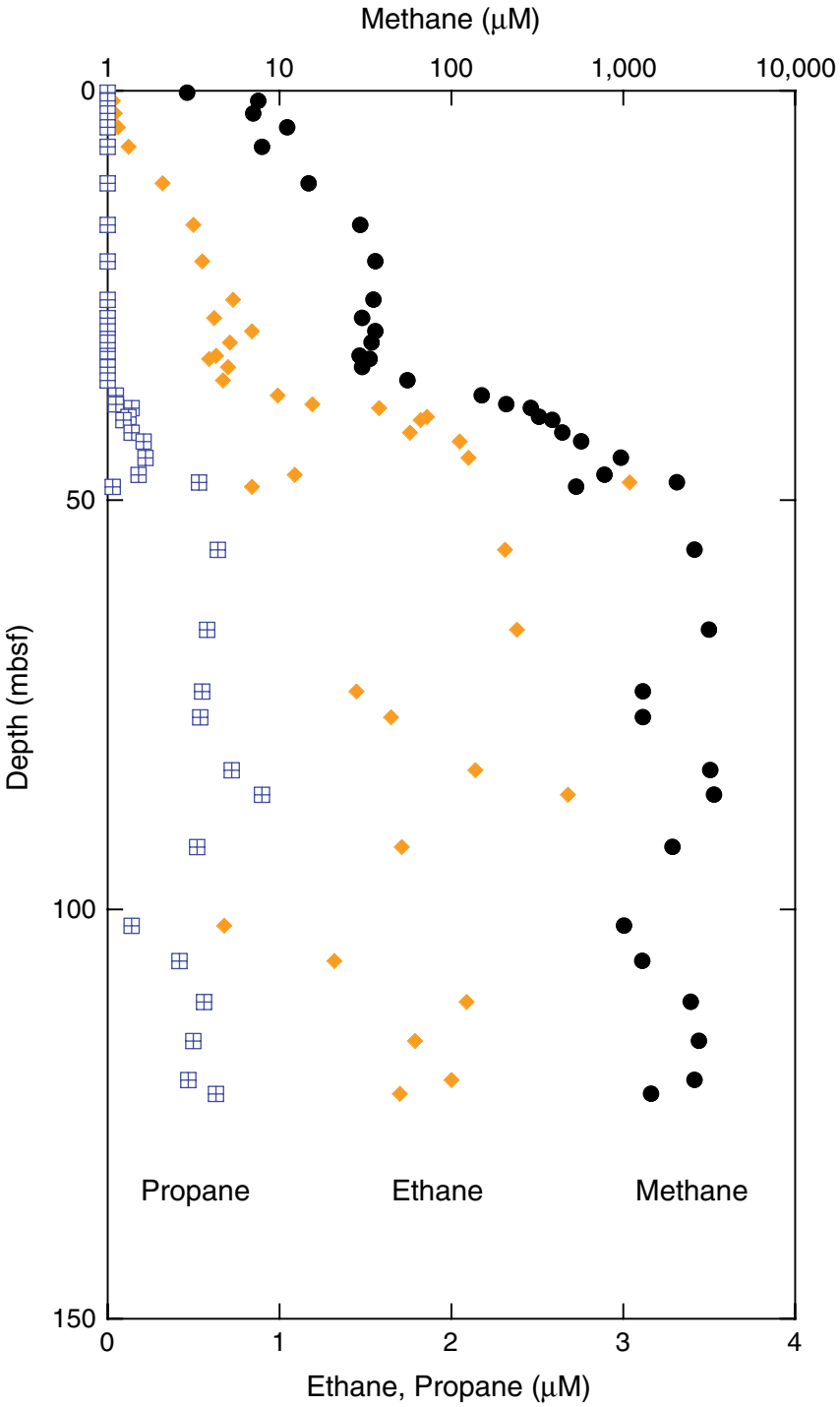

Figure F11. Dissolved nitrate concentrations at open-ocean Sites 1225 and 1231.

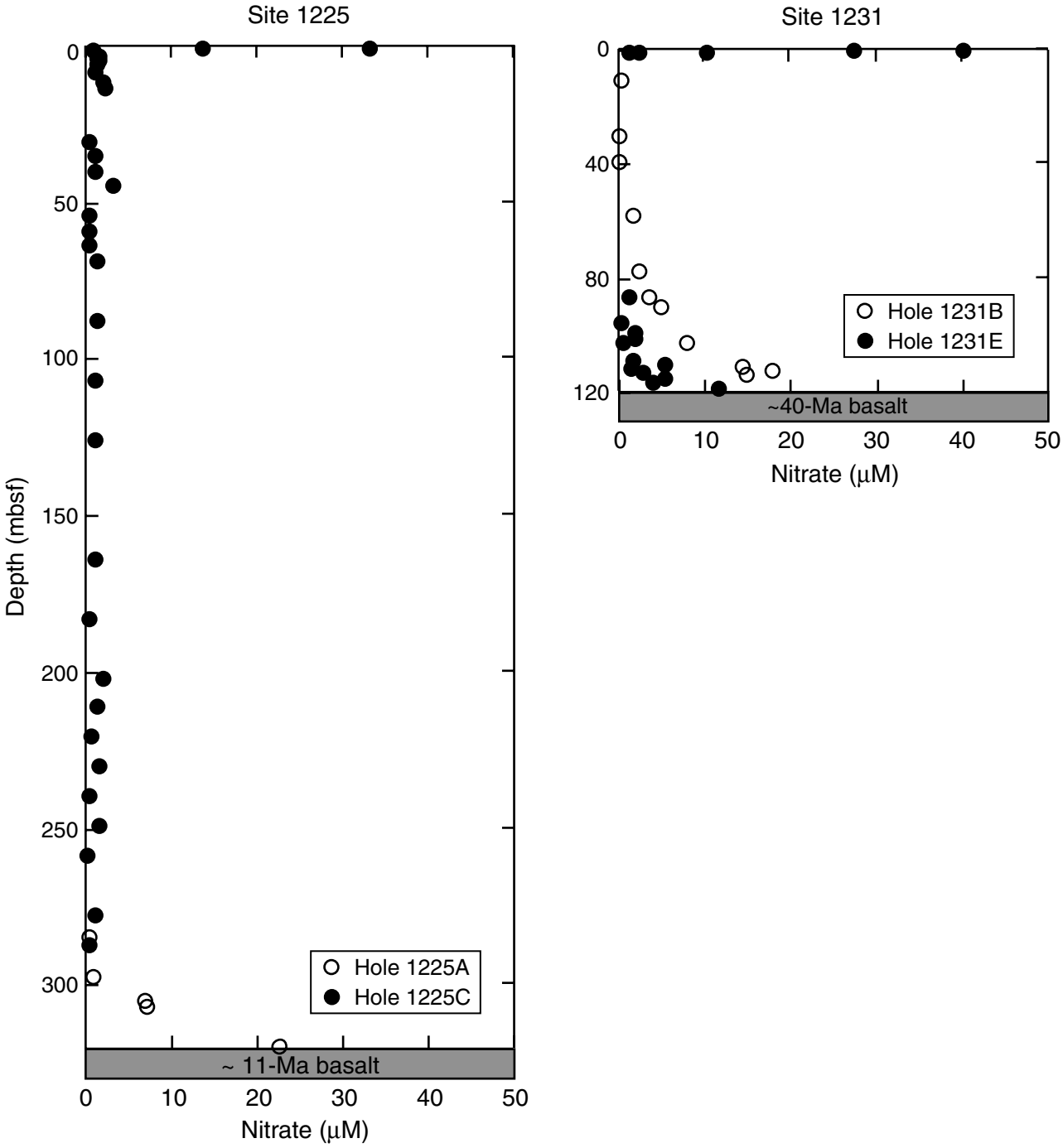

Figure F12. Acridine orange direct count (AODC) of microbial cells and concentrations of dissolved sulfate, barium, methane, and acetate at Peru shelf Site 1229.

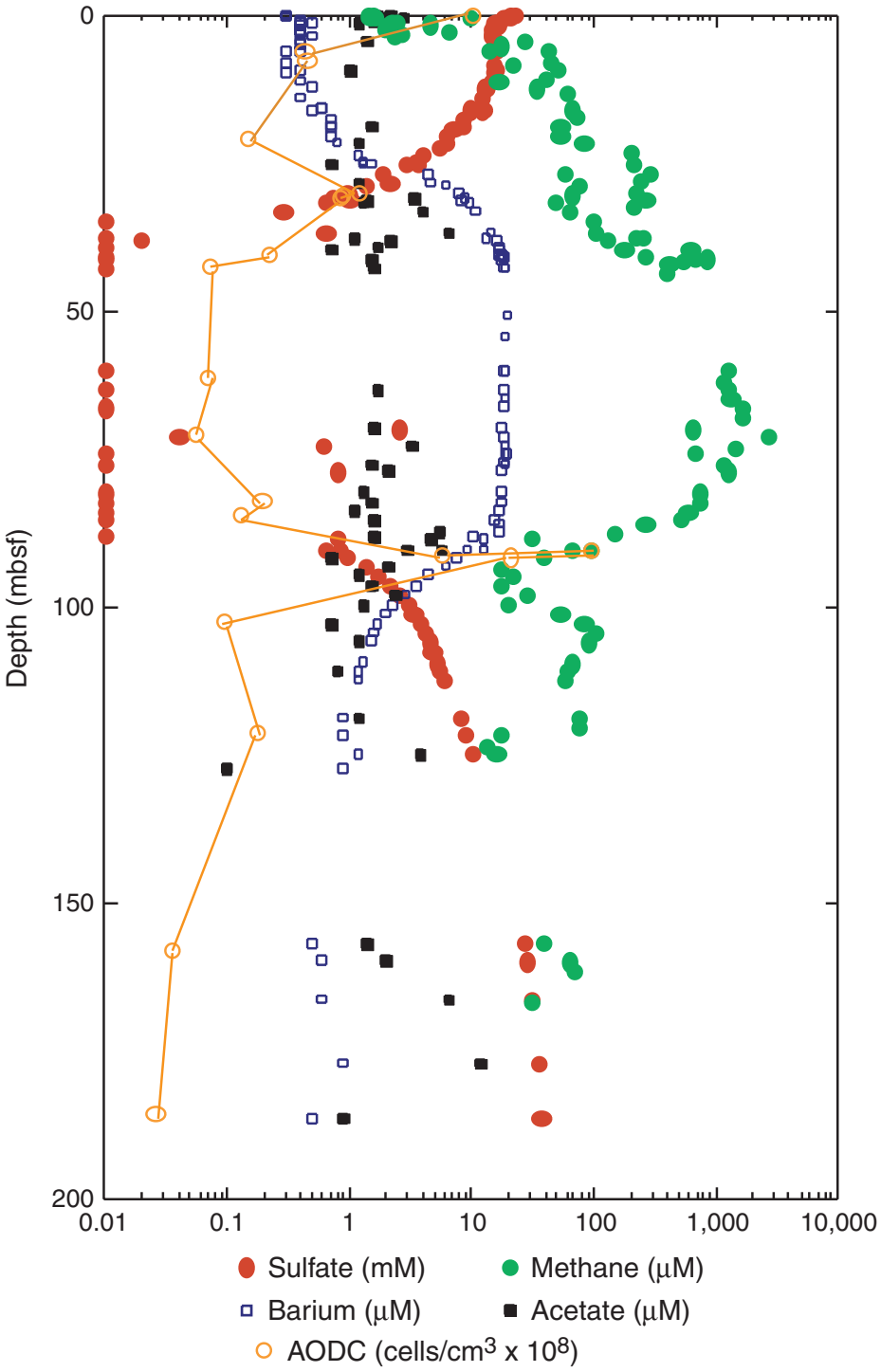

Figure F13. Dissolved iron profile and sediment magnetic susceptibility of equatorial Pacific Site 1225.

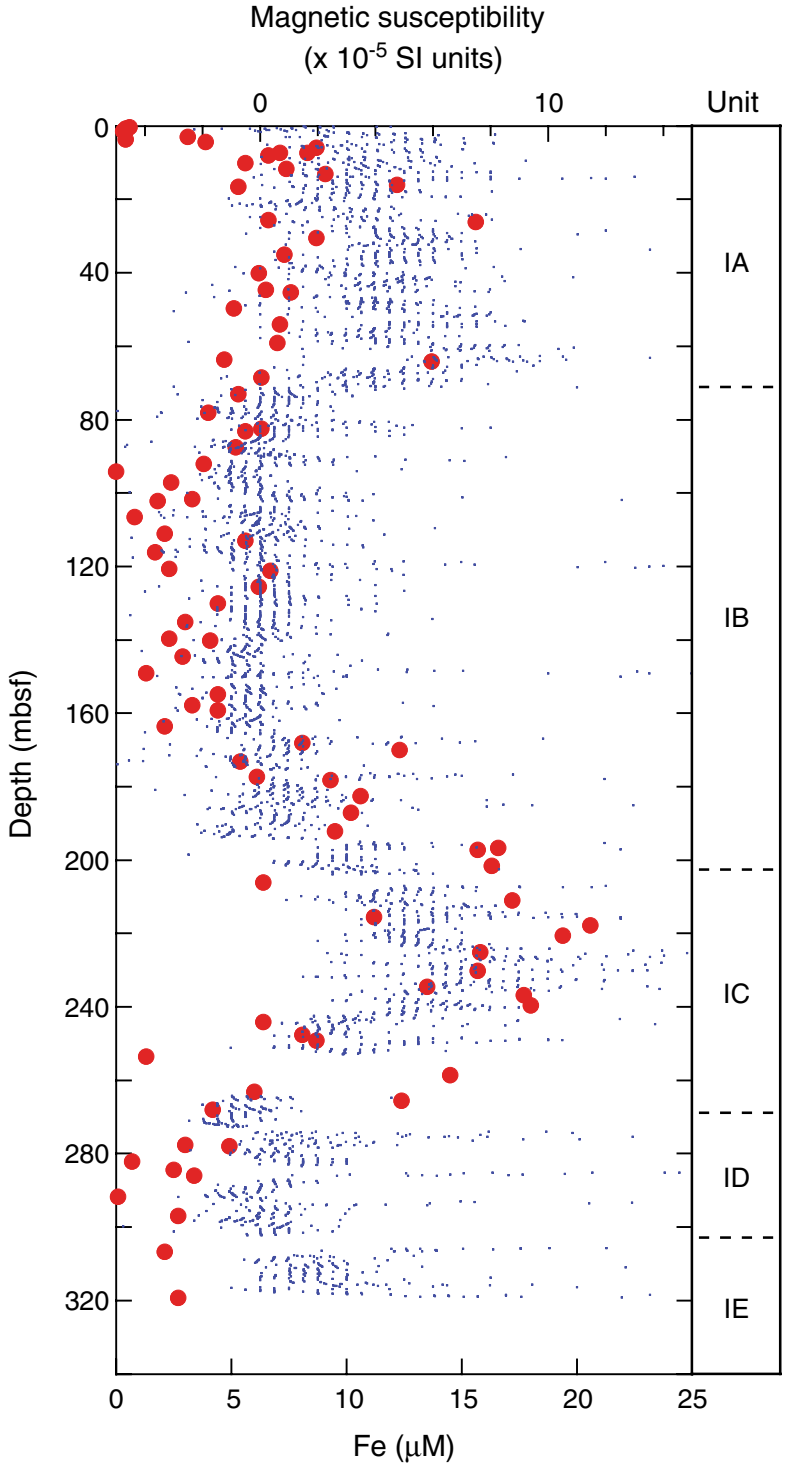

Figure F14. Dissolved manganese profile and natural gamma radiation of equatorial Pacific Site 1226.

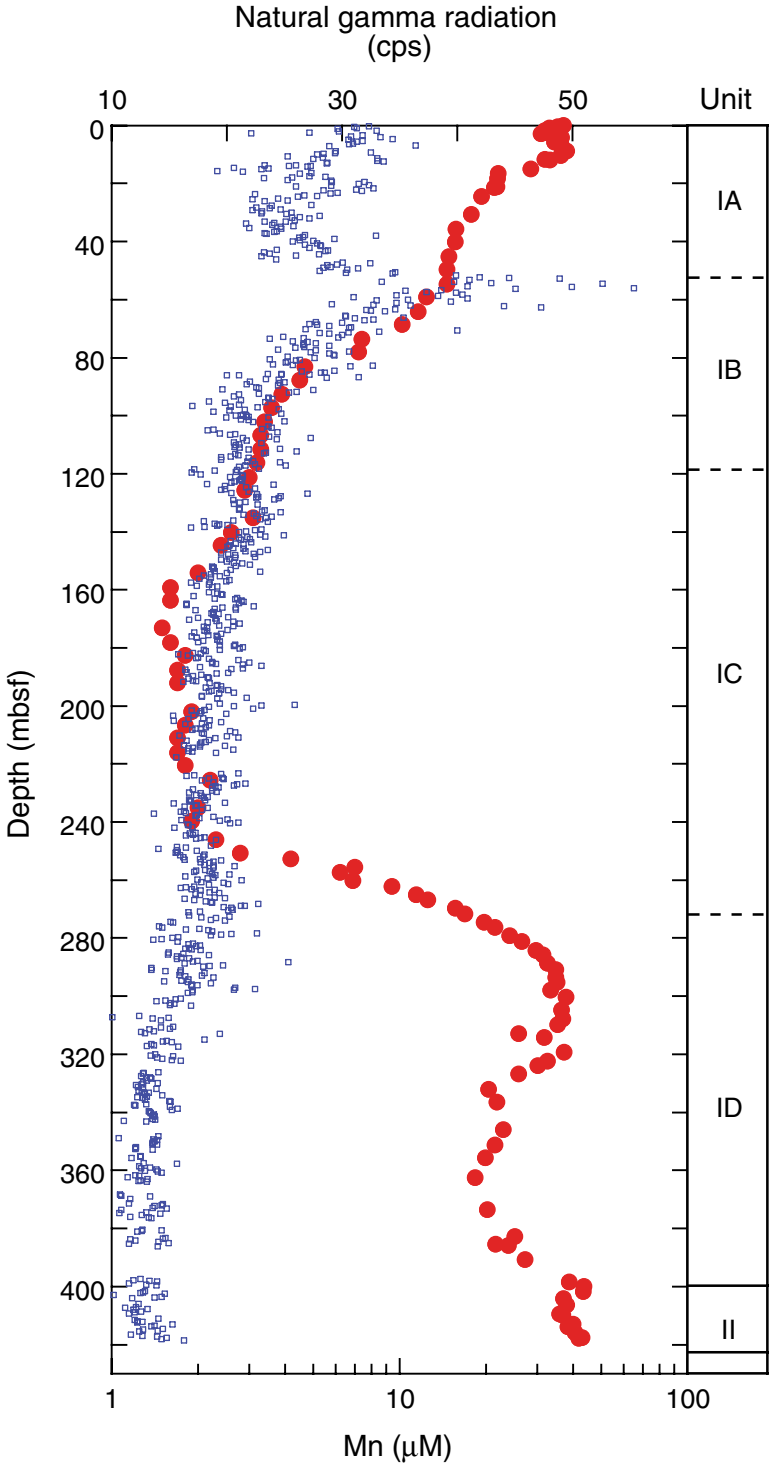

Figure F15. Dissolved iron profile and magnetic susceptibility of Peru shelf Site 1229.

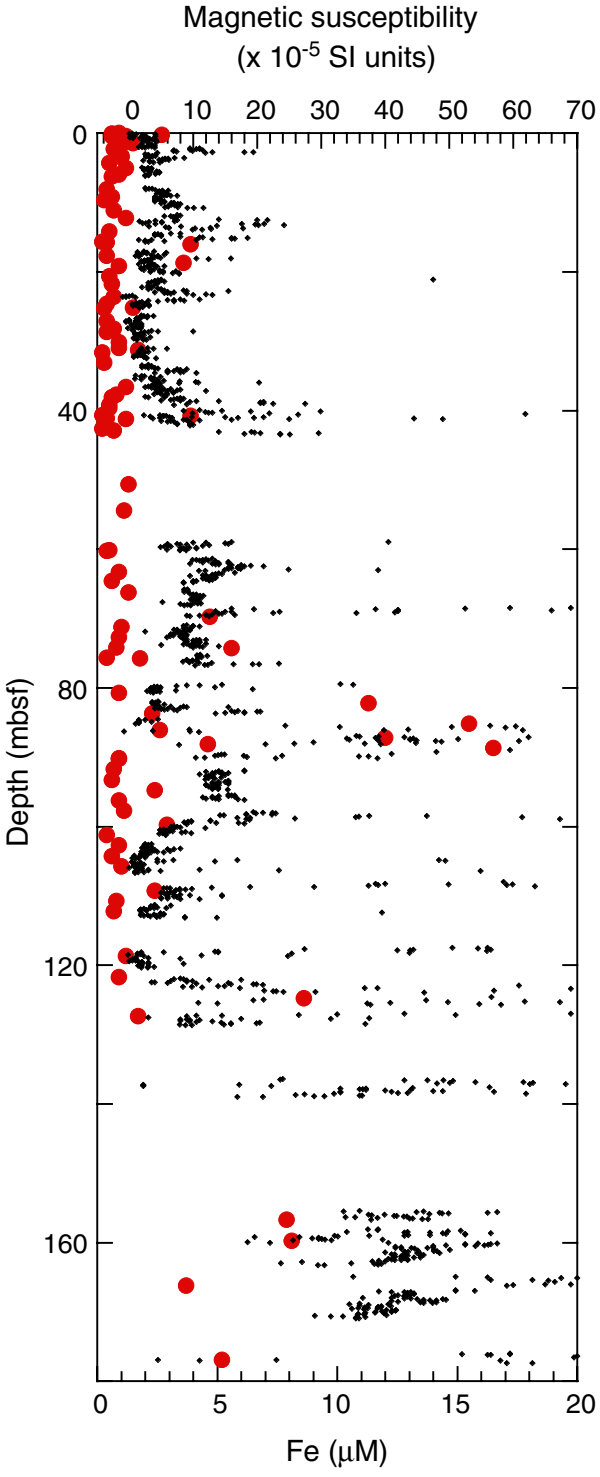

Figure F16. Dissolved manganese, iron, and methane profiles of Peru shelf Site 1229.

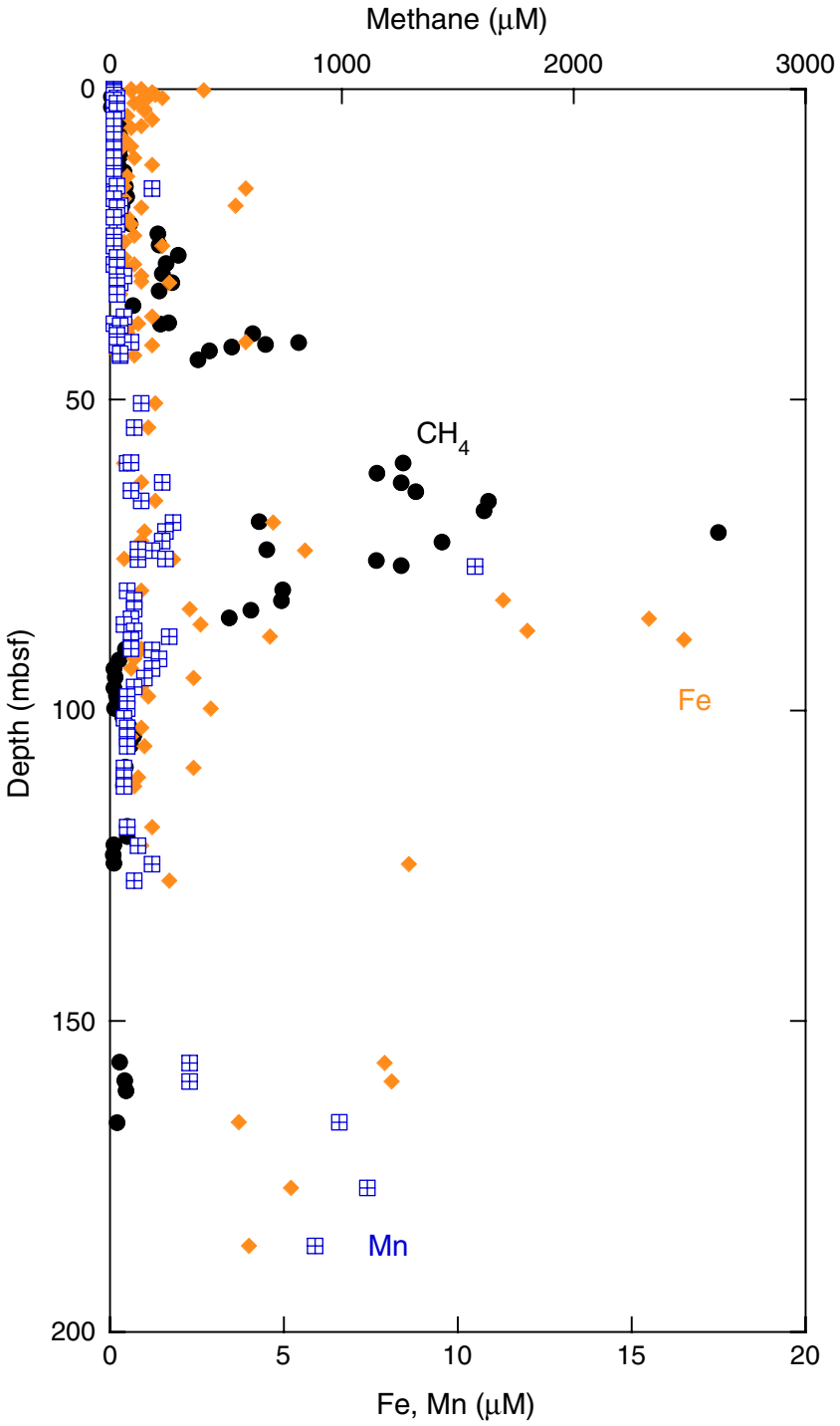

Figure F17. Grain density and dissolved methane and sulfate profiles at Peru shelf Site 1227.

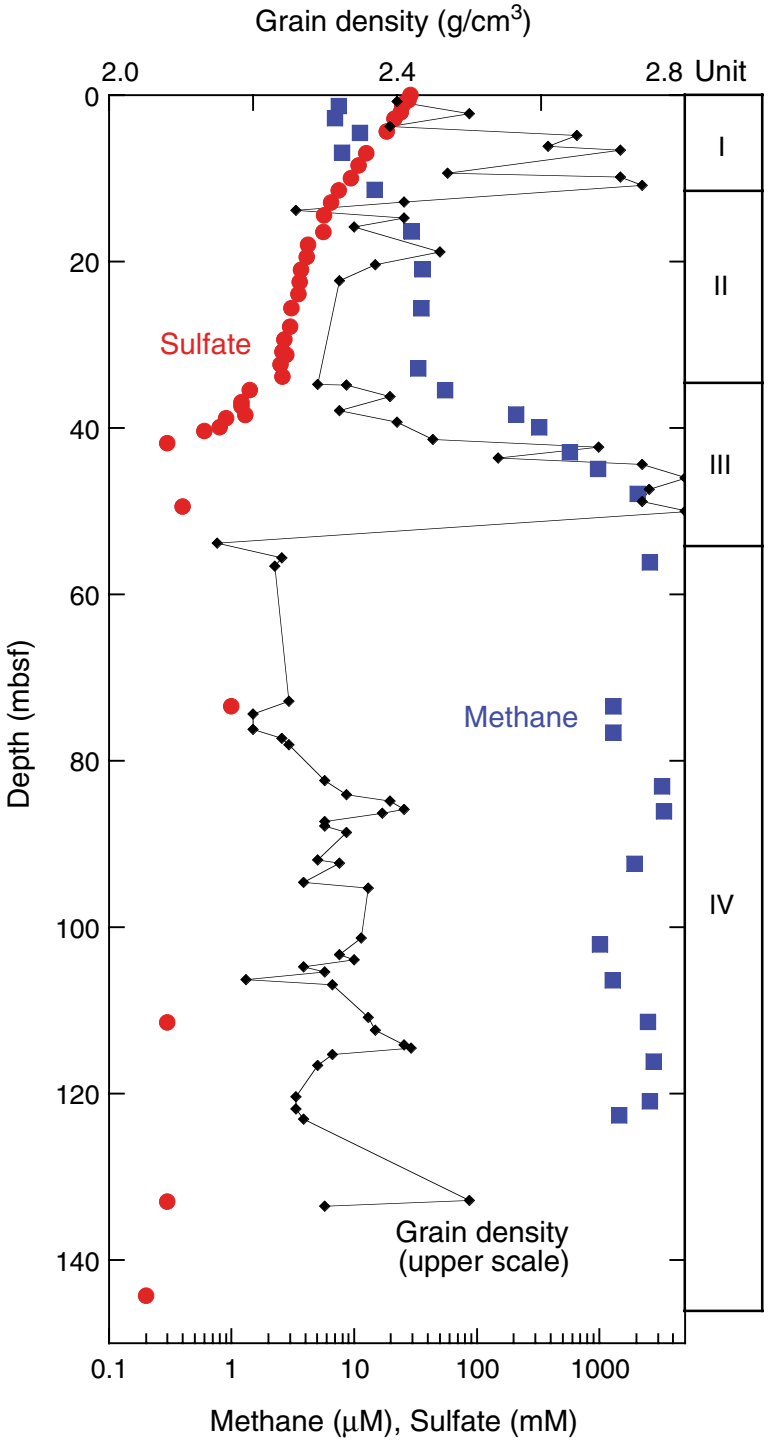

Figure F18. Dissolved sulfate profiles of Peru shelf Sites 1227, 1228, and 1229. Solid squares = Holes 1227A, 1228A, and 1229A. Solid circles = Holes 1227D, 1228C, 1228E, and 1229D.

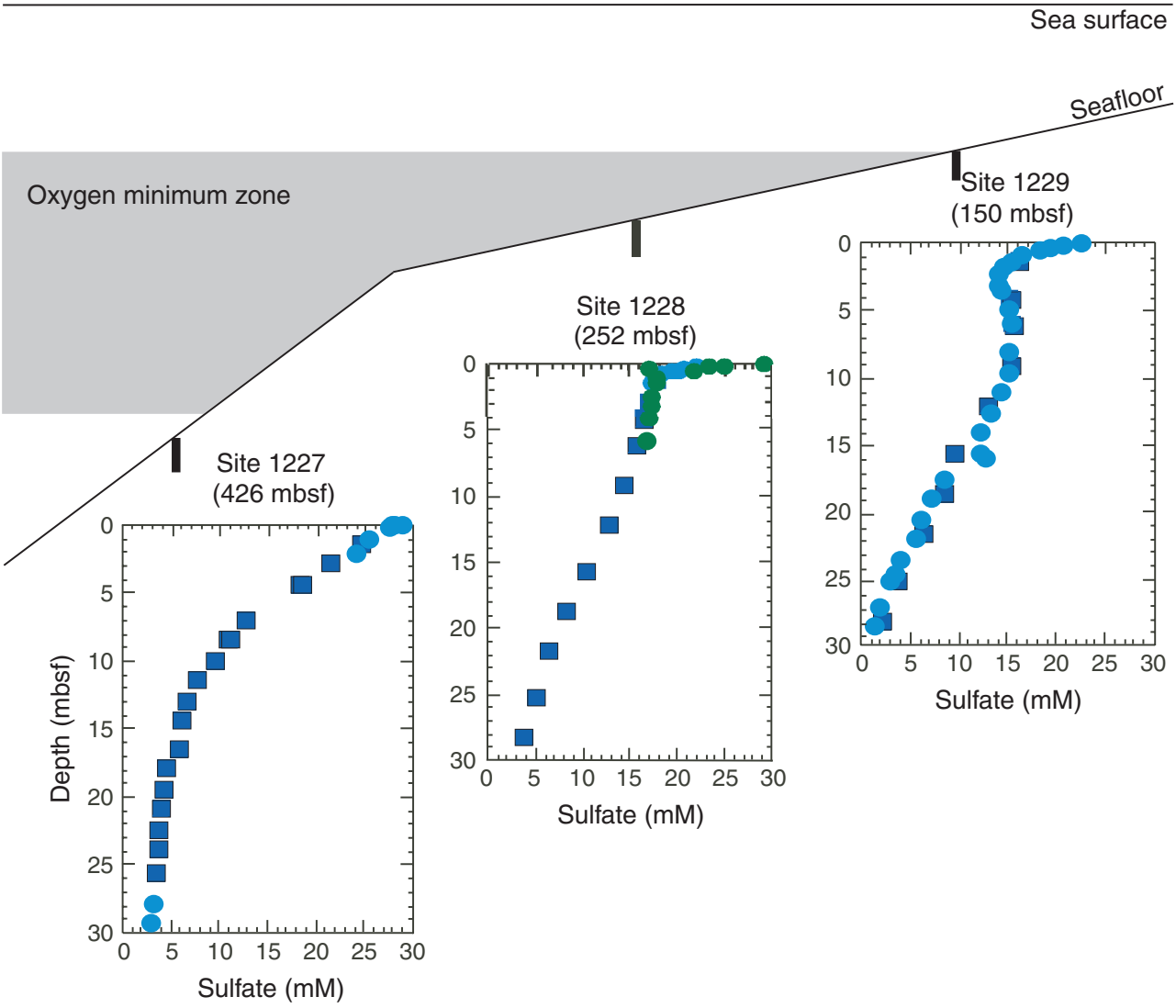

Figure F19. Dissolved barium and sulfate profiles of Peru slope hydrate Site 1230.

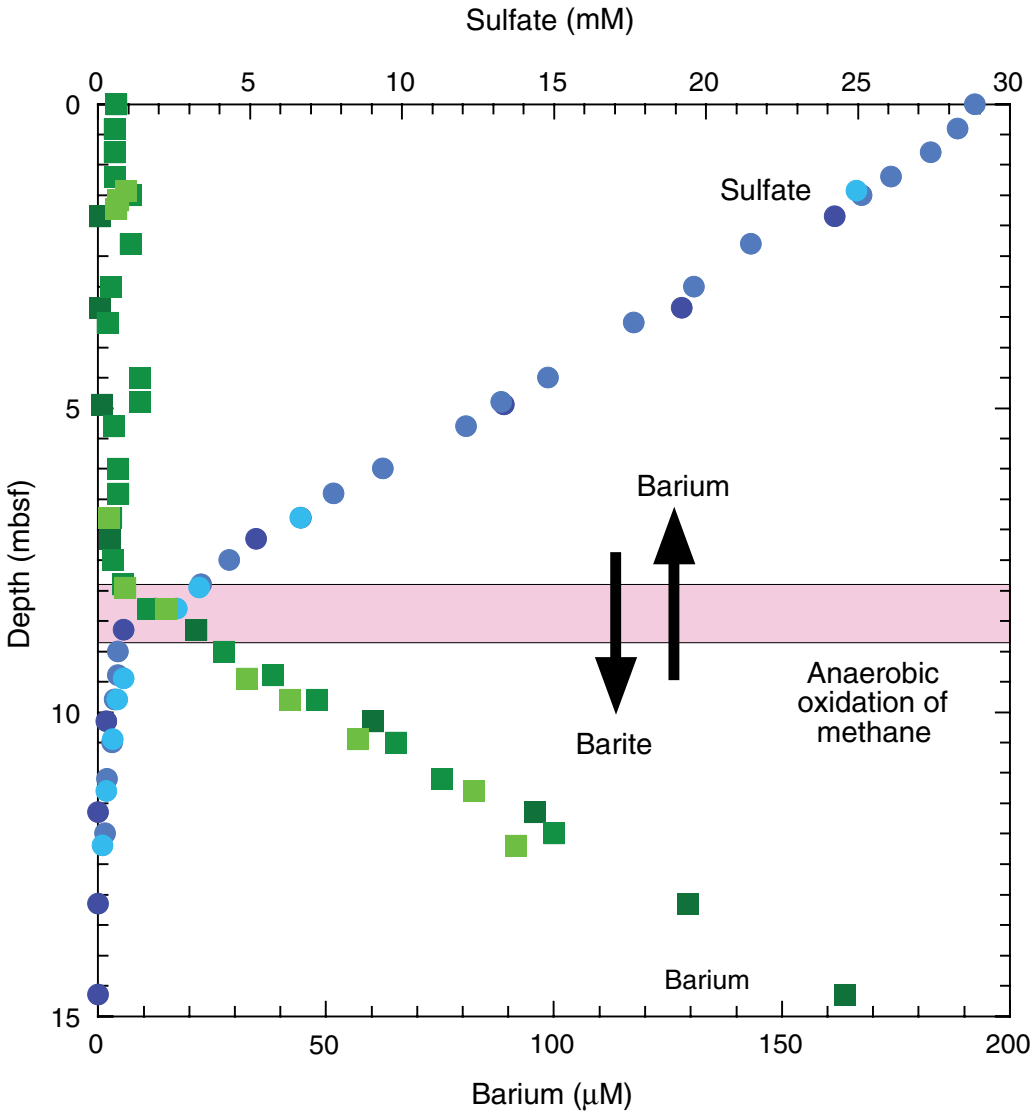

Figure F20. Comparison of perfluorocarbon tracer (PFT) and bead contamination tests in sediments cored by advanced hydraulic piston coring (APC) or extended core barrel (XCB). The PFT was recalculated to microliters of seawater potentially introduced into a gram of sediment in proportion to the tracer concentration. The lines indicate limits below which contamination was undetectable.

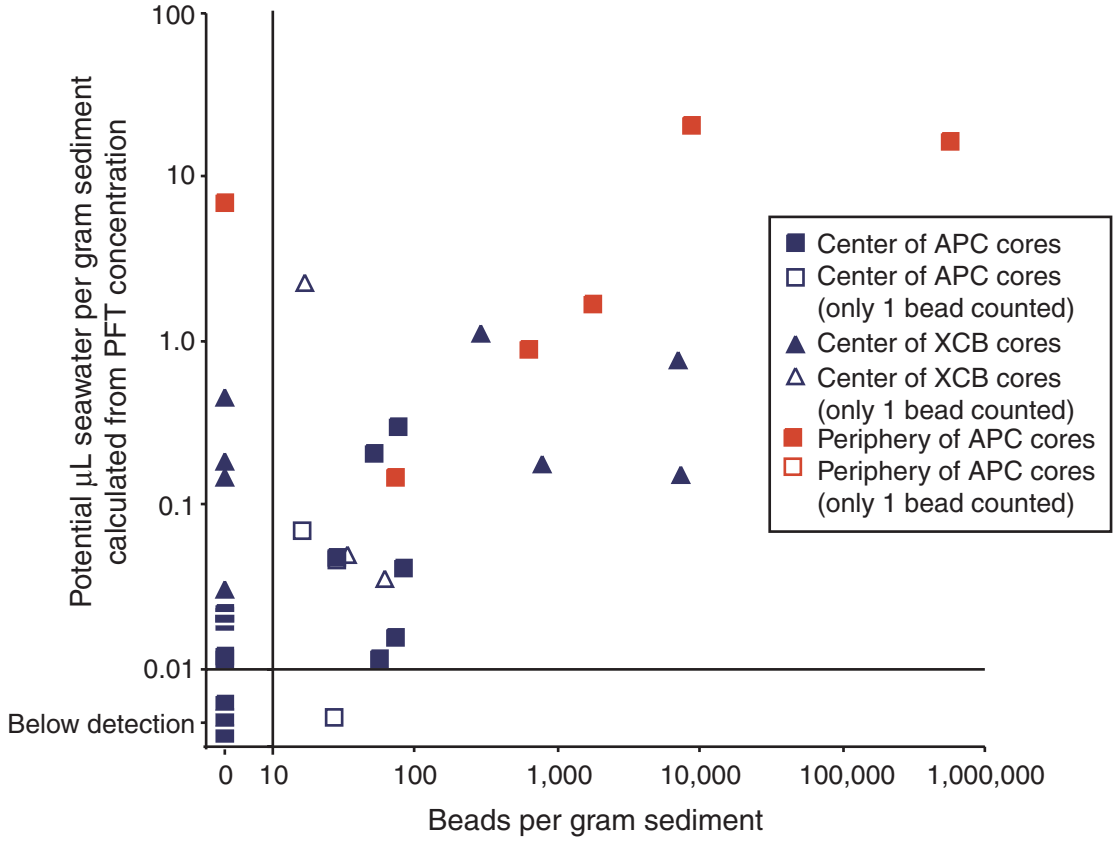

Table T1. Operations summary, Leg 201.

	Advanced piston corer				Extended core barrel				Pressure Coring System				Fugro Percussion Corer				Leg 201 totals				
Site/hole	*N*	Cored (m)	Recovered (m)	Recovery (%)	*N*	Cored (m)	Recovered (m)	Recovery (%)	*N*	Cored (m)	Recovered (m)	Recovery (%)	*N*	Cored (m)	Recovered (m)	Recovery (%)	Drilled	*N*	Cored (m)	Recovered (m)	Recovery (%)
1225A	32	298.8	312.99	104.7	2	15.8	7.25	45.9	1	1.0	1.41	141.0	0	0.0	0.00	0.0	4.0	35	315.6	321.65	101.9
1225B	1	9.0	8.96	99.6	0	0.0	0.00	0.0	0	0.0	0.00	0.0	0	0.0	0.00	0.0	0.0	1	9.0	8.96	99.6
1225C	32	303.3	304.49	100.4	0	0.0	0.00	0.0	1	1.0	1.00	100.0	0	0.0	0.00	0.0	1.0	33	304.3	305.49	100.4
Site 1225 totals:	65	611.1	626.44	102.5	2	15.8	7.25	45.9	2	2.0	2.41	120.5	0	0.0	0.00	0.0	5.0	69	628.9	636.10	101.1
1226A	1	9.5	9.43	99.3	0	0.0	0.00	0.0	0	0.0	0.00	0.0	0	0.0	0.00	0.0	0.0	1	9.5	9.43	99.3
1226B	29	270.4	284.43	105.2	17	148.5	129.26	87.0	1	1.0	1.66	166.0	0	0.0	0.00	0.0	2.5	47	419.9	415.35	98.9
1226C	1	7.9	7.91	100.1	0	0.0	0.00	0.0	0	0.0	0.00	0.0	0	0.0	0.00	0.0	0.0	1	7.9	7.91	100.1
1226D	1	7.6	7.64	100.5	0	0.0	0.00	0.0	0	0.0	0.00	0.0	0	0.0	0.00	0.0	0.0	1	7.6	7.64	100.5
1226E	20	188.1	196.38	104.4	4	39.4	30.58	77.6	1	1.0	1.02	102.0	0	0.0	0.00	0.0	190.9	25	228.5	227.98	99.8
Site 1226 totals:	52	483.5	505.79	104.6	21	187.9	159.84	0.0	2	2	2.68	0.0	0	0	0	0.0	193.4	75	673.4	668.31	99.2
1227A	16	148.1	100.40	67.8				0.0	1	2.0	0.00	0.0	1	1.0	0.15	15.0	0.0	18	151.1	100.55	66.5
1227B	3	24.0	24.67	102.8				0.0				0.0				0.0	0.0	3	24.0	24.67	102.8
1227C	3	26.8	27.25	101.7				0.0				0.0				0.0	0.0	3	26.8	27.25	101.7
1227D	8	74.0	54.84	74.1				0.0				0.0				0.0	0.0	8	74.0	54.84	74.1
1227E	3	25.9	26.28	101.5				0.0				0.0	1	1.0	0.44	44.0	0.0	4	26.9	26.72	99.3
Site 1227 totals:	33	298.8	233.44	78.1	0	0.0	0.00	0.0	1	2.0	0.00	0.0	2	2.0	0.59	29.5	0.0	36	302.8	234.03	77.3
1228A	21	193.9	125.85	64.9				0.0	1	2.0	0.07	3.5	1	1.0	0.39	39.0	4.0	23	196.9	126.31	64.1
1228B	6	54.3	50.68	93.3				0.0				0.0	1	1.0	0.42	42.0		7	55.3	51.10	92.4
1228C	1	7.5	7.53	100.4				0.0				0.0				0.0		1	7.5	7.53	100.4
1228D	3	26.6	27.27	102.5				0.0				0.0				0.0		3	26.6	27.27	102.5
1228E	1	7.3	7.33	100.4				0.0				0.0	1	1.0	1.90	190.0		2	8.3	9.23	111.2
Site 1228 totals:	32	289.6	218.66	75.5	0	0.0	0.00	0.0	1	2.0	0.07	3.5	3	3.0	2.71	90.3	4.0	36	294.6	221.44	75.2
1229A	21	191.9	132.84	69.2				0.0				0.0	1	1.0	0.26	26.0	1.5	22	192.9	133.10	69.0
1229B	3	24.4	24.84	101.8				0.0				0.0	1	1.0	0.00	0.0		4	25.4	24.84	97.8
1229C	1	8.8	8.80	100.0				0.0				0.0				0.0		1	8.8	8.80	100.0
1229D	14	113.8	100.02	87.9				0.0	1	2.0		0.0				0.0		15	115.8	100.02	86.4
1229E	13	121.5	99.64	82.0				0.0				0.0				0.0		13	121.5	99.64	82.0
Site 1229 totals:	52	460.4	366.14	79.5	0	0.0	0.00	0.0	1	2.0	0.00	0.0	2	2.0	0.26	13.0	1.5	55	464.4	366.40	78.9
1230A	27	219.6	161.26	73.4	6	46.2	21.57	46.7	6	11.5	4.50	39.1				0.0	1.0	39	277.3	187.33	67.6
1230B	11	96.0	94.73	98.7				0.0	3	6.0	3.65	60.8				0.0	3.0	14	102.0	98.38	96.5
1230C	2	14.0	14.42	103.0				0.0				0.0				0.0	0.0	2	14.0	14.42	103.0
1230D	2	13.5	14.22	105.3				0.0				0.0				0.0	0.0	2	13.5	14.22	105.3
1230E	4	32.5	34.47	106.1				0.0	1	2.0		0.0				0.0	1.5	5	34.5	34.47	99.9
Site 1230 totals:	46	375.6	319.10	85.0	6	46.2	21.57	46.7	10	19.5	8.15	41.8	0	0.0	0.00	0.0	5.5	62	441.3	348.82	79.0
1231A	1	9.5	10.13	106.6				0.0				0.0				0.0		1	9.5	10.13	106.6
1231B	13	112.9	115.20	102.0	1	2.9	0.10	3.4				0.0				0.0	1.5	14	115.8	115.30	99.6
1231C	2	15.1	15.27	101.1				0.0				0.0				0.0		2	15.1	15.27	101.1
1231D	12	112.3	109.17	97.2	1	9.6	2.40	25.0				0.0				0.0		13	121.9	111.57	91.5
1231E	14	119.1	118.57	99.6				0.0				0.0				0.0		14	119.1	118.57	99.6
Site 1231 totals:	42	368.9	368.34	99.8	2	12.5	2.50	0.0	0	0.0	0.00	0.0	0	0.0	0.00	0.0	1.5	44	381.4	370.84	97.2
Leg 201 totals:	322	2887.9	2637.91	91.3	31	262.4	191.16	72.9	17	29.5	13.31	45.1	7	7	3.56	50.9	377	3186.8	2845.94	89.3	377

Note: *N* = number of cores.

Table T2. Summary of pressure coring sampler operations, Leg 201.

Run	Core	Date (2002)	Depth (mbsf)	Recovered (m)	Pressure (psi)	Gas volume	Comments
	201-						
1	1225A-29P	10-Feb	262.2	0.41	1200	70 mL	
2	1225C-32P	13-Feb	293.8	1.00	4800	70 mL	
3	1226B-42P	22-Feb	378.0	0.66	6200	60 mL	
4	1226E-21P	25-Feb	378.0	1.02	0		Chert prevented ball valve from closing
5	1227A-15P	1-Mar	129.1	0.00	0		Actuation mechanism failed
6	1228A-23P	5-Mar	198.9	0.07	35	60 mL	Cutting shoe lost in hole
7	1229D-10P	9-Mar	77.8	0.86	400	2.88 L	
8	1230A-7P	12-Mar	52.3	1.00	6278	1.16 L	
9	1230A-16P	13-Mar	127.3	1.00	7794	3.11 L	
10	1230A-20P	13-Mar	156.8	0.65	5930	6.33 L	
11	1230A-25P	14-Mar	196.8	0.18	8050	0.200 L	
12	1230A-36P	15-Mar	254.6	0.41	8086	1.16 L	
13	1230A-39P	15-Mar	276.8	0.62	280	1.53 L	
14	1230B-4P	17-Mar	22.0	1.00	7400	0.775 L	
15	1230B-10P	17-Mar	71.5	1.00	7416	1.14 L	
16	1230B-14P	18-Mar	103.0	1.00	8030	1.765 L	
17	1230E-5P	18-Mar	34.0	1.00	6134	0.26 L	

Table T3. Summary of Fugro Percussion Corer operations, Leg 201.

Run	Core	Date (Mar 2002)	Depth (mbsf)	Comments
	201-			
1	1227A-16M	1	131.1	A few centimeters of gravel recovered. Autoclave not under pressure due to gravel in valve.
2	1227E-4M	2	25.8	40 cm sandy clay recovered, data logger failed, no pressure measured.
3	1228A-13M	4	109.4	50 cm of gravel recovered, core liner collapsed, seals damaged, no pressure retained.
4	1228B-7M	6	54.3	42 cm of clay recovered, valve stuck open, seals damaged, pawls inside housing damaged, no pressure retained.
5	1228E-2M	6	7.3	65 cm of clay recovered, valve stuck open, seals damaged, no pressure retained.
6	1229A-20M	8	174.4	40 cm of gravel with some clay, valve stuck open, seals damaged, no pressure retained.
7	1229B-4M	8	24.4	Inner barrel did not fully retract, jammed due to previous seal failure, previously damaged pawls in housing sheared off, damaged beyond repair at sea, no core recovered, no pressure retained.